Administration of Chemically-Modified Poly(lactide-co-glycolide) Nanoparticles to Engineer the Immune Response for Tolerance Induction

By

Robert Kuo

A dissertation submitted in partial fulfillment
of the requirements for the degree of
Doctor of Philosophy
(Chemical Engineering)
in the University of Michigan
2017

Doctoral Committee:

Professor Lonnie D. Shea, Chair
Associate Professor Omolola Eniola-Adefeso
Assistant Professor James J. Moon
Professor Bethany B. Moore
Assistant Professor Fei Wen

Robert Kuo

robertkuo@outlook.com

ORCID: 0000-0001-8271-4602

Acknowledgements

I wish to recognize the mentors, colleagues, friends, and family who have invested in me over the past 10 or so years of my formal scientific training and helped me unlock my potential to accomplish the work that follows.

I would first like to extend my heartfelt gratitude to Dr. Brian West who gave me my first opportunity to work in scientific research. I learned so much during my summer at Plexxikon under Brian's direction, and working alongside Hoa Nguyen, a great teacher who set a strong example with her remarkable laboratory knowledge and experience. From my time at Plexxikon, I also saw firsthand the beneficial impact that scientific research can have for improving human health which I found to be inspiring and motivating.

I am also very thankful for the excellent education I received at UC Berkeley and the wonderful opportunity to work with Dr. Michael Samoilov and Dr. Adam Arkin in synthetic biology.

My time at UCSF was instrumental for preparing me to succeed in graduate study. Under the guidance of Dr. Hua Su, and working alongside Dr. Fanxia Shen, I gained experience performing many new experimental techniques important for biomedical investigations and also learned how to design experiments and develop a research project. Thank you for teaching me so many things and providing a lot of encouragement.

I wish to also extend my gratitude to Dr. Lonnie Shea for accepting me into his laboratory and providing the creative space for me to conduct studies that interested me. A big thank you also to Dr. Ryan Boehler, who helped me settle into the lab when I first arrived and

was so generous in sharing his time and experience. Many thanks to Dr. Eiji Saito, who I could always ask for support and guidance on my research. Thank you to the Particle People subgroup for the input and teamwork. And thank you to the many who came before me in the lab, developing the nanoparticle and cell array platforms. I did my best to build off their work and I hope the next group of lab members can use my contributions to continue advancing the technologies further.

I recognize that while many set out to obtain a Ph.D., not everyone is able to complete this goal. I consider myself fortunate to have a family that is encouraging and supportive. I am grateful to my mother who showed me that getting a Ph.D. is indeed possible, and to my father, who is a model for tenacity and perseverance. Thank you to my sister and brother-in-law for their support and I hope my niece and nephew will consider a scientific career path when they grow up.

Table of Contents

List of Figures

Abstract

Autoimmune diseases are the result of a severe immune response targeted against native tissues. Current strategies in the clinic to treat autoimmunity involve administering immunosuppressant medications which suppress broad components of the immune system. While effective for managing symptoms, reduced immune competency leads to harmful side effects such as increased risk for infection. Therefore, developing more targeted approaches to induce immune tolerance in the treatment of autoimmunity are highly desirable.

One approach to induce antigen-specific tolerance has been to administer antigen coupled to poly(lactide-co-glycolide) (PLG) nanoparticles. These nanoparticles have been effective in treating models of autoimmunity, allergy, and transplant rejection, however the mechanism of action is poorly understood. Herein contains investigations of downstream cellular and molecular events following nanoparticle internalization by antigen-presenting cells (APCs). Increasing the amount of both administered nanoparticles and coupled antigen led to higher levels of antigen presentation on the APC surface. Co-stimulatory analysis of APCs with detectable MHC-restricted antigen revealed a significant reduction of positive co-stimulatory molecules (CD86, CD80, and CD40) as nanoparticle concentration was increased. These trends in co-stimulatory expression were not observed in APCs administered increasing amounts of soluble antigen, suggesting the critical role of antigen coupling to nanoparticles.

Cell signaling activity of APCs treated with either antigen-coupled nanoparticles (PLG-OVA) or antigen-coupled splenocytes (SP-OVA) were compared to identify tolerance mechanisms resulting from different antigen delivery vehicles. Network analysis revealed NF-

KB had an integral role within macrophages to connect signaling among several different transcription factors while NF-KB was less critical to integrate signaling across dendritic cell networks. Macrophages treated PLG-OVA or SP-OVA before co-culture with activated T cells did not dramatically affect T cell response. Dendritic cells treated SP-OVA compared to PLG-OVA were more effective to attenuate not only IL-2Rα expression but also other indicators of T cell activity. Inhibiting NF-KB signaling in macrophages treated with SP-OVA led to reduced T cell expression of IL-2Rα, suggesting a potential role for targeting NF-KB activity to improve tolerance induction.

Nanoparticles encapsulating small interfering RNA (siRNA) were investigated to inhibit autoimmune signaling pathways. A feasibility study was conducted focusing on CCR2, a chemokine receptor correlated with worse prognoses in models of multiple sclerosis. An siRNA mixture targeting CCR2 expression (siCCR2) was complexed to polyethylenimine prior to PLG encapsulation. Complexed and encapsulated siCCR2 were evaluated by measuring CCR2 levels and cell migratory potential. Encapsulated siCCR2 were also examined by administering 1.0 mg in a mouse model of multiple sclerosis on Days 7, 9, and 11 following disease induction. Mean clinical scores were significantly reduced compared to administering either encapsulated non-specific siRNA complexes or buffered solution. These findings suggest encapsulated siRNA complexes may have clinical applications for the treatment of multiple sclerosis and other autoimmune diseases.

This work identified several mechanisms, including IL-10 production, T cell apoptosis, and reduced T cell proliferation affected by antigen-coupled nanoparticle treatment. Intracellular signaling activity of treated APCs revealed a central role of NF-KB to mediate macrophage signaling. Macrophages treated with SP-OVA and an NF-KB inhibitor prior to co-culture with

activated T cells resulted in attenuated T cell activity. More targeted approaches to inhibit molecules of interest were explored using PLG nanoparticles encapsulating siRNA. Initial studies focused on CCR2, whose expression during autoimmunity is correlated with worsening prognosis. Encapsulated CCR2-targeting siRNA had good feasibility for reducing both *in vitro* and *in vivo* inflammatory responses.

Chapter 1: Introduction

1.1 Motivation

Autoimmune diseases represent a severe worldwide health burden. There are currently 81 identified autoimmune diseases, affecting approximately 4.5% of the world's population. [1] Many autoimmune diseases are chronic in nature, leading to a reduced life expectancy as well as a diminished quality of life. [2] Typical therapeutic strategies for autoimmune diseases focus on systemic immune suppression. However, the harmful side effects of disrupting immune competency motivates the development of antigen-specific interventions. These approaches would specifically target autoimmune pathways for inactivation while preserving the remainder of the immune system to prevent opportunistic infections.

Antigen-specific approaches to desensitize the immune system have been used for nearly a century, primarily to treat allergies by administering a gradually increasing dose of allergen over an extended period of time. This type of approach has shown promise to also treat models of autoimmune disease through the administration of escalating doses of autoantigen. [3] However, the difficulty with controlling dose escalation, length of treatment window, and risk for anaphylaxis has limited widespread adoption of these hyposensitization therapies. Interestingly, instead of soluble administration of autoantigen, attaching the autoantigen to nanoparticles prior to administration has led to rapid and long-lived antigen-specific tolerance. [4] The use of nanoparticles to treat autoimmune diseases holds potential for clinical translation, but a better understanding of the cellular and molecular mechanisms would help ensure safety and efficacy.

Nanoparticles are not the exclusive antigen delivery vehicle to induce antigen-specific tolerance. In fact, attaching autoantigen to donor cells has been previously demonstrated to also induce antigen-specific tolerance. [5] The use of cell-based vehicles is a logical platform, as the immune system routinely removes apoptotic cells from circulation without triggering an immune response. Interestingly, the chemical treatment used to attach autoantigens to donor cells results in apoptosis, [6] thus it is highly probable that administering antigen attached to donor cells triggers endogenous signaling pathways that overlap with apoptotic cell clearance. A comparison of the signaling pathways used by antigen-coupled nanoparticles and antigen-coupled cells would therefore provide interesting insights to identify additional signaling molecules whose activity could be modulated to enhance the tolerance induction efficiency of nanoparticle-based antigen-specific therapy. Antigen-coupled nanoparticles offer several advantages in the therapeutic setting compared to antigen-coupled cells, which include ease of manufacturing and storage.

Concern over an anaphylactic reaction will undoubtedly overshadow any antigen-specific approaches that reintroduce antigen into a sensitized patient. Studies of the cellular and molecular mechanisms contributing to autoimmunity have identified several pathways that may be targeted directly to reduce the occurrence of autoimmunity. [7] The use of siRNA molecules represent an effective approach to target these signaling pathways and suppress an unwanted immune response. The research that follows seeks to better understand how existing antigen-specific therapies work, with the goal of improving the safety and efficacy of these therapies to facilitate their clinical translation which will help to reduce the worldwide clinical burden of autoimmune diseases.

1.2 Outline

This dissertation focuses on engineering strategies that leverage polymer nanoparticles to modulate the immune response towards tolerance. The following chapters provide background information, experimental methodology, results, conclusions, and future directions of the different strategies explored in this work. Chapters 2 and 3 contain relevant background information with regard to the immune system and biomaterials, respectively. Chapters 4 through 6 describe the completed experimental work. Chapter 7 discusses the conclusions and potential future directions revealed by the investigations herein.

Chapter 2 presents an overview of the immune system with particular focus on the steps to activate an immune response. Different hypotheses are explored with regard to the initiation of autoimmunity, followed by an evaluation of various antigen-specific treatments previously explored in research. Chapter 3 introduces biomaterials, particularly emphasizing a synthetic polymer, poly(lactic-co-glycolic acid), already used in several FDA approved drugs and medical devices. This chapter focuses on uses of this material at the nanoscale to deliver therapeutic molecules to effect disease prognosis.

Chapter 4 closely examines tolerance mechanisms triggered by treatment with antigen-conjugated nanoparticles. This investigation particularly emphasized the variables of nanoparticle dose and conjugation levels of antigen. Nanoparticle efficacy for tolerance induction was first demonstrated *in vivo* with a mouse model of multiple sclerosis administered different doses of nanoparticles with different levels of antigen conjugation. Several *in vitro* studies then examined cell signaling activities following nanoparticle internalization by antigen-presenting cells and the efficiency of antigen processing and presentation. T cells which mediate autoimmunity in this disease model were isolated and co-cultured with innate immune cells

administered nanoparticles to identify the specific antigen-specific tolerance mechanisms at work.

Chapter 5 focuses on the role of the antigen delivery vehicle for tolerance induction. Nanoparticle-mediated and cell-mediated delivery of antigen is compared with regard to activating effector T cell responses. Cell signaling pathways were inferred and constructed based on the signaling activities of innate immune cells following internalization and presentation of antigen. A small molecule inhibitor was used to reduce the activity of an important signaling molecule to validate the network and attempt to replicate tolerance mechanisms triggered by cell-mediated antigen delivery with nanoparticle-mediated antigen delivery.

Chapter 6 explores loading a bioactive molecule, siRNA, into the nanoparticle formulation to disrupt key chemokine signaling that regulates inflammatory cell migration. Several *in vitro* studies examine the intracellular nanoparticle localization, chemokine signaling, and cell migration. These nanoparticles are then used *in vivo* to test for ameliorated disease symptoms in a mouse model of multiple sclerosis.

Chapter 7 draws conclusions from the research studies conducted in this work and provides guidance in possible future lines of investigation based on the findings reported herein.

Chapter 2: The Immune System: Autoimmunity and Tolerance

2.1 The Human Immune System

A healthy human immune system functions to protect the body from harmful infection by pathogens. Cells comprising the immune system are found throughout the body, allowing for a quick response to pathogenic invasions that may occur at any time or place. Immune cells circulate throughout the body using both blood vessels of the cardiovascular system as well as lymphatic vessels of the lymphatic system. [8] Blood and lymphatic vessels connect through the spleen and lymph nodes, respectively, which serve as important locations for coordinating immune cell activity and the immune response. [9]

2.1.1 Innate and Adaptive Immunity

The immune system is quite complex, but is often organized into two major components: innate and adaptive immunity. When a pathogen breaches the body's surface barriers, it is typically met first by components of innate immunity. Innate immunity responds immediately with non-specific mechanisms to attempt to resolve the invasion. [10] The cell-mediated mechanisms of the innate response consist primarily of phagocytosis, the internalization of extracellular material that binds receptor molecules located on the phagocytic cell's surface. [11] Innate immunity also consists of a humoral-mediated mechanism that includes complement proteins and antibodies which opsonize or decorate the surface of pathogens to increase their likelihood of phagocytosis. [12]

A small number of cell types are capable of phagocytosis, including macrophages, dendritic cells, monocytes, and neutrophils. Phagocytosis internalizes extracellular material into the cell via membrane-bound cellular compartments called endosomes, or more specifically, phagosomes, the endosomes resulting specifically from phagocytosis. [11] As phagosomes are shuttled further inside the cell along the endocytic pathway, the compartmental pH decreases as enzymes are introduced and become activated to break down contents of the phagosome. [13] At the end of the pathway, phagosomes fuse with lysosomes that contain a variety of different hydrolytic enzymes to thoroughly degrade remaining materials within the phagosome.

The degradation process generates small molecular fragments, or antigens that are loaded onto major histocompatibility complex (MHC) molecules for antigen presentation at the cell surface. There are two classes of MHC molecules, including class I (MHC-I) and class II (MHC-II) molecules. MHC-I are expressed by most cell types in the body and typically associate with antigens from proteins synthesized by the cell. In contrast, MHC-II expression is primarily limited to phagocytic cells, such as macrophages and dendritic cells, also referred to as antigen-presenting cells (APCs). [14] MHC-II typically associate with antigens from proteins internalized from the extracellular space. Surface availability of MHC-restricted antigen is critical for signaling to T cells to induce adaptive immune responses.

Adaptive immunity is comprised of T cell and B cell responses that are highly efficient for pathogen elimination due to their antigen-specificity. Different T cell subsets preferentially interact with either MHC-I or MHC-II depending on surface expression of CD8 or CD4, respectively. [15] CD4+ T cells are typically associated with providing helper functions while CD8+ T cells predominantly possess a cytotoxic-suppressor phenotype. [16] CD4+ T cells help activate B cells to produce antibodies which tag pathogens using antigen specificity to facilitate

their elimination. CD8+ T cells induce cell death when cells present the specific MHC-restricted antigen.

There are two main signals provided by APCs necessary for effective CD4+ and CD8+ T cell activation. The first signal consists of MHC-restricted antigen. [17] Not all T cells can detect the MHC-restricted antigen on the APC surface. Initially, only a small number of T cells in the body express the specific T cell receptor necessary to detect a particular MHC-restricted antigen. However, upon binding its cognate antigen through the T cell receptor, T cells can rapidly proliferate to create a substantial population to detect and respond to the specific antigen. Alternatively, T cells may also enter a state of inactivity, or anergy, when their T cell receptors are engaged. [18] The T cell fate depends heavily on the presence or absence of a second signal from APCs, co-stimulatory molecules.

Interactions between co-stimulatory molecules on the APC surface and receptors on the T cell surface are critical for an effective immune response. [19] Among the most well-known interactions are those between CD80 and CD86 on the APC surface with CD28 on the T cell surface. In addition, CD40 interactions with T cells can help mature APCs to elicit stronger effector T cell responses. Without these co-stimulatory molecules, engagement of the T cell receptor complex can result in deletion or anergy of the T cell. APCs may also express negative co-stimulatory molecules, such as PD-L1, which play a major role in immune tolerance. [20]

Both macrophages and dendritic cells are capable of activating T cells, although each cell type makes contributions to different aspects of the activation process. Dendritic cells have a higher surface density of MHC-II compared to macrophages, and thus provide more of the cell-cell input signals necessary to activate CD4+ T cells. [21] Macrophages can adopt different phenotypes depending on whether they received classical activation or alternative activation

signals. The phenotype influences the signaling mediators that macrophages produce, which can either be pro-inflammatory and facilitate T cell activation or anti-inflammatory and suppress T cell activation. [22]

2.1.2 Intercellular and Intracellular Immune Signaling

Many of the immune processes mentioned above are directed and regulated by receptor-mediated signaling. Extracellular cues are first detected by cell surface receptors, which trigger a cascade of intracellular signaling activity that results in changes to cell behavior which may include increased production of signaling molecules to engage additional cells in a coordinated response. For example, the immune response is first initiated upon detection of extracellular molecules known as pathogen-associated molecular patterns (PAMPs), structures typically found only in bacteria or viruses. Most phagocytic cell types possess toll-like receptors (TLRs) which bind PAMPs, an event that triggers the propagation of signal transduction pathways leading to upregulated surface expression of co-stimulatory molecules, trafficking to the spleen or lymph nodes, and secretion of chemical mediators to promote inflammation. [23]

Cytokines are important intercellular chemical mediators, synthesized and secreted by cells to influence the behavior of their surrounding cells. Many cell types ranging from macrophages to T cells are capable of producing cytokines. While these cells may produce related cytokines to amplify a particular immune response, one cell type's cytokines may also work to inhibit the actions of other cytokines already present in the environment. [24] Cytokines can include interleukins (IL), such as IL-2 and IL-4, which promote proliferation and differentiation of T cells, respectively. Another class of cytokines is the interferons (IFN), such as IFN-γ, which activates macrophages, and along with IL-1 and IL-12, work to promote inflammation. One other

important cytokine group is the chemokines, such as CCL2, which drives inflammation by inducing cell chemotaxis.

Transcription factors (TFs) play an important role in the intracellular signaling that converts extracellular cues into the appropriate cell behavioral changes. TFs bind to gene promoter regions in the cell nucleus and recruit cellular machinery needed to initiate gene expression. TFs can be categorized by the specific DNA sequence that they bind to, and over 1,000 different TFs have been identified in humans. [25] TFs can also be characterized by signaling pathways they are involved with. Several TFs have been identified in TLR signaling pathways, including NF-KB and AP-1. The STAT family has also been identified in the IFN signaling response.

RNA interference represents a sequence-specific approach for controlling gene expression. Several molecules are capable of mediating RNA interference, one of which is short interfering RNA (siRNA). Molecules of siRNA are first formed when Dicer enzyme cleaves long double-stranded RNA or small hairpin RNAs into siRNA, which are approximately 21 to 24 base pairs in length. [26] When siRNA is in the cytosol, it can associate with RNA-induced silencing complex (RISC) and possibly other factors which then scan mRNA transcripts for sequence complementarity. When complementary mRNA sequence is detected, the RISC complex degrades the mRNA to prevent its further translation into protein and thereby inhibit gene expression. The use of siRNA to downregulate transcription factor activity has been demonstrated to attenuate cancer growth. [27]

2.2 Autoimmune Diseases

The immune system contains regulatory mechanisms to ensure its response is directed only toward pathogens, but at times, the immune system can still mistakenly attack the body's own

molecules. This undesirable response often leads to an autoimmune disease. There are over 80 identified autoimmune diseases which affect an estimated 23.5 million Americans. [28] Diseases manifest with markedly different symptoms, ranging from impaired motor function in multiple sclerosis to hypoglycemia in Type 1 diabetes, but all share the common underlying physiology of an immune response directed against molecules normally found in the body.

2.2.1 Central and Peripheral Tolerance

To limit the occurrence of autoimmunity, central tolerance is used by the immune system to remove self-reactive T cells from circulation. These self-preservation processes occur in the thymus once T cell precursors undergo genetic recombination to form their T cell receptor. [29] Many variations of the T cell receptor may result from recombination, producing cell populations with a variety of different receptors able to bind a wide range of antigens. Inevitably, recombination also produces self-reactive T cells able to cause autoimmunity, and so subsequent T cell maturation includes a two-step selection process. First, positive selection identifies T cells able to bind MHC molecules. Those that fail positive selection do not survive, ensuring that T cells respond only to antigen that is MHC-restricted. Next, negative selection is used to remove self-reactive T cells. Within the thymus, T cells are introduced to MHC molecules loaded with several different self antigens. T cells that bind any of these antigens with high affinity will undergo apoptosis. [29] While positive and negative selection reduce the likelihood of developing autoimmunity, they do not eliminate all self-reactive T cells from entering circulation, requiring additional tolerance mechanisms to suppress their activity in the periphery.

Peripheral tolerance describes mechanisms for suppressing the activity of self-reactive T cells already in circulation. One mechanism is the stringent activation threshold for T cells. Circulating self-reactive T cells must still encounter both MHC-restricted antigen and co-

stimulatory molecules on the surface of antigen-presenting cells in order to become activated. Without an infection, antigen-presenting cells are unlikely to encounter the PAMPs which trigger expression of co-stimulatory molecules. [30] Self-reactive T cells that receive only the antigen signal alone will adopt a non-responsive state of anergy. [31] Other mechanisms to suppress self-reactive T cells include production of immunosuppressive cytokines, such as IL-10 and TGF-β. [32] These cytokines are typically secreted by regulatory T cells, which are T cells that possess receptors for self antigens. But instead of producing an autoimmune response when their cognate antigen is detected, activated regulatory T cells work to suppress the immune response.

Certain tissues and organs maintain an environment biased towards immune tolerance. These regions of the body are often referred to as immune privileged sites, where foreign antigen can be introduced without provoking an immune response. Among these sites include the brain, eyes, and placenta. [33, 34] Tolerance is maintained through a combination of reduced entry for immune cells, low expression of MHC molecules, and continuous production of immunosuppressive cytokines.

2.2.2 Possible Causes of Autoimmune Diseases

While the causes of autoimmune diseases are not precisely known, several factors, including both genetic predisposition and environmental exposures have been implicated. Molecular mimicry describes one possible hypothesis that there exists a potential cross-reactivity between native and pathogenic antigens. [35] Certain pathogens are believed to possess antigens with a similar peptide sequence or structure to those found on human cells. When invaded by these pathogens, the immune system cannot distinguish the difference and will attack both sources of antigen, resulting in autoimmunity. In this case, a patient who develops an autoimmune disease due to molecular mimicry had both a genetic predisposition, with the

preexistence of a potentially cross-reactive antigen, as well as environmental exposure to the pathogen.

Epitope spreading is another hypothesis to describe the initiation of autoimmunity. When activated T cells migrate to the infection site, they destroy infected cells and release cytokines to remodel the local environment. In the process, cells in the vicinity may also suffer damage, releasing their own peptides that become internalized by phagocytes. [36] Although phagocytes routinely display native antigens loaded onto MHC molecules at the cell surface, when pathogens are present, these phagocytes will also express co-stimulatory molecules which provide the necessary signals to activate self-reactive T cells.

2.2.3 Current Treatments of Autoimmune Diseases

Autoimmune diseases are chronic conditions that lack cures, and any prescribed treatments primarily serve to manage the disease symptoms. The mechanism of action used by these treatments is typically broad and non-specific, resulting in suppression of large components of the immune system. [37] For example, corticosteroids are a powerful immunosuppressant which are administered in situations that include autoimmunity, allergy, and organ transplants. However, these types of drugs compromise the patient's immune system, often resulting in unfortunate side-effects, which can include increased susceptibility to opportunistic infections. [38]

The development of antigen-specific therapeutic strategies would be a major improvement in the treatment of autoimmune diseases. This type of approach would focus action on self-reactive T cells and the related immune components that directly contribute to autoimmunity. Although not all autoimmune diseases have a well-defined self antigen implicated for causing autoimmunity, multiple sclerosis is one disease where several myelin peptides have been

identified as the antigens. [39] Treatments currently prescribed to patients with multiple sclerosis include IFN-β and glatiramer acetate. IFN-β works non-specifically by inhibiting expression of MHC class II molecules, IL-12 production, and T cell proliferation. [40] On the other hand, glatiramer acetate is a polymer of four amino acids found in myelin. Delivered subcutaneously, this treatment is believed to activate regulatory T cells which help suppress the autoimmune response. [41] Studies comparing the two treatment courses have not found much difference in disease prognosis. [42] However, the targeted approach of glatiramer acetate may be more effective to reduce undesirable side-effects of broad immune suppression.

The efficacy of novel therapeutic approaches to treat autoimmunity are often tested using a disease model, called experimental autoimmune encephalomyelitis (EAE). EAE is a mouse model of human multiple sclerosis. Disease is established in mice by inducing an immune response against myelin antigen. [43] The immune response leads to activation and proliferation of myelin-reactive CD4+ T cells which enter the central nervous system and promote inflammation. [44] Massive infiltration of inflammatory cells results in tissue injury and paralysis.

Antigen-specific approaches to treat autoimmunity often incorporate the antigen targeted by self-reactive T cells into the therapeutic formulation. [45] There remain safety concerns surrounding the reintroduction of antigen to a patient with autoimmunity, as the immune system is already sensitized to the antigen which could potentially trigger anaphylaxis. However, one effective strategy has been to load the self antigen onto apoptotic cells using a chemical cross-linker, such as ethyl carbodiimide. [46, 47] Administering the antigen-conjugated apoptotic cell intravenously results in upregulated anti-inflammatory cytokines, negative co-stimulatory molecules, and the activity of T regulatory cells. [48] Human clinical trials have shown good

safety indications with this approach, first collecting the patient's own cells and loading with several myelin peptides before intravenously administering the modified cells back into the patient. [49] One major improvement being explored for this approach has been to use an off-the-shelf product for antigen coupling, which would eliminate the expensive and complicated step of removing cells from the patients. [50] Strategies from biomaterial engineering, such as loading antigen onto synthetic particles instead of the patient's cells may improve the ease of clinical translation for antigen-specific therapies to treat autoimmune diseases.

Chapter 3: Biomaterial Strategies for Immune Modulation

3.1 Advances in Biomaterials and Drug Delivery

A biomaterial describes any material used in the construction of medical devices. Natural materials, such as wood and metal, have functioned as biomaterials throughout history, often to replace appendages lost to disease or trauma. More recently, synthetic materials such as alloys, composites, and polymers have become the biomaterials of choice. [51] These advanced materials offer improved functionality, enabling the development of new applications, especially those occurring within the body.

One application benefitting from advancements in biomaterials is drug delivery. [52] In drug delivery, biomaterials are infused with pharmaceutical products for controlled release inside the body. Initial drug delivery formulations were developed as once-a-day tablets, which could be taken orally and used to treat chronic conditions. [53] However, larger drug molecules, such as peptides or proteins were not suitable for oral delivery, and thus required a more advanced delivery system. [54] In the 1980s, drug manufacturers found an innovative solution by encapsulating peptide within injectable microparticles made of a biodegradable and biocompatible polymer. [55] This major achievement brought widespread attention to particle-based drug delivery systems which continue to be an actively researched technology area within this field.

Over the past several years, the field of drug delivery has increasingly focused on improving the targeting of therapeutic delivery. The primary goal is to deliver therapeutic

interventions to regions of the body that require treatment, while minimizing off target effects and toxicity. Developing particles on the nanoscale has been shown to provide a certain level of specificity for nanoparticle accumulation in particular regions and cell types of the body. [56] Continued advances in the research of nanoparticle-based therapeutics has resulted in many experimental therapies currently under clinical study. [57]

3.2 Poly(lactic-co-glycolic acid) Nanoparticles

Synthetic polymers, including poly(lactic acid), poly(glycolic acid), poly(ethylene glycol), and their copolymers, are commonly used in the design of nanoparticle therapeutics. [58] One copolymer which has been successfully used in several commercially available drugs is poly(lactide-co-glycolide), or PLG. When introduced with water, PLG undergoes hydrolytic degradation, causing the copolymer to break down into its constituent monomers that are naturally found in the body. [59] The good biodegradable and biocompatible properties of PLG were likely major factors leading the Food & Drug Administration to approve PLG products for medical use in humans. [59] As such, experimental medical devices or drugs that incorporate PLG into their design may be at an advantage when seeking future regulatory approval.

3.2.1 Fabrication

The classical approach to fabricating PLG nanoparticles is the emulsification solvent evaporation technique. The process begins by dissolving polymer in organic solvent and then creating an emulsion by the addition of water and a surfactant. Sonication or homogenization of this mixture generates droplets that give rise to nanoparticles when the solvent within each droplet traverses the aqueous phase and evaporates at the emulsion-air interface. [60] This fabrication technique is often specified as single emulsion, which can produce nanoparticles that encapsulate hydrophobic molecules dissolved in the initial polymer solution. A variation of this

technique, called double emulsion, is preferable to generate nanoparticles that encapsulate hydrophilic molecules. [61] In the double emulsion procedure, an initial emulsion is formed with polymer and an aqueous solution containing dissolved hydrophilic molecules. Following sonication or homogenization, water and a surfactant are added to create a secondary emulsion and the mixture is sonicated or homogenized once more to create the final droplets that give rise to nanoparticles.

Other approaches to fabricate PLG nanoparticles include nanoprecipitation and spray-drying. Nanoprecipitation, or interfacial deposition, involves dissolving polymer and drug in organic solvent which is then added dropwise to water. [62] The resulting nanoparticles are then collected after solvent evaporation. One improvement nanoprecipitation offers over emulsion methods is the ability to produce nanoparticles without the use of surfactants which can affect biological activities and contribute to toxicity. However, nanoprecipitation is limited primarily to entrapping hydrophobic molecules. Spray drying is another fabrication technique, using hot gas to rapidly dry a liquid to form solid nanoparticles. While this approach can result in good encapsulation efficiencies of hydrophilic molecules, it has been reported to suffer from burst release, or a quick initial release of the entrapped payload, compared to a sustained release of hydrophilic molecules provided by nanoparticles made by emulsification solvent evaporation techniques. [63]

3.2.2 Degradation

The copolymer composition can be adjusted in several ways to influence the PLG degradation rate and accommodate various biomedical applications. In general, increasing the glycolic acid content and decreasing molecular weight have been reported to accelerate PLG degradation and thereby drug release. However, glycolic acid content higher than a 50:50 ratio

with lactic acid is typically not used due to the reduced solubility during synthesis and uneven molecular weight distributions that result. [64] One study of tetanus toxoid release from microspheres compared PLG containing a 50:50 monomer ratio alongside PLA containing a 100:0 ratio of lactic acid to glycolic acid. [65] At 3,000 Daltons, PLG 50:50 had released about 69% of the encapsulated payload after 30 days while PLA had only released about 28% in the same time frame. Increasing molecular weight to 100,000 Daltons, the PLG 50:50 released about 32% of the encapsulated payload after 30 days while PLA had released about 16% in the same time frame. These trends show the potential large contributions of molecular weight and monomer ratio for determining degradation rate.

Other factors reported to affect PLG degradation include environmental acidity and end group modification. [66] Studies have correlated lower pH environments with faster PLG degradation compared to neutral pH environments. After 16 weeks, PLG macroporous foams placed in acidic pH 5.0 began degrading at a faster rate than foams placed at either physiological pH 7.4 or intermediate pH 6.4. After 30 weeks, the foams at pH 6.5 and 7.4 had lost 30% of their initial mass, whereas foams at pH 5.0 had lost 90% of their initial mass. [67] Environmental pH governs the morphological changes to PLG, which may help to explain differences in the degradation rate. Degradation results in acidification of the PLG microsphere core, causing surface erosion and channel formation at physiological environments. [68] In contrast, an acidic environment has a pH balance with the PLG core, preserving the smooth microsphere structure during degradation, although it is hypothesized that monomer accumulation within microspheres resulting from insolubility at low pH leads to microsphere brittleness and fracturing. Neutralizing or capping the carboxylic acid chain ends of PLG with esters helps to extend their half-life.

When left free, polymer end chains induce autocatalysis of PLG hydrolysis to accelerate degradation.

3.2.3 Toxicity

PLG nanoparticles have good biodegradable and biocompatible properties, and investigations of their toxicity have largely concluded their safety for internal human use. Grabowski et al. [69] examined PLG nanoparticles measuring between 200 to 300 nm, fabricated with different surfactants to achieve either neutral, positively, or negatively charged nanoparticles. The cytotoxicity of A549 human lung epithelial cells was measured through mitochondrial activity and membrane integrity, which revealed good viability in response to PLG nanoparticles, especially compared to treatment with inorganic nanoparticles composed of titanium dioxide. In a separate study, Tulinska et al. [70] administered PLG nanoparticles to human peripheral blood cells and measured for changes in immune cell behavior indicative of allergy or toxicity. The studies showed PLG nanoparticles attenuated immune activity, as T cell proliferation was reduced following CD3 stimulation and lytic activity of natural killer cells decreased in the presence of tumor cells. While the reduced immune activity following nanoparticle treatment was concluded to be nanoparticle toxicity, the high cell viabilities would suggest rather that interactions between the immune system and PLG nanoparticles are favorable for applications in immune modulation.

3.3 Nanoparticles and Immune Modulation

The sub-micron size of nanoparticles enables deep tissue penetration and high rates of intracellular uptake. Further tuning of size can direct nanoparticles to accumulate in particular tissues and cells to either enhance or inhibit the immune response. [56] Additional control over interactions with the immune system can be achieved by loading nanoparticles with bioactive

molecules, such as adjuvants to stimulate an immune response or corticosteroids to suppress an immune response. [71] Controlling the immune response following nanoparticle administration is important to ensure their successful therapeutic function.

3.3.1 Nanoparticle Localization

Controlling the size of nanoparticles during the fabrication process can predictably influence their internal distribution following *in vivo* administration. One approach to adjust the size of nanoparticles made from emulsification solvent evaporation is to vary surfactant concentration. Increasing the concentration of poly(vinyl alcohol) from 0.5% (w/v) to 5.0% (w/v) helped stabilize smaller emulsion droplets, decreasing the mean particle size from 522 nm to 380 nm. [72] Similarly, the average volume of spheroids decreased from 1,000 μm^3 to 160 μm^3 as surfactant concentration increased from 1% (w/v) to 4% (w/v). [73] The higher surfactant concentration was reported to increase aqueous phase viscosity, producing greater shear forces to break down droplets into smaller structures.

Nanoparticle size plays a major role in their localization within the body. Size-dependent nanoparticle accumulation in tissues was determined by HPLC quantification 4 h following intravenous administration of polystyrene nanoparticles of varying sizes. [74] As size increased, the percent of total nanoparticle retention also increased, most dramatically in the liver, lungs, and spleen, compared to the blood, brain, and heart. Nanoparticles smaller than 100 nm more easily permeated the vasculature into the renal system and also into peripheral tissues such as the skin, muscle, and fat. In a separate study, tissues were analyzed using gel permeation chromatography following intravenous administration of 200 and 500 nm PLG nanoparticles. [75] Nanoparticle accumulation occurred primarily in the liver, spleen, and lungs, relative to the blood, brain, heart, kidneys, and stomach.

Route of administration may also play an important role to influence nanoparticle localization and disease outcome. Subcutaneous injection of PLG nanoparticles with an average size of approximately 200 nm were strongly detected in the brain, heart, kidneys, and lungs, and to a lesser extent, the liver, spleen, and lymph nodes. [76] This study was conducted in the context of experimental autoimmune encephalomyelitis (EAE), a mouse model of multiple sclerosis. Consistent abrogation of EAE disease was seen only when both disease-relevant myelin antigen and IL-10 were co-delivered in the PLG nanoparticles. Researchers have also attempted to establish EAE using dendritic cells pulsed with myelin antigen co-administered with pertussis toxin. [77] After three subcutaneous injections of dendritic cells and pertussis toxin over a period of 4 weeks, mice displayed mild EAE symptoms. However, mice receiving the same dosing regimen through intravenous or intraperitoneal injections did not develop symptoms. These studies suggest the reduced efficacy of establishing tolerance via the subcutaneous route, especially compared to intravenous or intraperitoneal administration.

3.3.2 Post-Internalization Cell Response

The tissues in which intravenously administered nanoparticles accumulate contain an abundance of immune cells, such as macrophages and dendritic cells. These cells are quick to internalize nanoparticles and reshape the local immune environment. Macrophages efficiently internalized PLG nanoparticles with approximate diameter of 389 nm compared to microparticles with approximate dimeter of 6.5 μm. [78] The secretion of IL-1β and TNF-α were significantly lower in nanoparticle-treated compared to microparticle-treated macrophages, and nuclear translocation of NF-KB was also significantly reduced. Dendritic cells were able to internalize PLG nanoparticles with average diameter of 280 nm resulting in little effect on the

expression of CD40, CD86, or MHC-II molecules. [79] These observations of cell behavior following internalization suggest the nanoparticle vehicle is relatively inert.

Incorporating bioactive molecules into the nanoparticles can further modulate the immune response. While molecules activating the immune system are not explored in the work that follows, a class of molecules called, toll-like receptor agonists have previously been loaded into PLG nanoparticles to stimulate immune responses in applications such as vaccines. [80] But rather, we focus here on immune suppressing molecules, such as IL-10 and rapamycin. It was previously mentioned that IL-10 encapsulation with antigen delivery resulted in better abrogation of EAE. [76] It has also been demonstrated that the presence of rapamycin further suppresses the immune response and abrogates EAE clinical score. [79, 81] Oligonucleotides, such as siRNA, have also shown therapeutic potential when encapsulated and delivered within nanoparticles for immune suppression. [82] These aforementioned studies reporting immune suppression or tolerance induction mediated by PLG nanoparticles are of great interest for further investigation with regards to immune mechanisms and nanoparticle formulations to provide better targeting and specificity over current approaches to treat autoimmune diseases.

The following chapters discuss research studies that examined and engineered the mechanisms of action used by antigen-coupled nanoparticles for immune tolerance. Antigen-coupled PLG nanoparticles have been effective for reducing the occurrence of EAE symptoms which are mediated by CD4+ T cells. Thus, assays were conducted to determine the impact of nanoparticle treatment on the CD4+ T cell response. Dynamic measurement of intracellular signaling activity following APC internalization of antigen-coupled PLG nanoparticles were compared to intracellular signaling activity following APC internalization of antigen-coupled cells. Similarities in intracellular signaling activity suggested a common mechanism between

nanoparticle processing and cell clearance. Differences in intracellular signaling activity would suggest possible signaling molecules to inhibit during nanoparticle treatment to better mimic cell clearance responses which suppress immune activity. The feasibility of encapsulating inhibitory molecules within PLG nanoparticles was explored using CCR2-targeting siRNA. These loaded nanoparticles were administered in vitro and in vivo to evaluate their inhibitory effects on inflammation and autoimmunity.

Chapter 4: Peptide-Conjugated Nanoparticles Reduce Positive Co-Stimulatory Expression and T Cell Activity to Induce Tolerance

4.1 Abstract

Targeted approaches to treat autoimmune diseases would improve upon current therapies that broadly suppress the immune system and lead to detrimental side-effects. Antigen-specific tolerance was induced using poly(lactide-co-glycolide) nanoparticles conjugated with disease-relevant antigen to treat a model of multiple sclerosis. Increasing the nanoparticle dose and amount of conjugated antigen both resulted in more durable immune tolerance. To identify active tolerance mechanisms, we investigated downstream cellular and molecular events following nanoparticle internalization by antigen-presenting cells. The initial cell response to nanoparticles indicated suppression of inflammatory signaling pathways. Direct and functional measurement of surface MHC-restricted antigen showed positive correlation with both increasing particle dose from 1 to 100 μg/mL and increasing peptide conjugation by two-fold. Co-stimulatory analysis of cells expressing MHC-restricted antigen revealed most significant decreases in positive co-stimulatory molecules (CD86, CD80, and CD40) following high doses of nanoparticles with higher peptide conjugation while expression of a negative co-stimulatory molecule (PD-L1) remained high. T cells isolated from mice immunized against myelin proteolipid protein ($PLP_{139-151}$) were co-cultured with antigen-presenting cells administered $PLP_{139-151}$-conjugated nanoparticles, which resulted in reduced T cell proliferation, increased T cell apoptosis, and a

stronger anti-inflammatory response. These findings indicate several potential mechanisms used by peptide-conjugated nanoparticles to induce antigen-specific tolerance.

4.2 Introduction

Aberrant T cell recognition of host antigen can trigger an immune response resulting in autoimmune diseases, such as multiple sclerosis. Patients with multiple sclerosis are often administered immunomodulatory and immunosuppressive drugs, such as interferon beta and cyclophosphamide. These therapies act broadly on the entire immune system with the unfortunate side effect of high infection rates. [83, 84] However, targeted therapeutic approaches that are antigen-specific would focus action on immune cells involved in disease and preserve the remainder of the immune system to maintain immune competency. Multiple sclerosis is modeled in mice using experimental autoimmune encephalomyelitis (EAE), wherein autoreactive CD4+ T cells recognize and respond to myelin epitopes. [43, 85] Following activation and proliferation, these T cells migrate to the central nervous system (CNS) and initiate inflammation, causing large influxes of immune cells that demyelinate axons, resulting in the observable loss of sensorimotor functions. Strategies to attenuate disease and establish durable immune tolerance focus on suppression of the activated autoreactive T cells.[86]

Induction of an antigen-specific immune response is relatively complex, involving the interaction of multiple cell types. T cells first become activated based on signals received from antigen-presenting cells (APCs). [87] Consisting primarily of macrophages (MΦs) and dendritic cells (DCs), APCs internalize and digest proteins from the extracellular space, [80] generating peptides, or antigens that are preferentially loaded onto class II molecules of major histocompatibility complex (MHC) molecules for surface display. Antigen loaded onto MHC-II molecules is recognized only by CD4+ T cells that express the specific receptor. [18] The

number of T cells able to recognize a particular antigen is initially low. To shift the immune response, T cells specific for the particular antigen receive activation signals from co-stimulatory ligands which include CD80 and CD86 expressed by APCs. [19] CD40 interactions with T cells can also mature APCs to elicit stronger effector T cell responses. [88] Engagement of only the T cell receptor complex without co-stimulation results in a state of T cell unresponsiveness. APCs may also express negative co-stimulatory molecules, such as PD-L1, or anti-inflammatory cytokines, such as IL-10 which have been shown to be critical for immune tolerance. [20, 48]

Antigen-conjugated polymeric nanoparticles, such as those made with the biodegradable and biocompatible material, poly(lactide-co-glycolide) (PLG), have demonstrated the ability to induce immune tolerance in models of autoimmunity, allergic responses, and cell transplantation. [50, 81, 89] Intravenously delivered fluorescent PLG nanoparticles co-localized with MARCO-positive and SIGN-R1-positive cells in the liver and spleen, suggesting selective uptake by APCs. Autoreactive T cells were reported to undergo apoptosis, anergy, and suppression by regulatory T cells [50] and the importance of IL-10 and PD-L1 for immune tolerance was established by several studies. [48, 90, 91] However, the fate of delivered antigen, the efficiency of antigen processing and T cell signaling, and the impact of antigen conjugation levels and nanoparticle dose remain key factors to be investigated.

In this chapter, we investigate cellular and molecular tolerance mechanisms resulting from antigen-conjugated nanoparticle treatment. Initially, *in vivo* studies were performed to correlate amounts of antigen conjugation and nanoparticle dose with the severity of EAE disease course. Subsequently, several *in vitro* assays were used to investigate key steps including cell signaling upon internalization, MHC-restricted antigen presentation, and co-stimulatory expression. Tolerance induction was then evaluated by co-culturing nanoparticle-treated antigen-presenting

cells with autoreactive T cells. These studies provide mechanistic insights to assist in the development of nanoparticle-based therapeutics.

4.3 Materials and Methods

4.3.1 PLG nanoparticle synthesis and characterization

PLG nanoparticles were prepared using a single emulsion-solvent evaporation method as previously described. [92] Briefly, PLG purchased from Lactel Absorbable Polymers (Birmingham, AL) was dissolved at 20% (w/v) in dichloromethane. Poly(ethylene-alt-maleic acid) (PEMA) was purchased from Polysciences, Inc. (Warrington, PA) and reconstituted in water at 1% (w/v). Sonicating a mixture of the PLG and PEMA produced nanoparticles, which following solvent evaporation, were washed three times and finally lyophilized in a solution of 4% w/v sucrose and 3% w/v D-mannitol. Nanoparticle size and ζ-potential were measured using a Zetasizer Nano ZSP from Malvern Instruments Ltd (Worcestershire, UK).

4.3.2 Conjugation of antigen or fluorophore onto PLG nanoparticles

$PLP_{139-151}$ and Ea_{52-68} were purchased from Genscript (Piscataway, NJ) and $OVA_{323-339}$ was purchased from Celtek Peptides (Franklin, TN). FITC-cadaverine was purchased from Thermo Fisher Scientific (Waltham, MA). Lyophilized PLG nanoparticles were washed three times using phosphate-buffered solution (PBS) at pH 7.4. Approximately 4 mg of PLG nanoparticles was recovered and activated using 1-ethyl-3-(3-dimethylaminopropyl) carbodiimide (EDC), purchased from Sigma-Aldrich (St. Louis, MO), at 16 mg/mL. Peptide or fluorophore was immediately added at the appropriate concentration to achieve desired higher or lower conjugation levels. The coupling reaction proceeded for 1 h under constant agitation. Uncoupled peptide was removed with three PBS washes. Total peptide conjugation was measured using the Micro BCA Protein Assay Kit manufactured by Pierce Biotechnology (Rockford, IL).

4.3.3 Mice

Female 6 to 8 week old SJL/J mice were purchased from the Jackson Laboratory (Bar Harbor, ME) and Envigo (Indianapolis, IN). Female 6 to 8 week old C57BL/6 mice were purchased from Charles River Laboratories (Wilminton, MA). OT-II mice, transgenic for a TCR specific to $OVA_{323-339}$, were purchased from the Jackson Laboratory and subsequently bred in-house. All experiments involving mice were approved by the University of Michigan Committee on the Use and Care of Animals.

4.3.4 EAE initiation and nanoparticle tolerance induction

EAE disease was initiated as described previously.[85] Briefly, SJL/J mice were injected subcutaneously with an emulsion of $PLP_{139-151}$ in complete Freund's adjuvant. To induce tolerance, a single dose of either PLG-PLP-Hi or PLG-PLP-Lo was administered intravenously 7 d after disease initiation. The control group was administered a single dose of PLG-OVA-Hi. Behavioral testing of mice was performed daily to determine clinical score, based on a 0-5 scale as follows: 0, healthy; 1, limp tail; 2, limp tail and impaired righting reflex; 3, hind-limp weakness; 4, hind-limb paralysis; and 5, moribund.

4.3.5 Harvesting and culturing of APCs

To obtain a primary population of APCs, bone marrow was harvested from the femurs and tibias of mice and differentiated in vitro. Cells were cultured in RPMI 1640 supplemented with 10% FBS, 4mM L-glutamine, and 1% penicillin/streptomycin, all purchased from Life Technologies (Carlsbad, CA). Culturing media was further supplemented with either 20% L929 conditioned media to obtain macrophages, or with 50 μM of 2-mercaptoethanol (Sigma-Aldrich, St. Louis, MO) and 20 ng/mL of GM-CSF purchased from PeproTech (Rocky Hill, NJ) to obtain dendritic cells. Media was replaced at 3 days and 6 days after initial culture. On Day 8,

macrophages were removed using Versene treatment and dendritic cells were obtained from suspension. APCs were seeded between 2.0 x 10^5 to 2.5 x 10^5 cells/mL in either 24-well untreated flat bottom cell culture plates or 96-well treated round bottom cell culture plates. APCs were activated with lipopolysaccharide (LPS) at 100 ng/mL to improve cell viability.

4.3.6 Internalization assays

Quenching of extracellular FITC was validated using APCs from C57BL/6 mice that were pre-treated for 30 minutes with 20 μg/mL of cytochalasin D, purchased from Life Technologies (Carlsbad, CA). PLG-FITC was administered to APCs at 1, 10, or 100 μg/mL. At several time intervals, APCs were collected. Following PBS wash, trypan blue was added at 1.2 mg/mL to quench extracellular FITC molecules. Fluorescence was measured using a CyAn ADP Analyzer manufactured by Beckman Coulter (Brea, CA), and data was analyzed using FlowJo v10. Cellular events were gated using forward scatter and side scatter. FMO controls were then used to identify cells with positive signal.

4.3.7 Cell signaling analysis of transcription factor activity

The reporter library consisted of lentiviral constructs, each with a consensus binding sequence for a specific transcription factor driving expression of the firefly luciferase reporter. The process of identifying consensus binding sequences and determining reporter specificity has been described previously.[93] APCs were batch transduced with a single lentiviral reporter and seeded in black 96-well plates for a minimum of 48 hours. Cultures were replaced with fresh media containing LPS to improve cell viability, and D-luciferin purchased from Perkin Elmer (Waltham, MA). Cells were treated with either soluble antigen or peptide-conjugated nanoparticles and bioluminescence measurements were acquired at 2.5, 5, 8, 19, 24, and 28 h

post-treatment. A minimum of four technical repeats was used per treatment group for each lentiviral reporter, and experiments were repeated two to three times.

4.3.8 Measuring antigen presentation and co-stimulation

APCs from C57BL/6 mice were cultured in 24-well flat bottom plates were administered PLG-Eα-Hi or PLG-Eα-Lo at 1, 10, or 100 μg/mL. After 24h, APCs were collected and Fc receptors blocked with TruStain fcX, purchased from BioLegend (San Diego, CA). To detect antigen presentation, APCs were stained with αI-Ab-Ea52-68-FITC (clone eBioY-Ae) purchased from eBioscience (San Diego, CA). Simultaneously, co-stimulatory expression was measured by staining with αPD-L1-Brilliant Violet 421 (clone 10F.9G2), αCD80-phycoerythrin (PE) (clone 16-10A1), αCD86-PE/Cy5 (clone GL-1), and αCD40-PE/Cy7, all purchased from BioLegend (San Diego, CA). Cell identity was confirmed through staining with αF4/80-APC-eFluor 780 (clone BM8) or αCD11c-APC-eFluor 780, both purchased from eBioscience (San Diego, CA). Viability was confirmed using Annexin V-Pacific Blue, purchased from BioLegend (San Diego, CA). Fluorescence signal was measured and analyzed similarly to the internalization assays.

4.3.9 T cell co-cultures with nanoparticle-treated APCs

T cells were obtained from murine spleen and lymph nodes (axillary, inguinal, brachial) using MACS LS columns. Naïve T cells were purified from OT-II mice using the Naïve CD4+ T Cell Isolation Kit and autoreactive T cells were purified from SJL/J mice 7 days following EAE disease initiation using the CD4+ T Cell Isolation Kit, both manufactured by Miltenyi Biotec (San Diego, CA).

Purified T cells were stained for 10 min at 37°C with 2.5 μM carboxyfluorescein succinimidyl ester (CFSE) purchased from Life Technologies (Carlsbad, CA). The staining was

immediately quenched with APC culturing media, supplemented with 1x non-essential amino acids, 1 mM sodium pyruvate, and 50 μM 2-mercaptoethanol.

Before the addition of T cells, APCs were activated with 100ng/mL of LPS for improved viability and seeded in 96-well round bottom plates. Following 24h of either soluble peptide or nanoparticle treatment, culture media was replaced with fresh media containing CFSE-stained T cells at a 2:1 ratio of T cells to APCs. After 3 to 5 days, T cells were collected to measure CFSE fluorescence signal.

Naïve T cells from OT-II mice were used for functional detection of antigen presentation following nanoparticle internalization. These T cells were co-cultured 3 days with APCs isolated from healthy C57BL/6 mice. Autoreactive T cells from EAE-immunized SJL/J mice were used to examine for tolerance induction. These T cells were co-cultured 5 days with APCs isolated from healthy SJL/J mice. Apoptosis was detected using Annexin V staining. Cytokine concentrations in the culture media were analyzed using ELISA kits from R&D Systems (Minneapolis, MN).

4.3.10 Statistical analyses

Comparisons between EAE disease courses of different treatment groups were analyzed by a Mann-Whitney test. Determination of transcription factors whose activities were significantly different due to nanoparticle-mediated rather than soluble antigen delivery was assessed for each measured time point by fitting normalized transcription factor activities to an empirical hierarchical Bayesian linear model using limma [94] independently for each biological repeat. Significant differences in co-stimulatory expression, T cell proliferation and apoptosis, and cytokine levels were identified using either a 1-way or 2-way ANOVA followed by the Tukey test for multiple comparisons.

4.4 Results

4.4.1 Peptide-conjugated PLG nanoparticles induce antigen-specific immune tolerance

PLG nanoparticles were manufactured using an emulsion process and subsequently evaluated for size and charge. The average diameter was 538 ± 21 nm and average ζ-potential was −43 ± 8 mV. Following peptide conjugation, nanoparticles showed an increase in size relative to unmodified nanoparticles, suggesting the development of some nanoparticle aggregates. No major impacts on zeta potential was observed. Peptides of myelin proteolipid protein ($PLP_{139-151}$), ovalbumin ($OVA_{323-339}$), and I-Eα ($E\alpha_{52-68}$) were chemically conjugated at multiple concentrations to yield two types of nanoparticles for each antigen, one with higher and one with lower levels of peptide as summarized in **Table 4.1**. The EAE disease model and in vitro studies of cells isolated from this model employed nanoparticles conjugated with $PLP_{139-151}$ and $OVA_{323-339}$. Nanoparticles conjugated with $E\alpha_{52-68}$ and $OVA_{323-339}$ were used for in vitro mechanistic studies to examine antigen processing and presentation.

Intravenous administration of a single 1.25 mg dose of PLG nanoparticles with higher conjugation of disease-relevant $PLP_{139-151}$ (PLG-PLP-Hi) significantly reduced clinical score during the course of relapse-remitting EAE compared to PLG nanoparticles conjugated with disease-irrelevant $OVA_{323-339}$ (PLG-OVA-Hi) which resulted in severe acute disease. (**Fig 4.1a**) Administering a single 2.0 mg dose of PLG nanoparticles with lower conjugation levels of $PLP_{139-151}$ (PLG-PLP-Lo) had strong knock-down of clinical scores early, but resulted in moderate clinical scores later in the disease course. (**Fig 4.1b**) Interestingly, administering a single 2.0 mg dose of PLG-PLP-Hi led to durable immune tolerance throughout the disease course, suggesting the importance of both total peptide and total administered dose of nanoparticles for induction of immune tolerance.

Table 4.1 Amount of peptide conjugated to PLG nanoparticles.

	Peptide Conjugation [μg/mg of PLG]
PLG-$OVA_{323-339}$-Hi	14.4 ± 1.7
PLG-$OVA_{323-339}$-Lo	7.6 ± 0.5
PLG-$PLP_{139-151}$-Hi	9.8 ± 2.5
PLG-$PLP_{139-151}$-Lo	4.1 ± 0.7
PLG-$E\alpha_{52-68}$-Hi	17.8 ± 2.0
PLG-$E\alpha_{52-68}$-Lo	9.8 ± 0.8

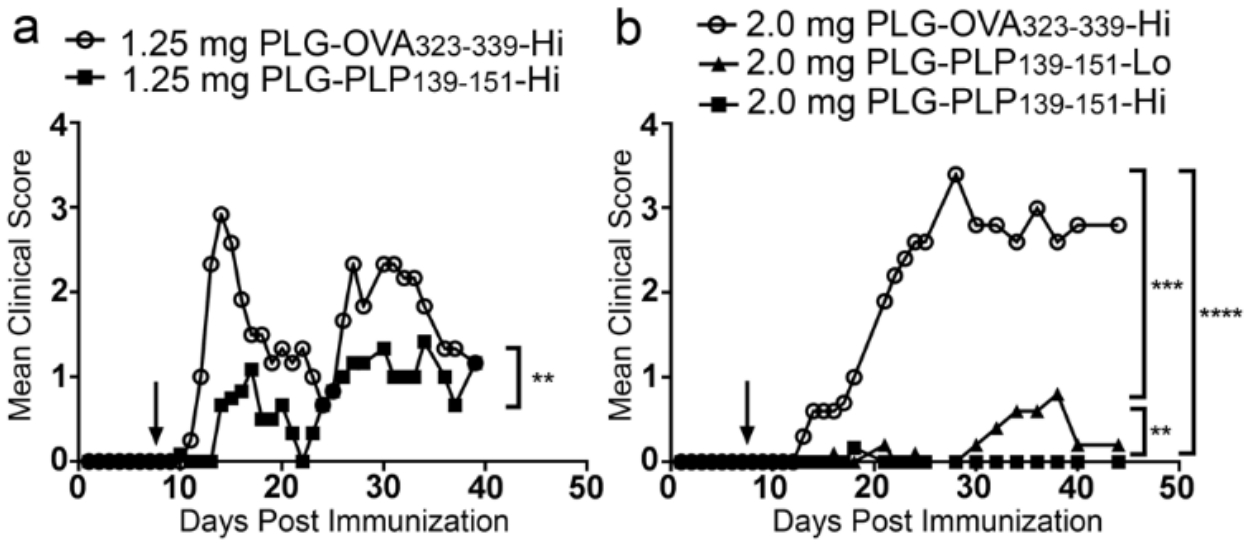

Figure 4.1 Peptide-conjugated nanoparticles induce antigen-specific tolerance to prevent EAE. Daily assessment of disease symptoms using mean clinical score following immunization against $PLP_{139-151}$ to induce EAE disease. (**a**) SJL/J mice intravenously administered 1.25 mg of peptide-conjugated PLG nanoparticles. Mice treated with PLG-PLP-Hi had significant reduction of clinical scores compared to mice treated with PLG-OVA-Hi. (**b**) SJL/J mice intravenously administered 2.0 mg of peptide-conjugated PLG nanoparticles. Mice treated with either PLG-PLP-Hi or PLG-PLP-Lo both had significantly lower scores compared to mice treated with PLG-OVA-Hi. Additionally, scores of mice treated with PLG-PLP-Hi were significantly lower than those of mice treated with PLG-PLP-Lo (**$p < 0.01$, ***$p < 0.001$, ****$p < 0.0001$, Mann-Whitney test). Each group had 5-6 mice and was representative of three separate experiments. Arrow indicates administration of peptide-conjugated PLG nanoparticles at day 7.

4.4.2 Cell signaling response following nanoparticle internalization

Nanoparticle internalization, a pre-requisite for antigen processing and presentation, was examined by administering PLG nanoparticles conjugated with fluorescein (PLG-FITC) to APCs for 24 h. Both MΦs and DCs exhibited high levels of fluorescence following quenching of extracellular fluorophores, indicating large amounts of nanoparticle internalization. (**Figs 4.2a, b**) To further confirm nanoparticle internalization, MΦs and DCs were treated with cytochalasin D to restrict cell internalization. Following treatment with PLG-FITC and quenching, these cells had low fluorescence signal, similar to that of untreated cells.

The internalization kinetics were measured following treatment with a range of PLG-FITC doses. At a low dose of PLG-FITC (1 μg/mL), the percentage of APCs with nanoparticle internalization increased at a steady rate over 24h. Higher doses of PLG-FITC, at 10 and 100 μg/mL, caused the percentage of APCs with nanoparticle internalization to increase exponentially within a few hours of treatment and level off by 24h. (**Figs 4.2c, d**) MΦs showed a moderate advantage over DCs in their internalization of PLG nanoparticles independent of dose administered.

The quantity of nanoparticles internalized per cell was evaluated using mean fluorescent intensity (MFI). After 24h of PLG-FITC treatment at 1, 10, or 100 μg/mL, the MFI of MΦs was 34.1 ± 2.3, 112.5 ± 13.1, or 301.7 ± 27.8, respectively. The MFI of DCs under the same dosing regimen yielded MFI values of 37.0 ± 3.8, 141.9 ± 36.9, or 268.3 ± 9.3. (**Figs 4.2e, f**) Overall, these studies indicated a strong correlation between the nanoparticle dose and the quantity of internalized nanoparticles. Taken together, these results indicate that MΦs and DCs had similar phagocytic capacity for internalizing PLG nanoparticles.

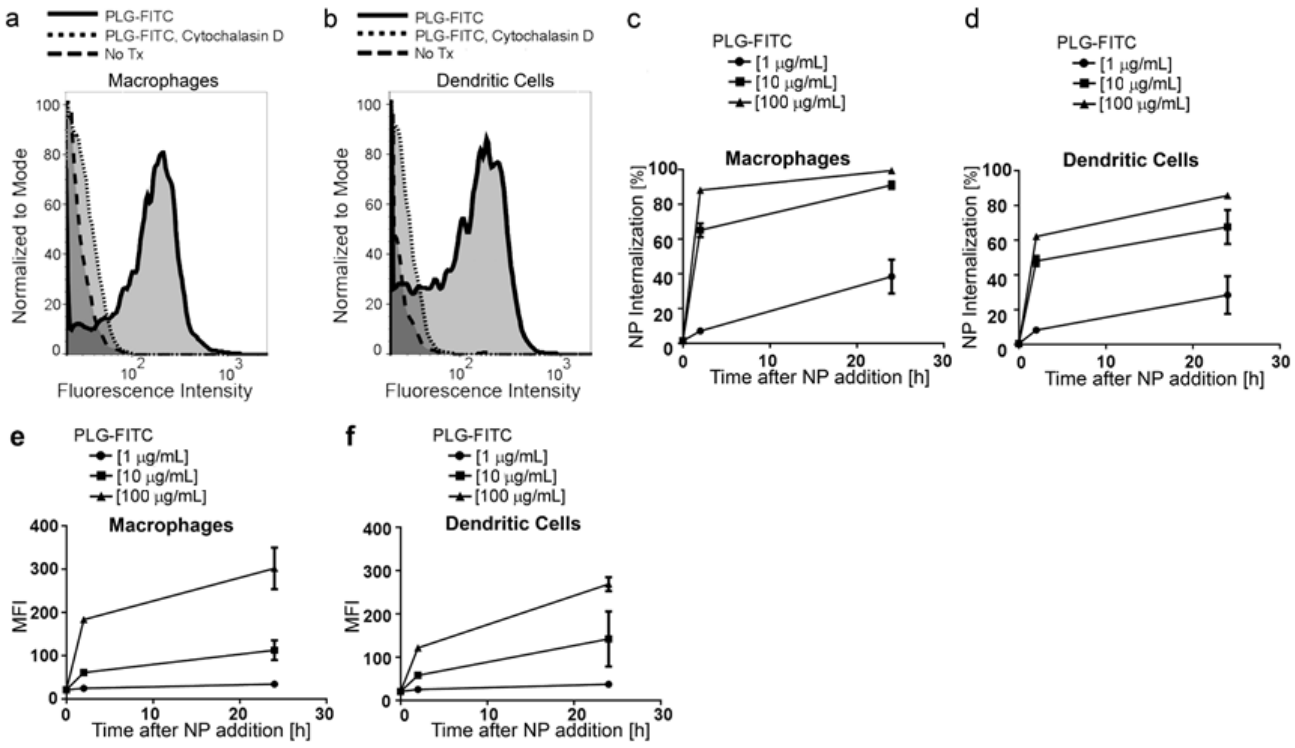

Figure 4.2 Macrophages and dendritic cells rapidly internalize PLG nanoparticles. Antigen-presenting cells administered PLG nanoparticles surface-conjugated with fluorescein (FITC). Extracellular fluorescence was quenched using trypan blue before flow cytometry analysis. (**a, b**) High fluorescence intensity was observed in cells 24 h after PLG-FITC treatment. Cells administered PLG-FITC in the presence of cytochalasin D had low fluorescence intensity, equivalent to the intensity of cells not administered PLG-FITC. **(c, d)** The percentage of cells with detectable nanoparticle internalization and (**e, f**) the mean fluorescence intensity after 2 and 24h of treatment with 1, 10, or 100 μg/mL of PLG-FITC. Macrophages in **a, c, e** and dendritic cells in **b, d, f**. Data show averages of three measurements ± standard error of mean (SEM).

Dynamic activity profiles of immune-related transcription factor activity were used to identify signaling pathways activated for delivery of $OVA_{323-339}$ antigen by nanoparticles relative to soluble peptide. The activity of 14 transcription factors was analyzed using a TRanscriptional Activity CEll aRray (TRACER). Several members of the signal transducer and activator of transcription (STAT) family were examined, which showed PLG-OVA treatment significantly decreased STAT-1 activity in DCs and significantly increased STAT-3 activity relative to soluble $OVA_{323-339}$ treatment in both cell types. (**Fig 4.3a-d**)The decrease in STAT-1 activity correlates with less signaling through the IFN-γ receptor, while the increase in STAT-3 activity indicates higher IL-10 receptor activity. Further transcription factor analysis included AP-1, NF-KB, and RUNX1, all of which had increased activity in both cell types in response to PLG-OVA compared to soluble $OVA_{323-339}$ treatment. (**Fig 4.3e-j**) The activity changes in these factors suggest increased cell differentiation and activation.

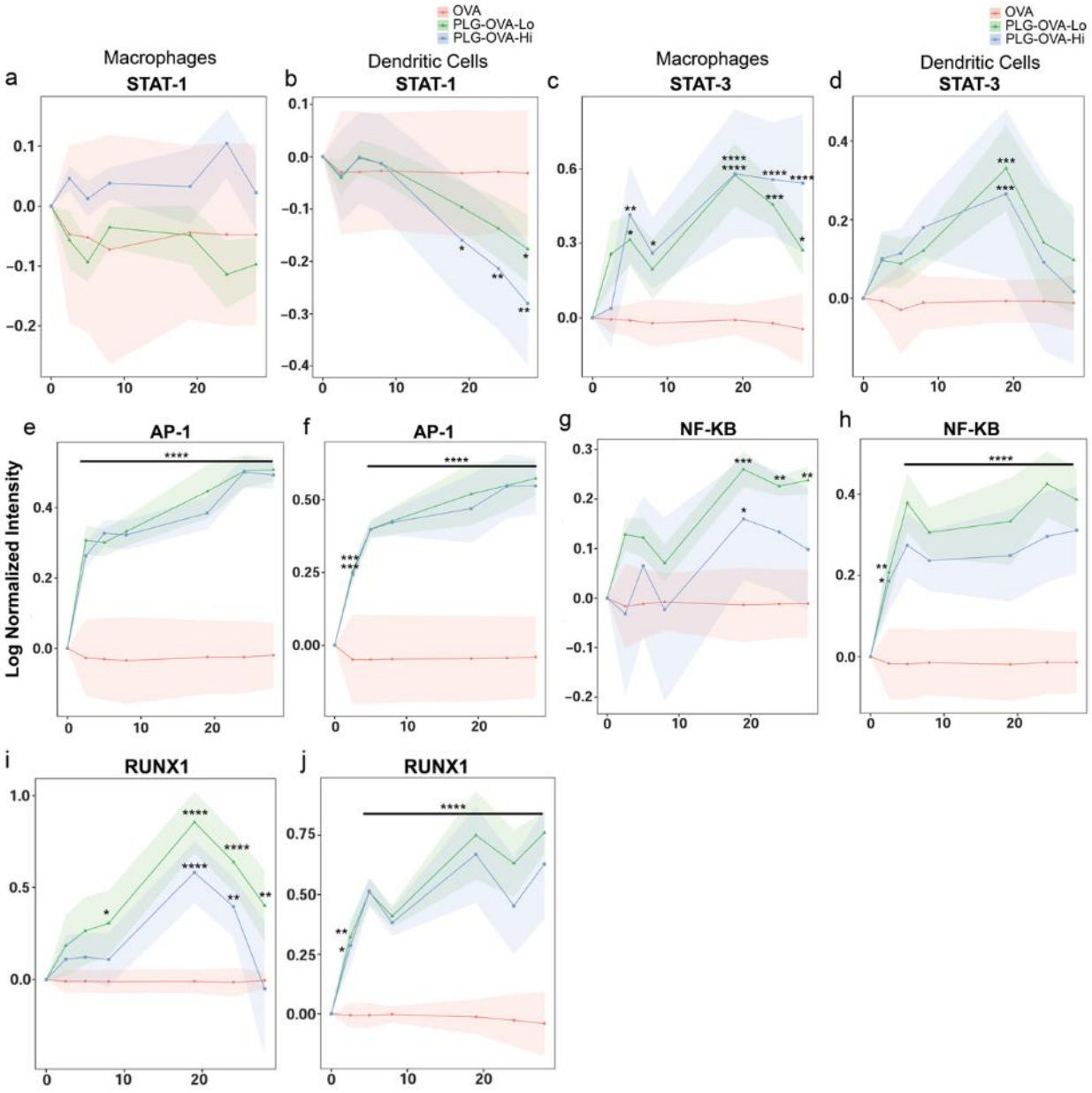

Figure 4.3 Cell signaling activity following soluble or nanoparticle-mediated antigen delivery. Dynamic activity of several transcription factors in the hours following APC treatment with either nanoparticle-conjugated (PLG-OVA-Lo or PLG-OVA-Hi) or soluble $OVA_{323-339}$. (**a, b**) STAT-1 activity did not change in MΦs, but significantly decreased in DCs at later time points following treatment with nanoparticle-conjugated $OVA_{323-339}$. (**c, d**) STAT-3 significantly increased in both MΦs and DCs administered nanoparticle-conjugated $OVA_{323-339}$. (**e-j**) AP-1, NF-KB, and RUNX1 were all significantly increased following treatment with nanoparticle-conjugated compared to soluble treatment of $OVA_{323-339}$. Macrophages in **a, c, e, g** and dendritic cells in **b, d, f, h**. Data show averages of four measurements ± standard error of mean (SEM).

4.4.3 Peptide-conjugated nanoparticles deliver functional antigen to APCs

Functional availability of surface MHC-restricted antigen for T cell signaling was measured by co-culturing nanoparticle-treated APCs with naïve CD4+ T cells specific for $OVA_{323-339}$. Activated MΦs and DCs were administered 100 μg/mL of blank or antigen-conjugated nanoparticles, or an equivalent dose of soluble $OVA_{323-339}$. The percentage of T cells undergoing proliferation was negligible in all conditions involving co-culture with MΦs. (**Fig 4.4a**) T cells co-cultured with untreated DCs or DCs administered PLG nanoparticles also had negligible proliferation. (**Fig 4.4b**) However, administering soluble $OVA_{323-339}$ resulted in 89.2% of T cells dividing, while administering PLG-OVA-Lo or PLG-OVA-Hi resulted in 94.9% or 94.5% of T cells dividing, respectively. These results demonstrated the efficacy of antigen delivery from PLG nanoparticles to trigger a T cell response, as well as the greater potency of DCs compared to MΦs for signaling to T cells.

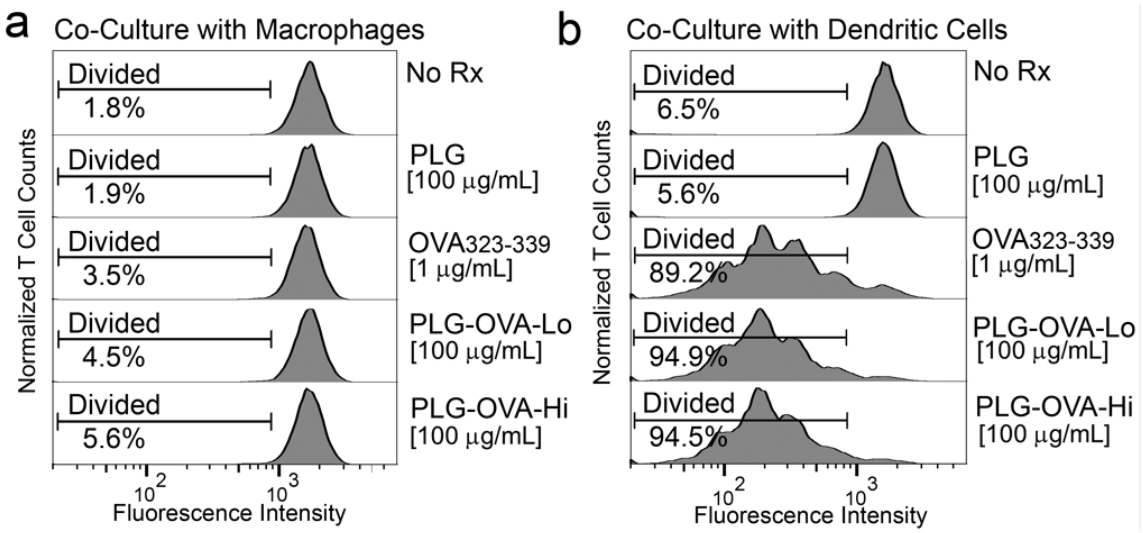

Figure 4.4 T cell signaling potential of macrophages and dendritic cells. T cell proliferation following 3d of co-culturing naïve T cells, isolated from OT-II transgenic mice, with (**a**) macrophages or (**b**) dendritic cells pre-treated 24h with either soluble $OVA_{323-339}$, blank nanoparticles, or nanoparticles conjugated with high or low levels of $OVA_{323-339}$. Data is representative of three separate experiments.

We subsequently used a peptide of I-Eα ($E\alpha_{52\text{-}68}$) to examine the APC surface for MHC-restricted antigen. Similar to both $OVA_{323\text{-}339}$ and $PLP_{139\text{-}151}$, $E\alpha_{52\text{-}68}$ forms complexes with MHC class II molecules for presentation on the APC surface to CD4+ T cells. The advantage of $E\alpha_{52\text{-}68}$ is the availability of a monoclonal antibody (Y-Ae) that only binds $E\alpha_{52\text{-}68}$ when complexed to MHC, allowing identification of cell subpopulations participating in antigen presentation.[95] Detection of surface MHC-restricted antigen was dose-dependent with the administered amount of either free peptide or peptide-conjugated nanoparticle. After soluble $E\alpha_{52\text{-}68}$ was administered at 0.1, 1, or 10 μg/mL for 24 h, the MΦ percentages with detectable MHC-restricted antigen were 0.9 ± 0.1%, 1.4 ± 0.1%, and 1.1 ± 0.1%, and the corresponding DC percentages were 0.6 ± 0.1%, 2.7 ± 0.1%, and 15.1 ± 0.1%. (**Figs 4.5a, b**) These results reflect a positive correlation between amount of antigen administered and antigen presentation levels. When PLG-Eα-Lo was administered at 1, 10 or 100 μg/mL, the MΦ percentages with detectable MHC-restricted antigen were 1.3 ± 0.1%, 1.8 ± 0.1, and 3.8 ± 0.3% and the corresponding DC percentages were 0.4 ± 0.1%, 1.8 ± 0.2%, and 19.4 ± 1.0%. (**Figs 4.5c, d**) Administering PLG-Eα-Hi at the same doses as PLG-Eα-Lo, MΦ percentages with detectable MHC-restricted antigen were 1.3 ± 0.1%, 2.0 ± 0.1%, and 7.1 ± 0.4%. (**Fig 4.5e**) Similarly, DC percentages were 0.8 ± 0.1%, 3.2 ± 0.1%, and 24.9 ± 1.4%. (**Fig 4.5f**) Both nanoparticle dose and levels of antigen conjugation to nanoparticles correlated with the percentage of cells with detectable MHC-restricted antigen. Although similar amounts of PLG-FITC was internalized among the APCs as seen in **Figure 4.2**, DCs were more efficient than MΦs for antigen processing and presentation. Moreover, comparing similar total quantities of antigen delivery, nanoparticle-mediated antigen delivery resulted in higher cell percentages of antigen presentation relative to soluble antigen delivery.

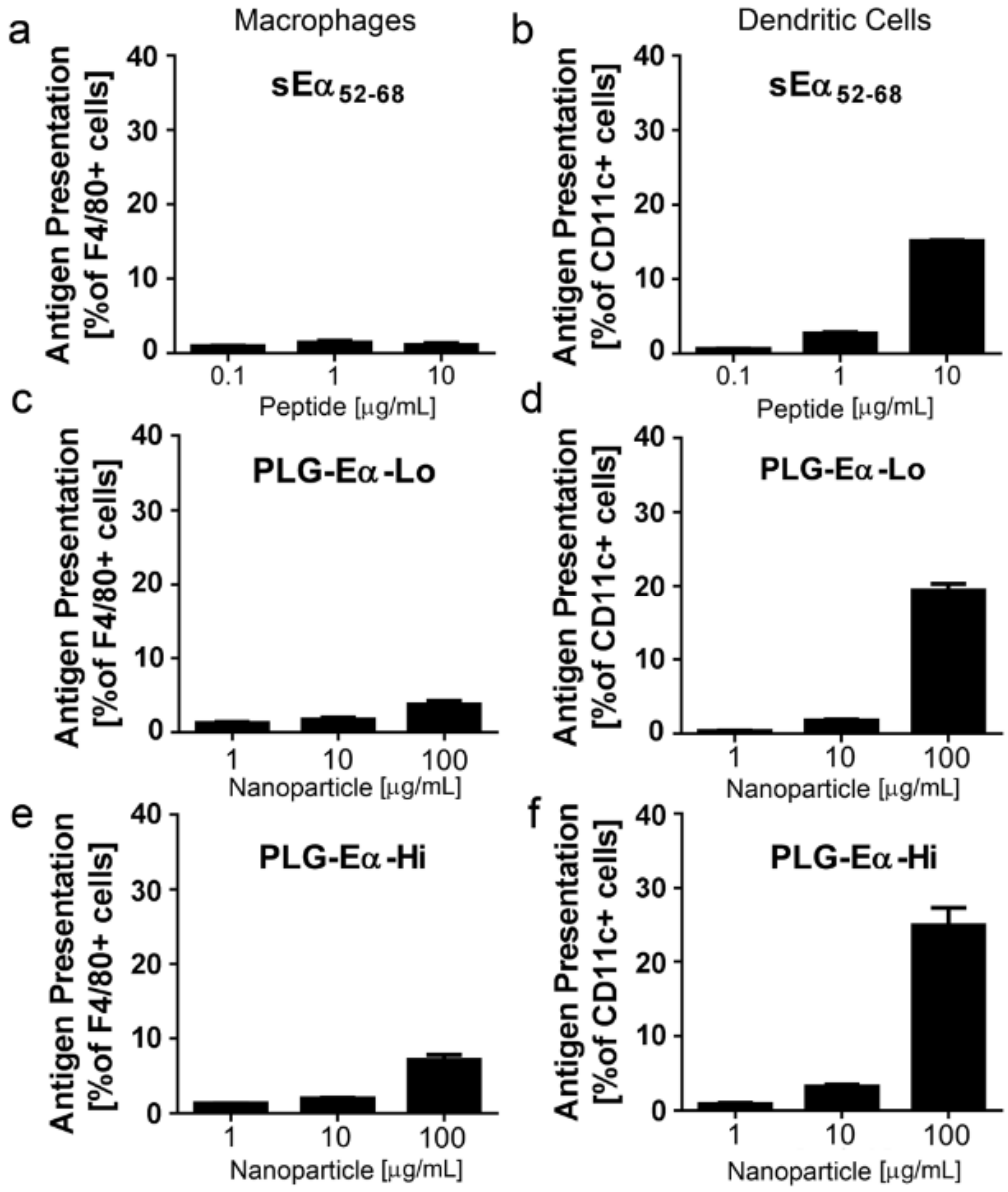

Figure 4.5. Dose-dependent correlation between antigen delivered and cell surface antigen presentation. Percentage of cells with detectable $E\alpha_{52\text{-}68}$ loaded on major histocompatibility complex (MHC) class II molecules after 24h of treatment with (**a, b**) 0.1, 1, or 10 μg/mL of soluble $E\alpha_{52\text{-}68}$, (**c, d**) 1, 10, or 100 μg/mL of PLG-Eα-Lo, or (**e, f**) 1, 10, or 100 μg/mL of PLG-Eα-Hi. Macrophages in **a, c, e** and dendritic cells in **b, d, f**. Data show averages of three measurements ± standard error of mean (SEM).

4.4.4 Reduced APC expression of positive co-stimulatory molecules

APC expression of CD86, CD80, CD40, and PD-L1, co-stimulatory molecules influencing the T cell response, were evaluated alongside antigen presentation. The ability to identify APC subpopulations expressing MHC-restricted $E\alpha_{52\text{-}68}$ enabled focusing analysis on cells exhibiting antigen presentation and thereby capable of signaling to T cells. Soluble $E\alpha_{52\text{-}68}$ administered at increasing doses to MΦs resulted in no significant changes to co-stimulatory expression. However, DCs exhibited a modest, but significant increase in the percentage of CD86-positive cells when the dose of soluble $E\alpha_{52\text{-}68}$ increased from 0.1 to 10 μg/mL. (**Figs 4.6a-b**)

Treatment with peptide-conjugated nanoparticles had a more noticeable effect on APC co-stimulatory expression. PLG-Eα-Lo administered at 100 μg/mL to MΦs significantly reduced CD86 and CD80 expression compared to their levels at either 1 or 10 μg/mL. (**Fig 4.6c**) However, PLG-Eα-Lo treatment did not significantly affect co-stimulatory expression in DCs. (**Fig 4.6d**) Interestingly, PLG-Eα-Hi elicited more significant reduction of co-stimulatory molecules at lower doses than PLG-Eα-Lo. Among MΦs, PLG-Eα-Hi reduced CD86 and CD80 expression at 10 μg/mL compared to their levels at 1 μg/mL, and again at 100 μg/mL compared to their levels at both 1 and 10 μg/mL. (**Fig 4.6e**) Among DCs, administering PLG-Eα-Hi significantly reduced CD86 at 10 and 100 μg/mL compared to their levels at 1 μg/mL, although a significant increase in CD86 occurred between 10 μg/mL and 100 μg/mL. (**Fig 4.6f**) Additionally, PLG-Eα-Hi resulted in significant reduction of CD80 between 10 and 100 μg/mL compared to its levels at 1 μg/mL. Further, PLG-Eα-Hi reduced CD40 levels at 100 μg/mL compared to its levels at 1 and 10 μg/mL. Expression of the negative co-stimulatory molecule PD-L1 was unchanged in all treatment conditions. Nanoparticle doses exceeding 100 μg/mL resulted in reduced APC viability and thus were not studied further.

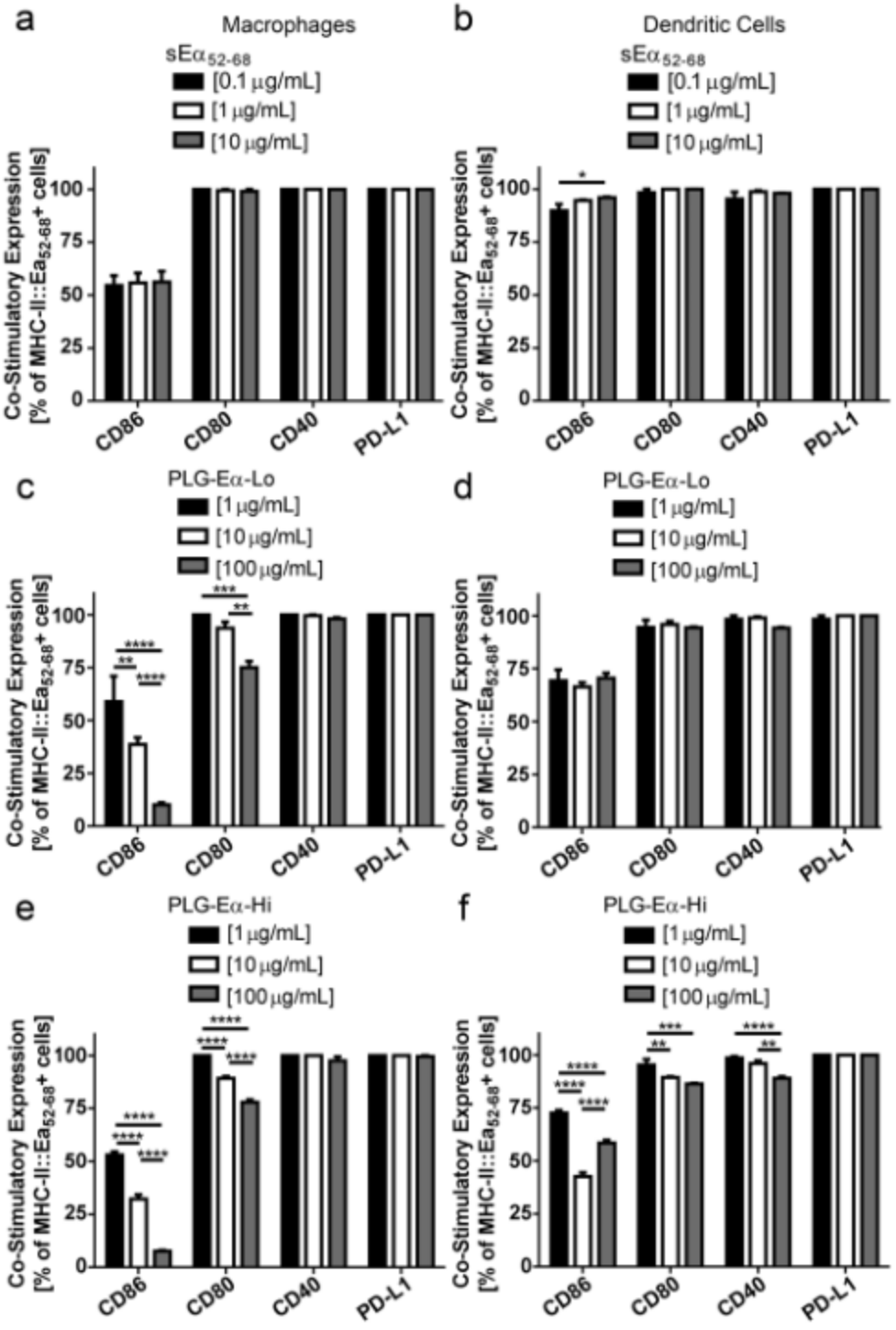

Figure 4.6 Effects of peptide-conjugated nanoparticles on expression of cell surface molecules. (**a, b**) Increasing the dose of soluble $E\alpha_{52\text{-}68}$ from 0.1 to 10 μg/mL had no detectable changes in MΦs, but a significant increase of CD86 was detected in DCs. (**c, d**) Higher doses of PLG-Eα-Lo significantly lower percentages of cells expressing CD86 and CD80 in MΦs compared to lower doses, but there were no significant differences in DCs. (**e**) Higher doses of PLG-Eα-Hi also led to significantly lower percentages of MΦs expressing CD86 and CD80

compared to lower doses. (**f**) Among DCs, higher doses of PLG-Eα-Hi resulted in significantly lower cell percentages expressing CD86, CD80, and CD40. No significant changes to PD-L1 were detected following a dose increase of any treatment condition tested. (*$p < 0.05$, **$p < 0.01$, ***$p < 0.001$, ****$p < 0.0001$, 2-way ANOVA followed by the Tukey test for multiple comparisons). Macrophages in **a, c, e** and dendritic cells in **b, d, f**. Data show averages of three measurements ± standard error of mean (SEM).

Collectively, these observations indicate that nanoparticle-mediated antigen delivery, particularly at the greater antigen loading (PLG-Eα-Hi), reduced expression levels of positive co-stimulatory molecules involved in activating T cell effector responses. When $E\alpha_{52\text{-}68}$ was administered directly to APCs, the subpopulations expressing MHC-restricted antigen showed no changes in co-stimulatory expression, even as the peptide dose was increased. However, the percentage of cells expressing positive co-stimulatory expression decreased with higher doses of peptide-conjugated nanoparticles, suggesting a critical role for nanoparticle-mediated peptide delivery to reduce APC co-stimulation. Notably, the trends in co-stimulatory expression following antigen-conjugated PLG nanoparticle administration were observed only on the cell subpopulations expressing antigen identified through the use of $E\alpha_{52\text{-}68}$ and the corresponding Y-Ae antibody.

4.4.5 Proliferation, apoptosis, and cytokine levels in co-cultures with T cells

T cell activity was examined following isolation from mice immunized against $PLP_{139\text{-}151}$ and subsequent co-culture with nanoparticle-treated APCs. T cells co-cultured with MΦs administered 100 μg/mL of either PLG-PLP-Lo or PLG-PLP-Hi had reduced levels of proliferation compared to untreated MΦs. No significant changes in proliferation were measured in T cells co-cultured with MΦs administered soluble $PLP_{139\text{-}151}$ or unmodified PLG compared to untreated MΦs. (**Fig 4.7a**) T cells co-cultured with DCs administered either $PLP_{139\text{-}151}$, unmodified PLG, PLG-PLP-Lo, or PLG-PLP-Hi had similar levels of proliferation as T cells co-cultured with untreated DCs. (**Fig 4.7b**) Levels of interleukin-10 (IL-10), an anti-inflammatory cytokine, were undetectable among T cells co-cultured with MΦs regardless of the treatment. (**Fig 4.7c**) However, levels of IL-10 significantly increased among T cells co-cultured with DCs treated with PLG or PLG-OVA-Hi compared to treatment with $PLP_{139\text{-}151}$. The IL-10 levels were

more significantly increased among T cells co-cultured with DCs administered PLG conjugated with disease-relevant antigen (PLG-PLP-Hi and PLG-PLP-Lo) compared to T cells co-cultured with DCs administered $PLP_{139-151}$. (**Fig 4.7d**).

T cell fate following co-culture with DCs was further evaluated for apoptosis. The percentage of T cells undergoing apoptosis did not significantly change when co-cultured with DCs administered increasing doses of PLG-PLP-Lo (**Fig 4.8a**). However, treatment with increasing doses of PLG-PLP-Hi resulted in a significant increase in T cell apoptosis at 100 μg/mL compared to 1 μg/mL of PLG-PLP-Hi. (**Fig 4.8b**). Results of the T cell co-culture studies suggest different tolerance mechanisms, which include proliferation, apoptosis, and cytokine production, used by MΦs and DCs to attenuate the activity of T cells contributing to EAE disease course.

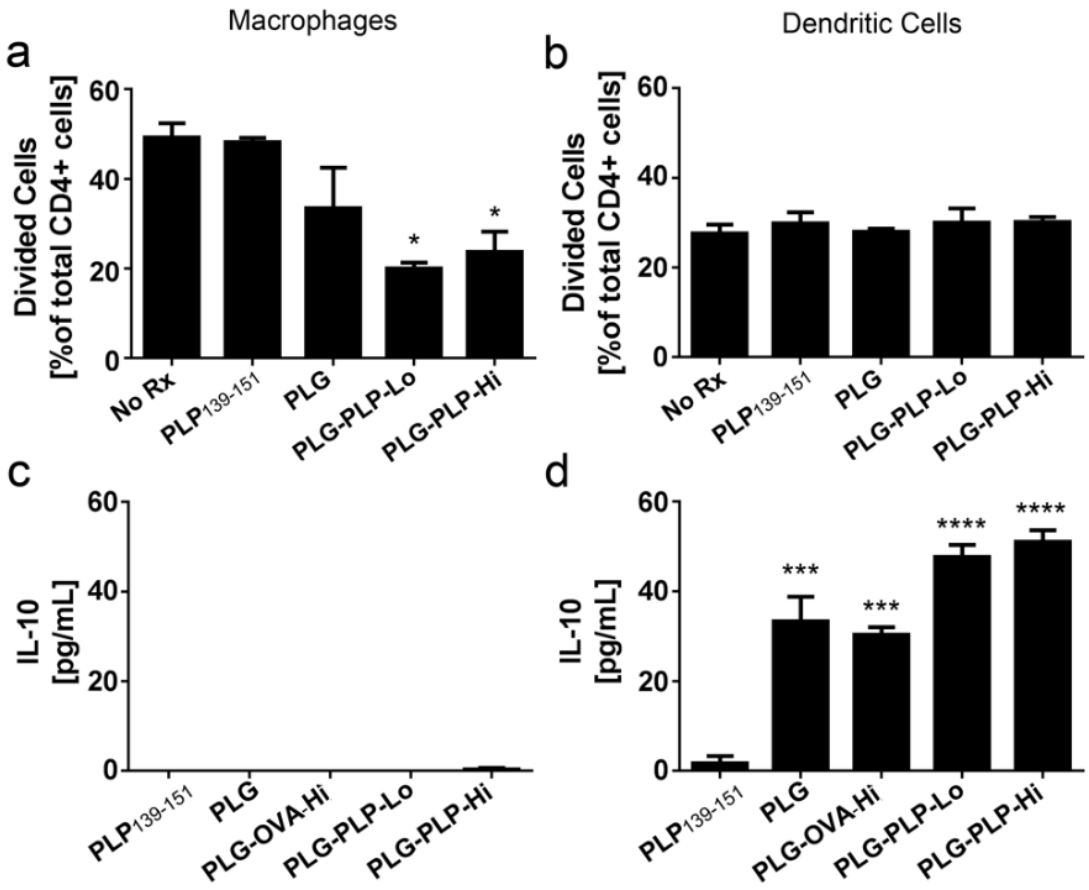

Figure 4.7 Changes in T cell proliferation and anti-inflammatory cytokine expression. (**a**) T cells isolated from mice immunized against $PLP_{139-151}$ had significantly reduced proliferation following 5 d of co-culture with MΦs administered 100 μg/mL of either PLG-PLP-Hi or PLG-PLP-Lo compared to MΦs administered no treatment. (**b**) T cell proliferation was not significantly changed in co-culture with DCs administered either soluble antigen or nanoparticle treatment. (**c**) IL-10 was largely undetectable in T cell co-cultures with MΦs. (**d**) T cells co-cultured with DCs treated with nanoparticles had significant increases of IL-10 compared to DCs administered soluble $PLP_{139-151}$. The increase of IL-10 was more significant when DCs were treated with nanoparticles conjugated with $PLP_{139-151}$, the T cell-specific antigen. (*$p < 0.05$, ***$p < 0.001$, ****$p < 0.0001$, 1-way ANOVA followed by the Tukey test for multiple comparisons) Data show averages of two to three measurements ± standard error of mean (SEM).

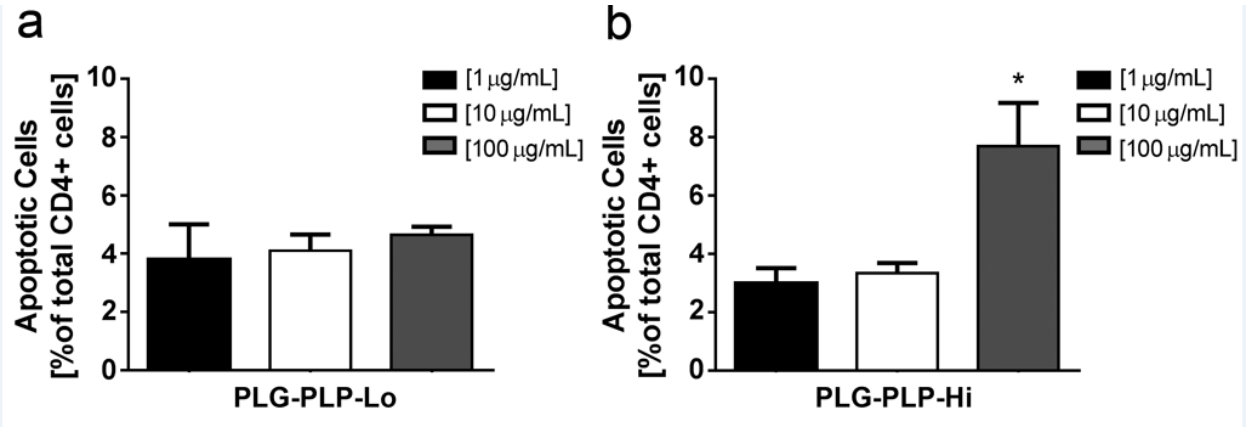

Figure 4.8 Effects of nanoparticle dose and antigen conjugation levels on T cell apoptosis. T cells isolated from mice immunized against $PLP_{139-151}$ and co-cultured 5 d with DCs administered (**a**) PLG-PLP-Lo or (**b**) PLG-PLP-Hi. Increasing the nanoparticle dose of PLG-PLP-Lo had no significant difference in the percentage of T cells with positive Annexin V staining, indicating apoptosis. However, increasing the nanoparticle dose of PLG-PLP-Hi from 1 to 100 μg/mL resulted in significant increase of the percentage of T cells with positive Annexin V staining. Data show averages of two to three measurements ± standard error of mean (SEM). (*$p < 0.05$, 1-way ANOVA followed by the Tukey test for multiple comparisons).

4.5 Discussion

Peptide-conjugated nanoparticles have been used by several groups to prevent or treat EAE via a targeted, antigen-specific approach.[76, 81, 92] Consistent with these reports, herein, we found nanoparticles conjugated with disease-relevant peptide ($PLP_{139-151}$) significantly improved EAE prognosis compared to nanoparticles conjugated with disease-irrelevant peptide ($OVA_{323-339}$). Our low nanoparticle dose (1.25 mg) did not provide the complete knock-down of EAE disease score as was seen with the high nanoparticle dose (2.0 mg). We further explored the impact of antigen conjugation levels, observing EAE relapse in later stages of the disease course following treatment with PLG-PLP-Lo. This relapse was abrogated by treatment with PLG-PLP-Hi, which contained approximately twice the amount of $PLP_{139-151}$. EAE relapses have been reported to result from epitope spreading, when the immune system recognizes an increasing set of myelin epitopes. [96, 97] Previous comparisons of CNS cell populations following treatment with PLG-PLP for EAE showed a reduction of total lymphocytes, total APCs, MΦs, and DCs relative to treatment with PLG-OVA.[92] It is likely the tolerance induction by PLG-PLP-Hi was more effective to curtail the immune response during early stages of EAE compared to PLG-PLP-Lo, which prevented the generation of epitope spreading and the subsequent relapse.

Many differences in transcription factor activity were detected between APCs administered soluble antigen and APCs administered antigen-conjugated nanoparticles. We examined several members of the STAT protein family, which play major roles in immune regulation. [98] STAT-1 activation is well-known for mediating interferon signaling to promote inflammation, while STAT3 has been reported to negatively regulate interferon responses. [99] We observed a decrease in STAT-1 activity along with an increase of STAT-3 activity, suggesting cell internalization of antigen conjugated to nanoparticles suppressed interferon-related cell

signaling. We also examined the activity of RUNX1 which synergizes with C/EBPβ and PU.1 to drive expression of microRNA-142 which regulates immunity. [100] However, when innate immune receptors such as TLR4 are triggered, AP-1 and NF-KB activity increases and negatively regulate microRNA-142 expression. We hypothesize that the higher intensity of RUNX1 detected would suggest a compensatory response of APCs to the AP-1 and NF-KB activity resulting from nanoparticle treatment. However, the complex interplay of intracellular immune signaling pathways will require further investigation to identify those pathways driving the phenotypic response.

Both MΦs and DCs internalized large amounts of nanoparticles, yet DCs showed much higher efficiency for antigen presentation. Additionally, when equivalent amounts of total antigen was delivered, higher levels of antigen presentation were detected on cells administered nanoparticles relative to soluble treatment. DCs have a reputation as the primary APCs for T cell signaling, due to DCs having a higher surface density of MHC-II molecules compared to MΦs. [21] Peptide-MHC complexes on the cell surface are crucial for signaling to T cells,[101] which may explain the high rates of naïve T cell proliferation observed in co-cultures with DCs not seen in co-cultures with MΦs. The studies with $E\alpha_{52\text{-}68}$ revealed lower percentages of APCs with detectable MHC-restricted antigen presentation compared to PLG-Eα treatments that delivered similar amounts of antigen. Moreover, nearly every cell internalized nanoparticles, but only a portion had detectable levels of antigen presentation. Studies of class I presentation have also reported low efficiency for antigen presentation wherein a 100-fold increase in the quantity of antigen delivered resulted in a less than two-fold increase of antigen presentation.[102] The class I and class II presentation pathways differ primarily by whether antigen escapes the endosome into the cytosol, or remains within the endosome until reaching the lysosome. Interestingly, using

a reducible chemical bond to link antigen with polymer nanoparticles resulted in a significant increase in class I antigen presentation compared to using a non-reducible bond.[103] Therefore tuning the linker strength between the antigen and polymer may have implications to augment class II presentation from nanoparticles.

Co-culturing autoreactive T cells with nanoparticle-treated APCs resulted in several indications of immune suppression. The onset of EAE occurs via autoreactive T cells producing large amounts of pro-inflammatory cytokines, including IFNγ.[104] However, EAE disease course can be tempered by the stimulated production or addition of IL-10.[76, 105] Administering either PLG-PLP-Hi or PLG-PLP-Lo to APCs likely resulted in reduced expression of co-stimulatory molecules as seen with administering PLG-Eα-Lo and PLG-Eα-Hi. When these APCs were co-cultured with autoreactive T cells, the presence of antigen without co-stimulation caused T cells to enter a state of unresponsiveness.[106] We detected this state by an absence of T cell proliferation and increase in T cell apoptosis. The increases in IL-10 concentration further suggest the activation of tolerance signaling pathways.

Collectively, these results identify cell types and mechanisms contributing to antigen-specific tolerance in animal models of R-EAE following nanoparticle treatment. We correlated the delivery of antigen-conjugated nanoparticles with surface levels of class II antigen presentation, expression of positive and negative co-stimulatory factors, and subsequent T cell proliferation or apoptosis. Furthermore, the assays used herein provide useful tools to evaluate the efficiency of nanoparticle designs for antigen delivery, APC phenotype shifting, and T cell activation, which may be useful to identify future formulations with greater potential to induce antigen-specific immune tolerance.

Chapter 5: The Role of NF-KB Signaling Due to Antigen-Coupled Nanoparticles or Cells Administered for Antigen-Specific T Cell Tolerance

5.1 Abstract

Reintroducing self-reactive antigen coupled to an antigen delivery vehicle has been shown to induce rapid and long-lived immune tolerance in models of autoimmune diseases. Several platforms have emerged as antigen delivery vehicles, including donor cells and synthetic nanoparticles. Both types of vehicles coupled with $OVA_{323-339}$ antigen were administered to antigen-presenting cells prior to co-culture with $OVA_{323-339}$-specific T cells. Macrophages were not sensitive to vehicle type, however, treating dendritic cells with antigen-coupled splenocytes (SP-OVA) reduced T cell proliferation and expression of IL-2Rα while enhancing T cell apoptosis and expression of L-selectin, indicators of tolerance. Inhibiting NF-KB signaling activity in macrophages led to major changes in the T cell response, but NF-KB disruption in dendritic cells had minimal effects. Signaling activity in antigen-presenting cells following antigen delivery was measured using TRanscriptional Activity CEll aRray (TRACER). Network analysis showed NF-KB played a critical role for maintaining network connectivity in macrophages. Moreover, the activity of transcription factors, PPAR and CEBP, were shown to be highly interconnected following treatment with SP-OVA which suggests their activity may provide more efficient induction of T cell tolerance.

5.2 Introduction

Self-reactive T cells that respond to autoantigens are normally found in the healthy T cell repertoire. Stringent T cell activation barriers are typically sufficient to maintain tolerance, but autoimmunity may still occur in instances such as following an infection that introduces pathogenic antigen cross-reactive with autoantigens. [107, 108] Activated T cells can be characterized by rapid proliferation, high expression of CD25 (IL-2Rα chain), and low expression of CD62L (L-selectin). [109] Cytokine expression is also an important indicator of T cell response, as increased GM-CSF levels have been implicated in T cell-mediated autoimmune pathogenesis, while IL-10 secretion assists in suppressing autoimmune responses. [32, 110]

Typical autoimmune treatments have focused on global immune suppression, however the harmful side effects from disrupting immune competency has provided strong motivation for developing antigen-specific interventions. These approaches involve reintroducing an autoantigen in such a way that skews the immune response against the autoantigen towards tolerance. [111] One of the earliest antigen-specific approaches developed was hyposensitization therapy to bring about allergen desensitization. [112] Low doses of allergen were subcutaneously injected directly into the patient, and over time, the dose was slowly increased. While effective, the extended treatment window and risk for anaphylaxis limited its clinical adoption.

The use of delivery vehicles to reintroduce autoantigens has been effective to induce rapid and long-lived immune tolerance. One type of vehicle is a donor cell, such as splenocytes, onto which autoantigens have been attached via chemical coupling which has induced tolerance in models of autoimmunity, allergy, and transplant rejection. [113] Another form of antigen delivery vehicle is a synthetic nanoparticle. Nanoparticles represent a versatile platform that can be modified in size and shape to target specific tissues and cell types. Functional groups on the

nanoparticle surface also allow for autoantigen attachment via chemical coupling and these antigen-coupled nanoparticles have also induced tolerance in models of autoimmunity. [4]

Both cell- and nanoparticle-mediated antigen delivery have demonstrated ability to induce tolerance, but direct comparisons of their mechanisms of action have yet to be explored. To effect tolerance induction, donor cells represent a more desirable delivery vehicle, as the immune system has many inherent homeostatic strategies to recognize cells and suppress an immune response. [114] The advantage of nanoparticles as a delivery vehicle is their ease of synthesis and storage. However, as a relatively inert platform, nanoparticles likely function primarily as an antigen depot, engaging tolerance mechanisms limited in scope to the antigen presentation process.

The following investigation applies an *in vitro* model of T cell activation to examine the impact of different vehicles for delivering antigen and inducing tolerance. Antigen-coupled cells (SP-OVA) or nanoparticles (PLG-OVA) are administered to antigen-presenting cells (APCs), either macrophages or dendritic cells, prior to their co-culture with activated T cells. Following co-culture, the T cell response is analyzed and the co-culture environment is profiled for cytokine expression. Using TRanscriptional Activity CEll aRray (TRACER), we measure the activity of immune-related transcription factors in APCs following antigen treatment. The results are used to construct networks that infer interactions among the transcription factors measured. Comparing the network activity of cells following antigen delivery will reveal common or distinct signaling pathways activated by the different vehicles that contribute to tolerance induction.

5.3 Materials and Methods

5.3.1 Mice

Female 6 to 12 week old C57BL/6 mice were purchased from Charles River Laboratories (Wilminton, MA). OT-II mice, transgenic for a TCR specific to $OVA_{323-339}$, were purchased from the Jackson Laboratory and subsequently bred in-house. All experiments involving mice were approved by the University of Michigan Committee on the Use and Care of Animals.

5.3.2 Preparation of donor splenocytes

Spleens from healthy C57BL/6 mice were harvested and passed through a 100 μm nylon membrane to generate a single cell suspension. After RBC lysis, cells were washed with phosphate buffer solution (PBS) and reconstituted at 3.2 $x10^6$ cells/mL. 1-ethyl-3-(3-dimethylaminopropyl) carbodiimide and $OVA_{323-339}$ were added at final concentrations of 30 mg/mL and 1 mg/mL, respectively. Chemical reaction proceeded for 1 h at 4°C under constant agitation. Cells were then washed three times with PBS and filtered through a 70 μm nylon membrane.

5.3.3 Preparation of nanoparticles

PLG nanoparticles were prepared using a single emulsion-solvent evaporation method as previously described. [92] Briefly, PLG purchased from Lactel Absorbable Polymers (Birmingham, AL) was dissolved at 20% (w/v) in dichloromethane. Poly(ethylene-alt-maleic acid) (PEMA) was purchased from Polysciences, Inc. (Warrington, PA) and reconstituted in water at 1% (w/v). Sonicating a mixture of the PLG and PEMA produced nanoparticles, which following solvent evaporation, were washed three times and finally lyophilized in a solution of 4% w/v sucrose and 3% w/v D-mannitol. Nanoparticle size and ζ-potential were measured using a Zetasizer Nano ZSP from Malvern Instruments Ltd (Worcestershire, UK).

Lyophilized PLG nanoparticles were washed three times using PBS. Approximately 4 mg of PLG nanoparticles was recovered and activated using 1-ethyl-3-(3-dimethylaminopropyl) carbodiimide (EDC) at 16 mg/mL. $OVA_{323-339}$ was immediately added at 1 mg/mL. The coupling reaction proceeded for 1 h under constant agitation. Uncoupled peptide was removed with three PBS washes.

5.3.4 T cell co-cultures with pre-treated APCs

A primary population of macrophages and dendritic cells was obtained as described previously. [90, 115] Briefly, bone marrow was harvested from femurs and tibias of C57BL/6 mice and differentiated *in vitro*. Between 8 to 10 days following harvest, cells were seeded at approximately 2.5 x 10^5 cells/mL in 60 mm untreated dishes and activated with lipopolysaccharide (LPS) at 100 ng/mL. The next day, cells were treated with 10 μg/mL of free peptide, 100 μg/mL of peptide-conjugated nanoparticles, or a 5:1 ratio of peptide-conjugated splenocytes to cells for 24 h before co-culturing with naïve T cells. BAY 11-7085, a small molecule targeting NF-KB activity was purchased from Cayman Chemical (Ann Arbor, MI) and used at 50 μM.

Naïve T cells were obtained from spleen and lymph nodes (axillary and inguinal) of OT-II mice using the Naïve CD4+ T Cell Isolation Kit, according to manufacturer specifications (Miltenyi Biotec, San Diego, CA). Purified T cells were stained with carboxyfluorescein succinimidyl ester (CFSE) purchased from Life Technologies (Carlsbad, CA) and mixed at a 2:1 ratio with either macrophages or dendritic cells in RPMI 1640 supplemented with 10% FBS, 4mM L-glutamine, 1x non-essential amino acids, 1 mM sodium pyruvate, and 50 μM 2-mercaptoethanol. Cells were seeded at 6.0 x 10^5 cells/mL in 24-well plates pre-treated for 2 h with αCD3 (10 ng/mL) and αCD28 (2 ng/mL).

Cells were collected after 4 days of culture for flow analysis. Fc receptors were first blocked with TruStain fcX before staining with L-selectin-APC, IL-2Rα-PE, and CD4-APC-eFluor 780 (eBioscience). Viability was measured using Annexin V-Pacific Blue. Except when indicated, all flow antibodies were purchased from BioLegend (San Diego, CA). Fluorescence signal was measured using a CyAn ADP Analyzer manufactured by Beckman Coulter (Brea, CA), and data was analyzed using FlowJo v10. Cellular events were gated using forward scatter and side scatter. FMO controls were then used to identify cells with positive signal. Cytokine concentrations in the culture media were analyzed using ELISA kits from R&D Systems (Minneapolis, MN).

5.3.5 TRACER experiments

Cells were aliquoted for separate batch infection with each lentiviral reporter. One μL of virus at approximately 1 x 10^9 IU/mL was administered per 25,000 cells. Cell and virus mixtures were seeded into black 96-well plates at 2.5 x 10^6 cells/mL and cultured for at least 48 h. Fresh media was replaced containing 1 mM D-luciferin (Perkin Elmer) and 100 ng/mL lipopolysaccharide (Sigma). Bioluminescence measurements were acquired at 2.5, 5, 8, 18, 24, and 27 h post-seeding using an IVIS Lumina LTE camera system (Perkin Elmer, Waltham, MA, USA). A minimum of three technical repeats was performed for each reporter.

5.3.6 Network analysis

Network analysis of TRACER measurements was performed using NTRACER, as described previously. [93] Briefly, normalized activity measurements were mean centered and an initial net topology was inferred using several linear and non-linear techniques. The network architecture was optimized with CellNOptR and a total of 500 runs was performed. Edge significance was determined by comparing the number of edge occurrences in the 500 optimized

networks to 500 networks generated from permutation samples from the same data. Significance was determined by a p-value of 10^{-6}. Features were selected from the top 10% of significant edges at each set of time points to ensure high-quality edge selection. Networks were visualized using the R package, iGraph.

5.4 Results

5.4.1 Antibody stimulation activates T cells in co-culture with treated APCs

Macrophages administered different treatments were subsequently co-cultured with naïve T cells isolated from OT-II mice. In the absence of stimulating antibodies (αCD3 and αCD28), T cells had low expression levels of IL-2Rα, an activation marker, and high levels of L-selectin, an inactivation marker following co-culture with untreated macrophages. (**Fig 1a, b**) The presence of stimulating antibodies resulted in T cell activation, as measured by a significant increase of IL-2Rα, when either soluble OVA or BAY 11-7085 (a compound that prevents NFkB activation) was used to treat macrophages. L-selectin was significantly decreased among T cells co-cultured with macrophages treated with BAY 11-7085. T cell apoptosis, measured by Annexin V, did not change in response to stimulating antibodies or macrophage treatment with soluble OVA, but stimulating antibodies and macrophages treatment with BAY 11-7085 resulted in a significant increase of T cell apoptosis. (**Fig 1c**) Dilution of carboxyfluorescein succinimidyl ester (CFSE) to indicate T cell proliferation was low in the absence of stimulating antibodies. However, proliferation increased dramatically when stimulating antibodies were added, and proliferation was moderately higher when macrophages were treated with OVA compared to BAY 11-7085. (**Fig 1d**)

Naïve T cells were also co-cultured with dendritic cells receiving various treatments. In the absence of stimulating antibodies, T cells had low IL-2Rα and high L-selectin expression

following co-culture with untreated dendritic cells. (**Fig 1e, f**) The presence of stimulating antibodies, regardless of dendritic cell treatment, resulted in a significant increase of IL-2Rα and a decrease of L-selectin, signifying T cell activation. A small significant increase of T cell apoptosis occurred in the presence of stimulating antibodies and dendritic cells treated with soluble OVA compared to the absence of stimulating antibodies or treating dendritic cells with BAY 11-7085. (**Fig 1g**) T cell proliferation increased dramatically when stimulating antibodies were present, with negligible differences between T cells co-cultured with dendritic cells receiving soluble OVA or BAY 11-7085 treatment. (**Fig 1h**)

These studies confirmed the use of stimulating antibodies for mimicking T cell activation and also described the impact of treating APCs with BAY 11-7085 to inhibit NF-KB signaling activity. In co-culture with macrophages or dendritic cells, T cells had low IL-2Rα and high L-selectin expression in the absence of antibody stimulation, which were reversed when stimulating antibodies were added. Interestingly, pre-treatment of macrophages but not dendritic cells with BAY 11-7085 had a significant impact on expression of L-selectin, apoptosis, and proliferation of T cells. This difference suggests a more critical role of NF-KB signaling in macrophages compared to dendritic cells for promoting T cell entry into lymph nodes, viability, and proliferation.

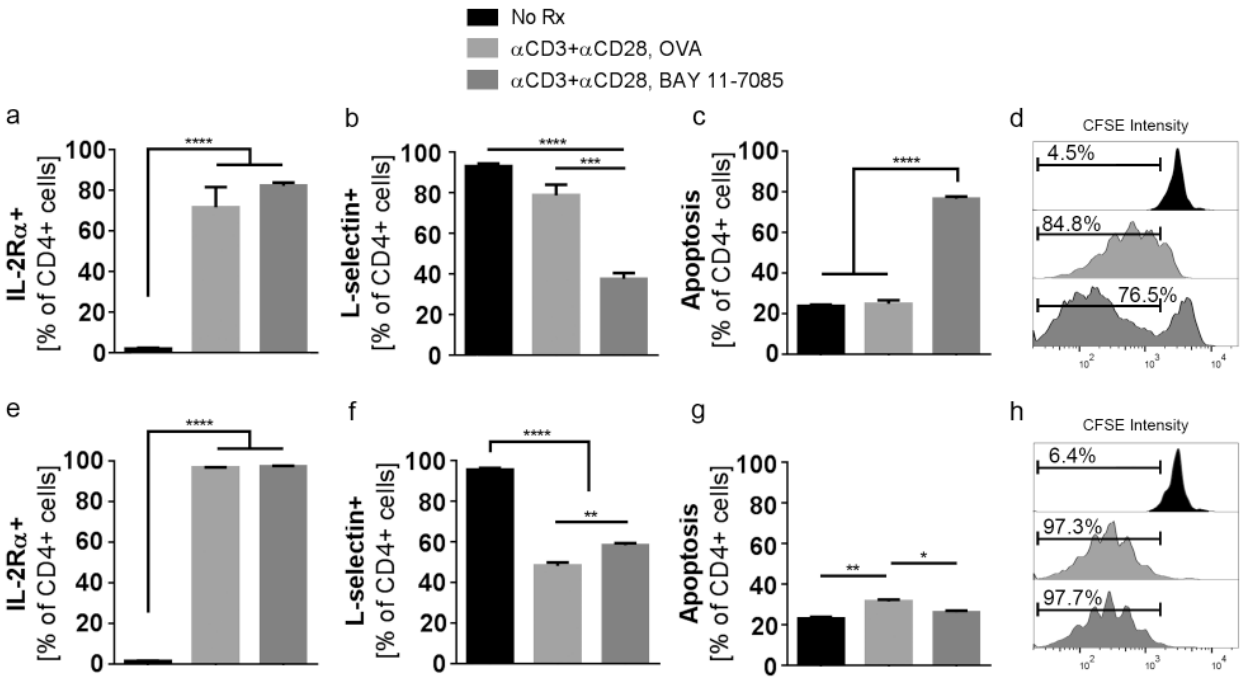

Figure 5.1 T cell response following antibody stimulation in co-culture with treated APCs. Co-culture of T cells with (**a-d**) macrophages or (**e-h**) dendritic cells administered the indicated treatment combinations. T cell expression of IL-2Rα in **a, e**, T cell surface expression of L-selectin in **b, f**, T cell apoptosis in **c, g**, and T cell proliferation in d, h. (*$p < 0.05$, **$p < 0.01$, ***$p < 0.001$, ****$p < 0.0001$, 1-way ANOVA followed by the Tukey test for multiple comparisons). Data show averages of three measurements ± standard error of mean (SEM) or representative population sample.

5.4.2 Cytokine profile from co-cultures of T cells and treated APCs

The co-culture cytokine profile revealed a strong sensitivity of macrophage treatment with BAY 11-7085. Naïve T cells co-cultured with untreated macrophages in the absence of stimulating antibodies had undetectable levels of GM-CSF, IFN-γ, and IL-10. (**Fig 2a-c**) The presence of stimulating antibodies and macrophages treated with soluble OVA resulted in a small increase of IFN-γ, although GM-CSF and IL-10 expression levels were still unchanged. A notable increase of GM-CSF, IFN-γ, and IL-10 was measured in co-cultures of T cells and macrophages treated with BAY 11-7085 in the presence of stimulating antibodies.

Stimulating antibodies and treatment of dendritic cells both influenced the cytokine profile in the co-culture environment. In the absence of stimulating antibodies, T cells co-cultured with untreated dendritic cells had undetectable levels of GM-CSF, IFN-γ, and IL-10. (**Fig 2d-f**) Adding stimulating antibodies and treating dendritic cells with soluble OVA resulted in significant increases of the measured cytokine levels. A significant increase of these three cytokines was also seen, although to a lesser extent, in co-cultures of T cells and dendritic cells pre-treated with BAY 11-7085 compared to co-culturing without stimulating antibodies.

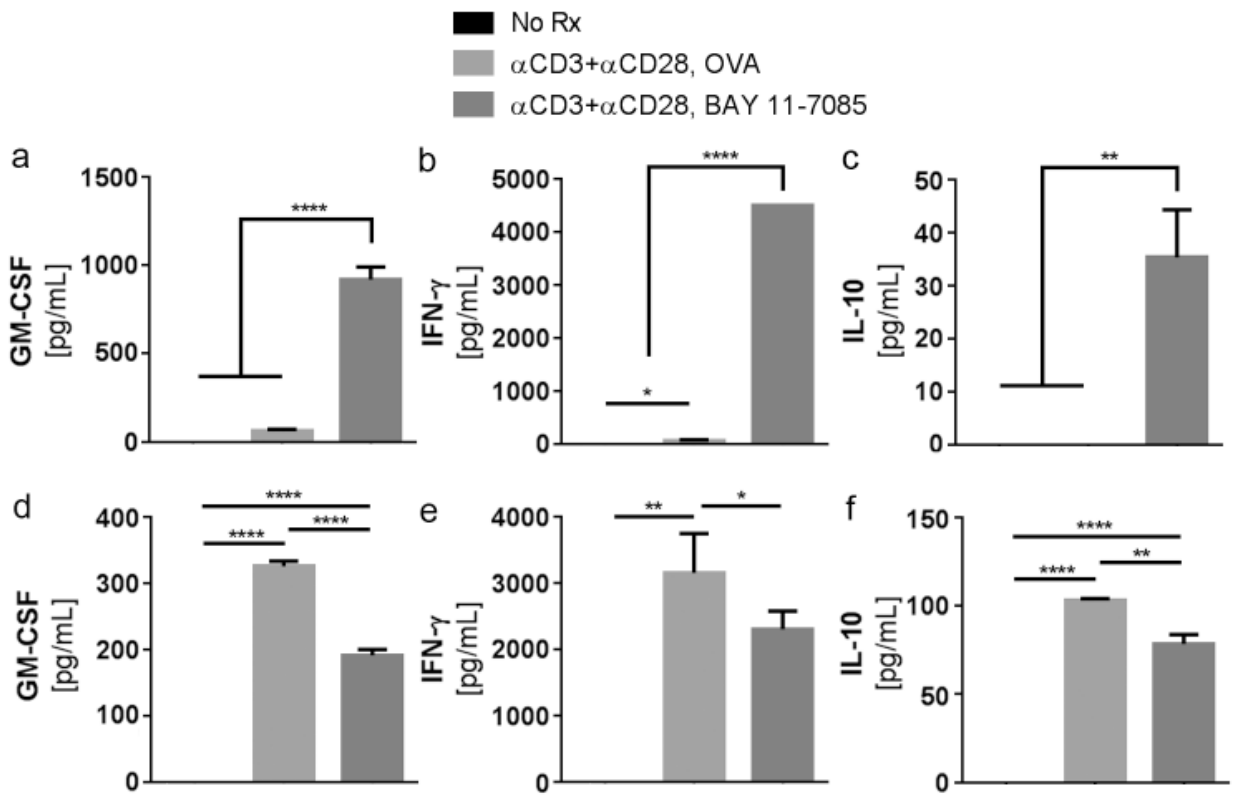

Figure 5.2 Cytokine profile of T cells following antibody stimulation in co-culture with treated APCs. Cytokine expression levels in co-cultures of T cells and (**a-c**) macrophages or (**d-f**) dendritic cells administered the indicated treatment combinations. GM-CSF in **a, d**, IFN-γ in **b, e**, and IL-10 in **c, f**. (*$p < 0.05$, **$p < 0.01$, ****$p < 0.0001$, 1-way ANOVA followed by the Tukey test for multiple comparisons). Data show averages of three measurements ± standard error of mean (SEM).

5.4.3 Role of antigen delivery vehicle on T cell response

The impact of delivering antigen to macrophages from different vehicles was examined via co-culture with naïve T cells in the presence of stimulating antibodies. IL-2Rα expression on T cells did not change significantly when macrophages were treated with PLG-OVA compared to soluble OVA. (**Fig 3a**) However IL-2Rα levels were significantly higher on T cells co-cultured with macrophages treated with SP-OVA relative to PLG-OVA. Interestingly, macrophage treatment with both SP-OVA and BAY 11-7085 resulted in a significant decrease of IL-2Rα expression by T cells compared to treating macrophages with both BAY 11-7085 and either soluble OVA or PLG-OVA. L-selectin expression did not change significantly due to different delivery vehicles, although L-selectin expression on T cells was generally lower when macrophages were treated with BAY 11-7085. (**Fig 3b**) T cell apoptosis was also not significantly affected by the different delivery vehicles but was notably higher when macrophages were treated with BAY 11-7085. (**Fig 3c**) T cell proliferation was not markedly changed in response to the different antigen delivery vehicles, but both BAY 11-7085 and either PLG-OVA or SP-OVA treatment of macrophages resulted in a moderate decrease of T cell proliferation. (**Fig 3d**)

T cell co-cultures were also used to examine the impact of different antigen delivery vehicles on dendritic cells. T cell expression of IL-2Rα was high when dendritic cells were treated with soluble OVA or PLG-OVA, but treating dendritic cells with SP-OVA resulted in a significant decrease of IL-2Rα expression. (**Fig 3e**) Additionally treating dendritic cells with BAY 11-7085 alongside the delivery vehicles resulted in similar trends to IL-2Rα expression. L-selectin expression on T cells was similar between co-cultures with dendritic cells treated soluble OVA or PLG-OVA, but treating dendritic cells with SP-OVA resulted in a significant increase of

L-selectin. (**Fig 3f**) Interestingly, the addition of BAY 11-7085 reversed the trend of L-selectin expression leading to a significant decrease when dendritic cells were treated with SP-OVA compared to soluble OVA. T cell apoptosis increased significantly when dendritic cells were treated with PLG-OVA compared to soluble OVA. (**Fig 3g**) Apoptosis was further increased in T cells co-cultured with dendritic cells treated SP-OVA. These trends in apoptosis were largely similar when dendritic cells were additionally pre-treated with BAY 11-7085. T cell proliferation was moderately attenuated in co-culture with dendritic cells treated with SP-OVA compared to soluble OVA or PLG-OVA. (**Fig 3h**) This attenuation due to SP-OVA was eliminated when dendritic cells were additionally pre-treated with BAY 11-7085.

Different vehicles for antigen delivery had negligible impact on T cells when applied via macrophages. In contrast, dendritic cells treated with SP-OVA compared to soluble OVA or PLG-OVA elicited T cell changes consistent with tolerance, such as lower levels of IL-2Rα expression and proliferation, and higher levels of L-selectin expression and apoptosis. When NF-KB signaling was inhibited in dendritic cells, the changes to T cell response brought on by different antigen delivery vehicles were still maintained, indicating redundancies or alternate signaling pathways used by dendritic cells to effect T cells. Interestingly, disruption of NF-KB signaling in macrophages led to dramatic changes in T cell response including decreased L-selectin expression, decreased proliferation, and increased apoptosis.

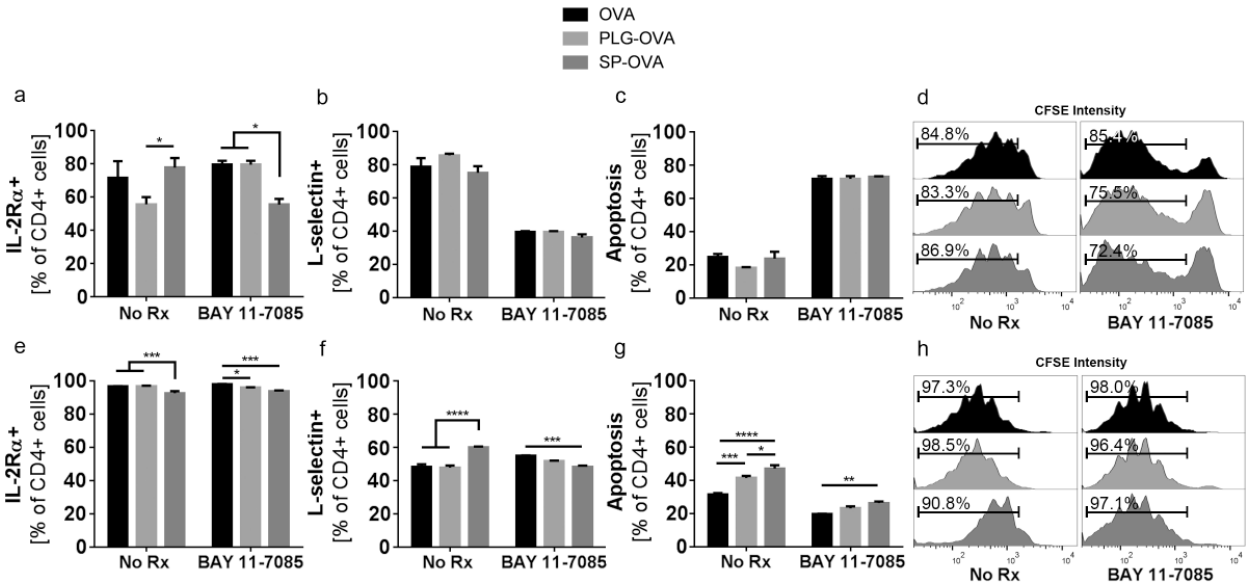

Figure 5.3 T cell sensitivity to APCs treated with different antigen delivery vehicles. Co-culture of T cells with (**a-d**) macrophages or (**e-h**) dendritic cells administered the indicated treatment combinations. T cell expression of IL-2Rα in **a, e**, T cell surface expression of L-selectin in **b, f**, T cell apoptosis in **c, g**, and T cell proliferation in **d, h**. (*$p < 0.05$, **$p < 0.01$, ***$p < 0.001$, ****$p < 0.0001$, 2-way ANOVA followed by the Sidak test for multiple comparisons). Data show averages of three measurements ± standard error of mean (SEM) or representative population sample.

5.4.4 Role of antigen delivery vehicle on co-culture cytokine profile

The cytokine profile resulting from co-culture of T cells and macrophages showed negligible differences due to antigen delivery vehicle but a strong influence of NF-KB signaling activity. Expression of GM-CSF, IFN-γ, and IL-10 were detected at low concentrations in co-cultures of T cells and macrophages treated either soluble OVA, PLG-OVA, or SP-OVA. (**Fig 4a-c**) When macrophages were additionally treated with BAY 11-7085, expression levels of these three cytokines increased substantially.

Co-cultures of T cells and dendritic cells produced cytokine profiles indicating the influence of both antigen delivery vehicle and NF-KB signaling. GM-CSF expression was unaffected by the vehicle delivering antigen to dendritic cells. (**Fig 4d-f**) However, lower GM-CSF levels were measured when dendritic cells were treated with BAY 11-7085 in addition to either soluble OVA or SP-OVA. Treating dendritic cells with SP-OVA compared to soluble OVA or PLG-OVA resulted in a significant reduction of IFN-γ that was reversed in the context of BAY 11-7085 treatment. Expression of IL-10 was also unaffected by the antigen delivery vehicle. However, additional treatment of dendritic cells with BAY 11-7085 reduced overall IL-10 expression, although SP-OVA treatment resulted in higher IL-10 levels compared to PLG-OVA.

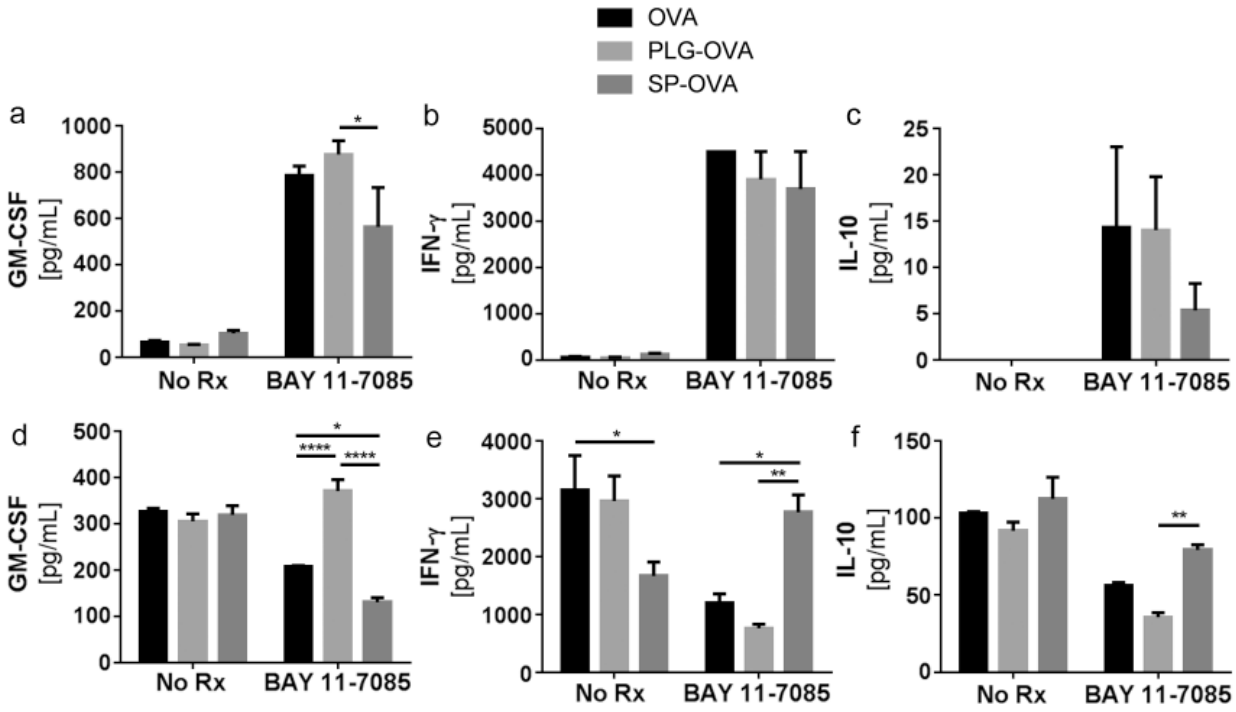

Figure 5.4 Cytokine expression in co-cultures of T cells and APCs treated with different antigen delivery vehicles. T cells co-cultured with (**a-c**) macrophages or (**d-f**) dendritic cells administered the indicated treatment combinations. GM-CSF in **a, d**, IFN-γ in **b, e**, and IL-10 in **c, f**. (*$p < 0.05$, **$p < 0.01$, ****$p < 0.0001$, 2-way ANOVA followed by the Sidak test for multiple comparisons). Data show averages of three measurements ± standard error of mean (SEM).

5.4.5 Comparison of dynamic TF activity between antigen delivery vehicles

TRACER was used to examine differences in APC signaling activity resulting from antigen delivery by different vehicles. Macrophages had a total of 50% (7/14) of examined factors that were significantly different between PLG-OVA and SP-OVA treatment. (**Fig 5a**) Of these factors, five were similarly different between PLG-OVA and SP-OVA treatment in dendritic cells. (**Fig 5b**) These transcription factors may be part of a common mechanism of APCs in response to antigen-coupled splenocyte or nanoparticle treatment. There were an additional 4 factors whose dynamic activity in dendritic cells was significantly different between PLG-OVA and SP-OVA treatment, which may be part of a cell-specific response. The majority of transcription factors in dendritic cells following SP-OVA treatment had reduced activity over time, which may suggest the induction of a homeostatic or regulatory cell phenotype.

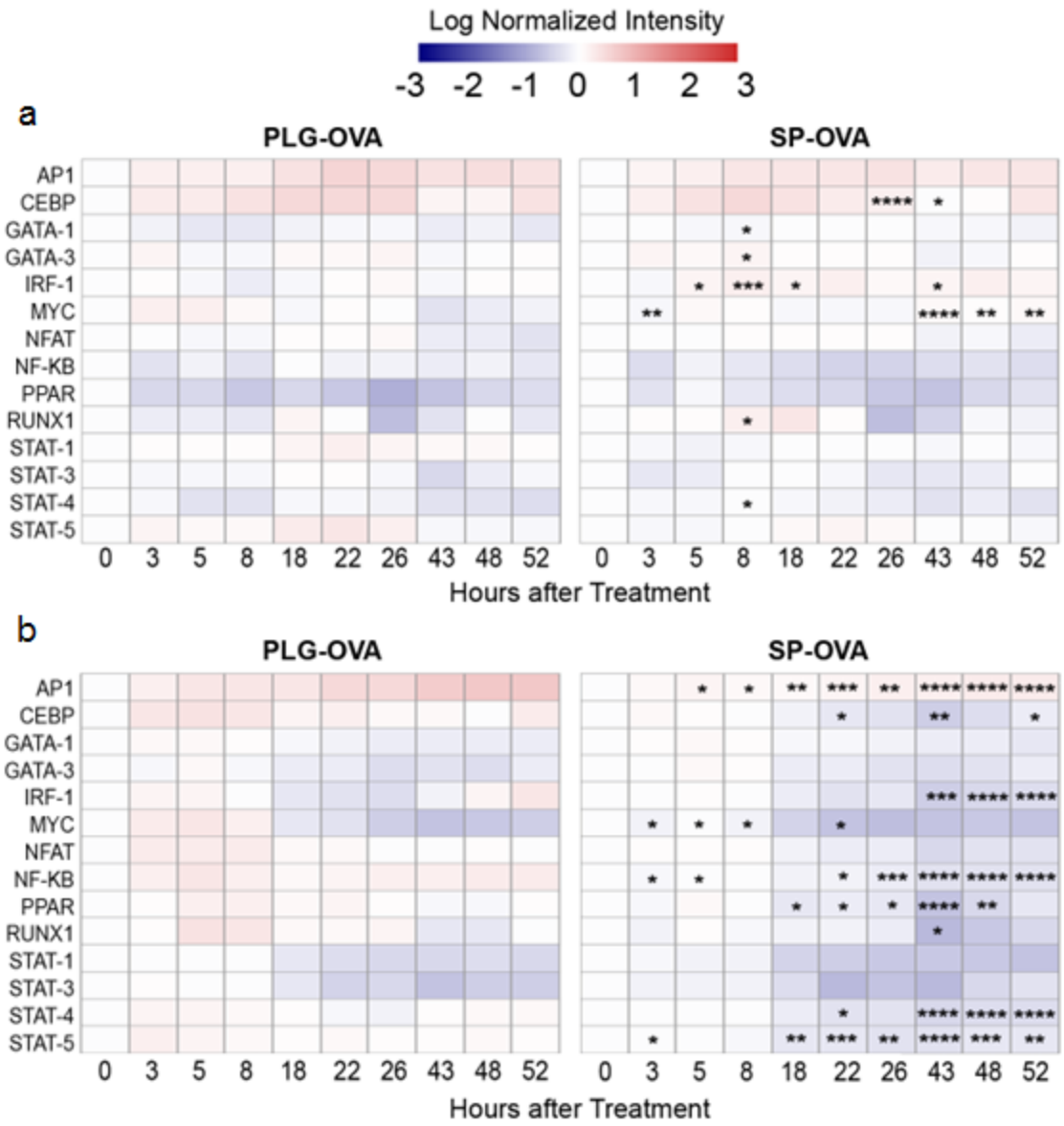

Figure 5.5 Dynamic transcription factor activity of APCs following antigen treatment. TRACER measurements of (**a**) macrophages or (**b**) dendritic cells in the hours following treatment with PLG-OVA or SP-OVA. Significance tests compared the PLG-OVA and SP-OVA treatments within each cell type. (*$p < 0.05$, **$p < 0.01$, ***$p < 0.001$, ****$p < 0.0001$, normalized activities were fitted to an empirical hierarchical Bayesian linear model). Data show averages of two separate experiments.

5.4.6 Inference networks of TF activity between antigen delivery vehicles

Signaling networks were constructed using inference methods to analyze the TRACER studies and identify potential interactions among the transcription factors examined. The networks resulting from macrophages and dendritic cells treated with PLG-OVA depicted the majority of transcription factors with few interaction partners and a few key transcription factors serving as bridges to link the entire network together. (**Fig 6a, b**) These linking factors included NF-KB and AP-1 in macrophages and RUNX1, IRF-1, and AP-1 in dendritic cells, which are likely important signaling molecules to determine cell activity and response to PLG-OVA treatment. Networks built from macrophages and dendritic cells treated with SP-OVA appeared more highly inter-connected compared to networks built from the PLG-OVA response. (**Fig 6c, d**) NF-KB, PPAR, and AP-1 in macrophages and CEBP, IRF-1, and AP-1 in dendritic cells were among the more highly inter-connected nodes. From these network diagrams, the critical role of NF-KB in macrophage signaling was apparent. Removing NF-KB from either macrophage network would sever interactions among many transcription factors, creating several disparate networks. In comparison, removing NF-KB from the networks of dendritic cells would not substantially affect the interactions between the remaining transcription factors. These networks help explain the major changes in T cell response when macrophages compared to dendritic cells were treated with BAY 11-7085 to inhibit NF-KB signaling.

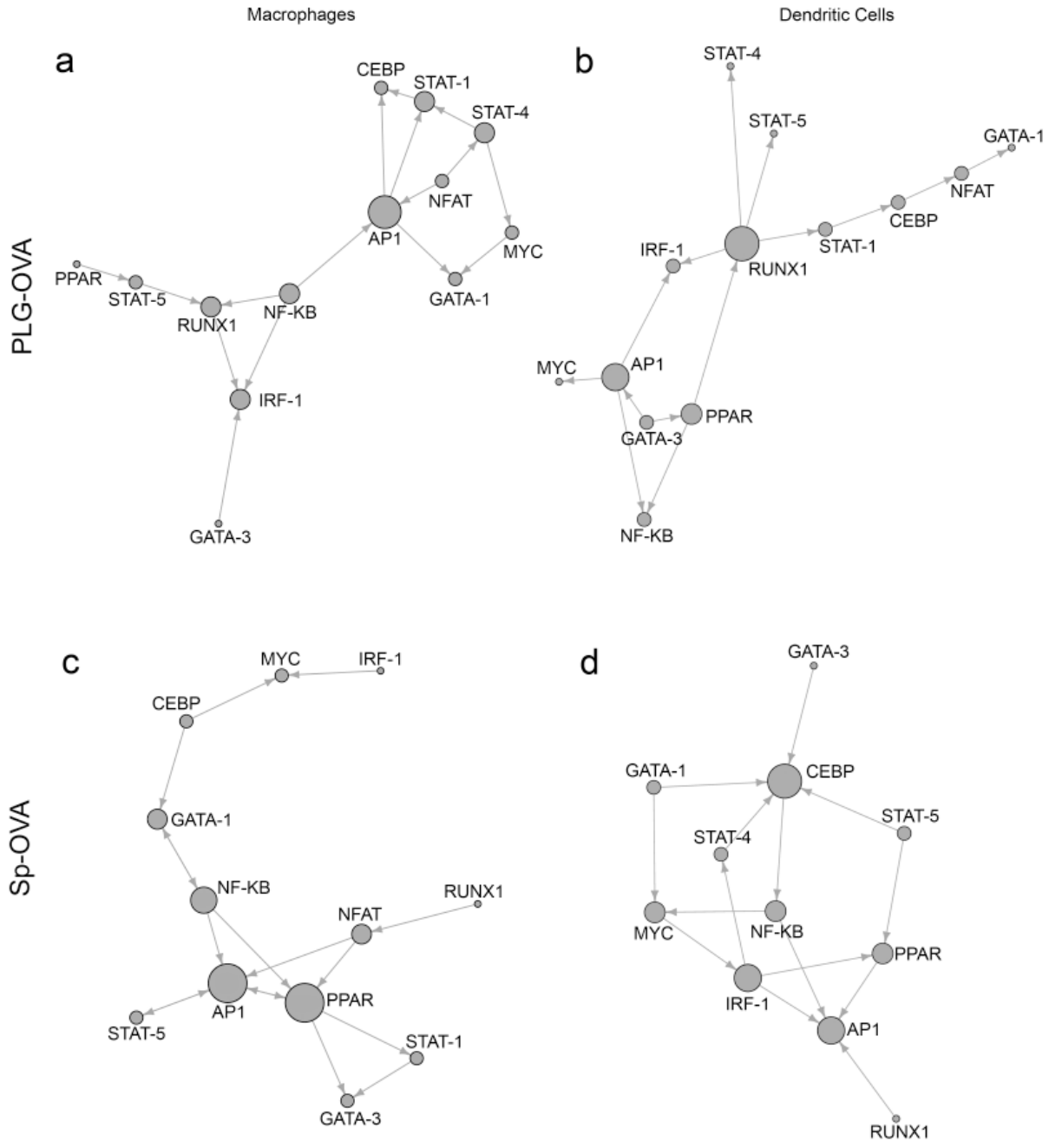

Figure 5.6 Network analysis of TRACER studies. Inference networks of transcription factor interactions following (**a, b**) PLG-OVA or (**c, d**) SP-OVA treatment. Macrophages in **a, c** and dendritic cells in **b, d**.

5.5 Discussion

We were interested to use stimulated naïve T cells as a surrogate for self-reactive T cells to detect differences in their responses to antigen delivery vehicles. T cell stimulation with αCD3/αCD28 has been widely used to expand naïve populations of T cells. [116] Raman spectroscopy has previously detected differences between T cells stimulated by αCD3/αCD28 and alloantigen-activated T cells. [117] However, a comparison using biological indicators, such as IFN-γ production, revealed similar responses from T cells stimulated with either αCD3/αCD28 or an infectious agent. [118] Moreover, several other groups have stimulated T cell activation using αCD3/αCD28 for *in vitro* models of autoimmunity. [119, 120] We observed that unstimulated T cells had low levels of the activation marker, IL-2Rα, and its levels increased significantly following T cell stimulation. Thus, we believe our experimental setup is sufficient for modeling tolerance responses to different antigen delivery vehicles.

NF-KB signaling in APCs can be triggered by ligand binding of Toll-like receptors (TLRs) on the cell surface resulting in an immune response. [121] Previous applications of the NF-KB inhibitor, BAY 11-7085, have shown reduced monocyte activation, as measured by lower levels of IL-1β and TNFα following co-culture with stimulated T cells or T cells isolated from rheumatoid arthritis. [122] When administered to dendritic cells, BAY 11-7085 attenuated maturation as measured by reduced expression of CD40, HLA-DR, CD83, and CD86 following exposure to haptens. [123] We found administering macrophages with antigen alongside BAY 11-7085 resulted in increases of cytokine production, which may have differed from the reported monocyte behavior due to a cell-specific response. Administering antigen and BAY 11-7085 to dendritic cells did yield noticeable trends in T cell activity or cytokine production, possibly due

to the reduced impact of antigen presentation and co-stimulatory expression on T cells in the presence of αCD3/αCD28.

The additional tolerance benefits from delivering antigen-coupled donor cells compared to antigen-coupled nanoparticles was evident in dendritic cells. Following SP-OVA treatment, dendritic cells brought about reduced T cell expression of IL-2Rα, increased T cell expression of L-selectin, increased T cell apoptosis, and reduced T cell proliferation. In addition, IFN-γ levels decreased while IL-10 levels remained high. These responses skewing towards tolerance are likely the result of triggering the same endogenous mechanisms used by dendritic cells to maintain peripheral tolerance to autoantigens found on apoptotic cells. [124] The mechanisms triggered by nanoparticle treatment, particularly in regard to inducing cytokine production are still unclear. [125]

Although NF-KB inhibition was not sufficient to explain the additional tolerance effects induced by SP-OVA, network analysis of dendritic cells administered SP-OVA showed other transcription factors of interest. Specifically, CEBP was the most highly connected node, which suggests it is highly involved in implementing the tolerance effects resulting from SP-OVA treatment. Others have identified CEBP to be triggered in DCs following IL-10 and LPS treatment, leading to upregulation of chemokines, transduction molecules, and other transcription factors. [126] Further investigation of CEBP and its downstream effector molecules may generate additional targets for nanoparticle treatment to target in order to replicate the superior tolerance induction ability of donor cells. Antigen-coupled nanoparticles that can make additional use of endogenous tolerance pathways would provide a highly attractive platform to develop antigen-specific therapeutics for autoimmune diseases.

Chapter 6: Encapsulated CCR2-Targeting SiRNA Reduces Inflammatory Cell Migration and Disease Symptoms in Multiple Sclerosis Model

6.1 Abstract

The therapeutic potential of delivering small interfering RNA (siRNA) from nanoparticles to silence gene expression important for multiple sclerosis has yet to be explored. We encapsulated within biodegradable poly(lactide-co-glycolide) nanoparticles a mixture of siRNA complexed to polyethylenimine PLG(siCCR2-PEI) to target expression of the CCR2 chemokine receptor. Nanoparticles encapsulating fluorescent nucleic acids were observed to escape the endocytic internalization pathway, a necessary precursor for siRNA function. The activity of complexed and encapsulated siCCR2 was demonstrated by directly measuring CCR2 expression and evaluating cell migration toward CCL2. Induction of experimental autoimmune encephalomyelitis, a mouse model of multiple sclerosis was followed by 1.0 mg administrations of PLG(siCCR2-PEI) on Days 7, 9, and 11 post-induction, which significantly reduced mean clinical scores compared with administering either PLG encapsulating non-specific siRNA or buffered solution. These findings suggest PLG(siCCR2-PEI) may be useful for further development in the clinical treatment of multiple sclerosis and other autoimmune diseases.

6.2 Introduction

The therapeutic potential of RNA interference (RNAi) received tremendous interest and investment at the start of the 21st century. Some predicted RNAi would soon become a potent tool within the healthcare provider's arsenal for treating a wide array of diseases. [127, 128] But

after many years of research and several clinical trials, a commercially available product has yet to emerge. Interestingly, several pharmaceutical companies have chosen instead to exit this research space. [129] While the difficulty of developing therapeutic RNAi may have initially been underestimated, advancements in nanoscale drug delivery systems offer potential solutions to overcome remaining challenges and enable RNAi to enter the clinic.

Therapeutic RNAi strategies focus primarily on the use of small interfering RNA (siRNA). When introduced into the cell cytosol, these short, double-stranded RNA molecules associate with RNA-induced silencing complex (RISC) and possibly other factors to cleave and inhibit translation of mRNA molecules containing complementary sequence. [130] The activity of siRNA depends critically on its presence in the cytosol in order to associate with RISC and disrupt mRNA translation. A number of synthetic materials have been investigated as delivery vehicles to facilitate siRNA delivery to the cytosol. [131]

Polymers are a versatile class of materials able to facilitate nucleic acid delivery into cells. Due to its negative charge, siRNA is often mixed with polycations, such as poly-L-lysine or polyethylenimine (PEI), resulting in self-assembly into more condensed structures, often called polyplexes. [132] The formation of polyplexes can improve the efficiency of siRNA encapsulation and subsequent release from poly(lactide-co-glycolide) (PLG) nanoparticles. [133] Several groups have previously used PLG nanoparticles to encapsulate siRNA for silencing TNFα expression and mitigating inflammation in both *in vitro* and *in vivo* models.[134, 135] These results demonstrate a possible role for siRNA to enhance or improve therapies currently used for autoimmune diseases.

Multiple sclerosis is one of 81 identified autoimmune diseases and affects approximately 58.3 per 100,000 people. [2] One of the most common treatments for multiple sclerosis is IFN-β,

which acts broadly and non-specifically to inhibit expression of MHC class II molecules, IL-12 production, and T cell proliferation. [40] Unfortunately, patient complaints of flu-like symptoms or skin reactions have contributed to 5-year drop-out rates for IFN-β treatment that in certain studies are as high as 42%. [136] Alternative therapeutic interventions to incorporate siRNA which possesses a more specific mechanism of action may help to reduce the occurrence of side effects and improve patient compliance.

Previous studies of immune components driving the pathogenesis of multiple sclerosis identified an important contribution of the CCL2/CCR2 chemokine signaling pathway. [137] Studies using experimental autoimmune encephalomyelitis (EAE), a mouse model of multiple sclerosis, found that mice with genetic deletion of CCR2 had reduced cell infiltration in their central nervous systems and did not develop EAE pathology. [138] Expressed primarily on monocytes, CCR2 activation leads to extravasation and transmigration. Administering encapsulated siRNA to inhibit CCR2 expression has resulted in reductions of monocyte accumulation that were therapeutically beneficial in mouse models of atherosclerosis, myocardial infarction, pancreatic islet allograft, and cancer. [139]

Herein we conducted several *in vitro* and *in vivo* studies to investigate the activity of siRNA designed specifically to inhibit CCR2 expression (siCCR2). Intracellular nanoparticle localization was first examined to verify their escape from the endocytic pathway into the cytosol to enable proper function. Subsequently, CCR2 expression was analyzed using direct measurement and also a cell migration assay following treatment of immune cells with siCCR2-PEI polyplexes as well as with polyplexes encapsulated within PLG nanoparticles. Finally, we tested the ability of nanoparticles encapsulating polyplexes to ameliorate EAE disease symptoms.

6.3 Materials and Methods

6.3.1 Materials

All siRNA was purchased from GE Dharmacon (Lafayette, CO) as mixtures containing four unique sequences. The siCCR2 mixture had the following sequences designed for specific silencing of mouse CCR2 expression: 5'CGAGUGAGCUCUACAUUCA3', 5'GGAGAGAAGUUCCGAAGGU3', 5'CCAGGAAUCAUAUUUACUA3', 5'GUACUUGGCUAUUGUUCAU3'. The siCTRL mixture had the following sequences designed to each have at least 4 mismatches to all mouse, human, and rat genes: 5'UAGCGACUAAACACAUCAA3', 5'UAAGGCUAUGAAGAGAUAC3', 5'AUGUAUUGGCCUGUAUUAG3', 5'AUGAACGUGAAUUGCUCAA3'.

The following DNA oligonucleotide sequences were purchased from Integrated DNA Technologies (Coralville, IA): 5'/6-FAM/AGCTCAACATTCTGATAAGCTAC3' and 5'GAGTAGCTTATCAGAATGTTGAG3'. The $PLP_{139-151}$ peptide was purchased from Genscript (Piscataway, NJ) and the MOG_{35-55} peptide was purchased from Celtek Peptides (Franklin, TN). Branched polyethylenimine (PEI), 25 kDa, and poly(vinyl alcohol), 30-70 kDa, were both purchased from Sigma-Aldrich (St. Louis, MO). Poly(lactide-co-glycolide) 50:50 (PLG) with inherent viscosity of 0.2 dL/g was purchased from Lactel Absorbable Polymers (Birmingham, AL).

6.3.2 Mice

Female 6 to 12 week old C57BL/6 mice were purchased from Charles River Laboratories (Wilminton, MA). Female 6 to 12 week old SJL/J mice were purchased from Envigo (Indianapolis, IN). All experiments involving mice were approved by the University of Michigan Committee on the Use and Care of Animals.

6.3.3 Preparation of fluorescent nanoparticles

PLG nanoparticles were synthesized using a single emulsion solvent evaporation technique as described previously. [92] Lyophilized nanoparticles were washed three times using phosphate-buffered solution (PBS) at pH 7.4. Approximately 4 mg of PLG nanoparticles was recovered and activated using 1-ethyl-3-(3-dimethylaminopropyl) carbodiimide (EDC), purchased from Sigma-Aldrich (St. Louis, MO), at 16 mg/mL. Fluorescein cadaverine, purchased from Thermo Fisher Scientific (Waltham, MA) was immediately added to a final concentration of 4 μg/μL and the coupling reaction proceeded for 1 h under constant agitation. Uncoupled fluorophore was removed with three PBS washes.

Complementary single-stranded DNA oligonucleotides containing a fluorophore molecule were combined at 40 μM in solution containing 5 mM NaCl, 1 mM Tris-HCl, 1 mM $MgCl_2$, and 0.1mM DTT. Sequences were heated at 95°C for 10 min before being cooled on ice for 10 min. The resulting double-stranded DNA was used within 24 h of annealing. PLG nanoparticles containing the annealed fluorescent DNA were formed in a similar process as the siRNA-encapsulated nanoparticles described below.

6.3.4 Fabrication of siRNA-encapsulated PLG nanoparticles

Complexes of siRNA and PEI (siRNA-PEI) were first formed by mixing together at an N:P ratio of 8:1 and incubating at room temperature for 30 min. A 200 μL solution of the complexes, containing approximately 2 nmol of siRNA, was added to 0.5 mL of PLG dissolved in dichloromethane at 10% (w/v). A primary emulsion was formed by sonicating the solution with a Cole-Parmer CPX130 Ultrasonic Processor for 30 s. Subsequently, 2.5 mL of poly(vinyl alcohol) at 0.5% (w/v) was quickly added to the solution which was sonicated an additional 30 s to form the secondary emulsion. The emulsion was poured into 25 mL of poly(vinyl alcohol) at 0.5%

(w/v) and stirred overnight to evaporate the solvent. The resulting nanoparticles were washed three times and finally lyophilized in a solution of 4% (w/v) sucrose and 3% (w/v) D-mannitol.

6.3.5 Nanoparticle characterization

Nanoparticle size and ζ-potential were measured using a Zetasizer Nano ZSP from Malvern Instruments Ltd (Worcestershire, UK). To measure siRNA loading, nanoparticles were first dissolved for 30 min in dichloromethane. An equal volume of Tris-EDTA buffer was then added, vortexed for 1 min, and centrifuged at 12,000x*g* for 10 min. Nucleic acids in the aqueous phase were collected and quantified with the Quant-iT Picogreen dsDNA Assay Kit purchased from Thermo Fisher Scientific (Waltham, MA) using a standard curve built from siRNA-PEI.

6.3.6 Intracellular localization of nanoparticles *in vitro*

A primary population of macrophages was obtained as described previously. [90] Briefly, bone marrow was harvested from femurs and tibias of C57BL/6 mice and differentiated *in vitro*. Between 8 to 10 days following harvest, macrophages were collected and seeded at approximately 5.0 x 10^5 cells/mL in a Lab-Tek Chamber Slide System and activated with lipopolysaccharide (LPS) at 100 ng/mL. Fluorescent nanoparticles were reconstituted in water and added to chambers at 100 μg/mL. After 24 h of culture, cells were stained with LysoTracker Red DND-99 purchased from Thermo Fisher Scientific (Waltham, MA) according to the manufacturer's instructions. Cells were fixed in 4% paraformaldehyde and cover slips were mounted on chamber slides with permount containing DAPI. Slides were imaged using either a Leica DM IRB fluorescent microscope or an Olympus FV 1200 confocal microscope.

6.3.7 EAE initiation

EAE disease was initiated as described previously. [85] Briefly, SJL/J and C57BL/6 mice were injected subcutaneously with emulsified $PLP_{139-151}$ or MOG_{35-55}, respectively, in complete

Freund's adjuvant. C57BL/6 mice were also IP injected with 100 μL of pertussis toxin (2 ng/mL) purchased from Tocris Biosciences (Minneapolis, MN) on the same day and again 2 days later.

For in vitro experiments, EAE-immunized mice were sacrificed 8 to 12 days after disease initiation, and blood within the heart was collected into Vacutainer tubes purchased from Becton, Dickinson and Company (Franklin Lakes, NJ). Red blood cells were lysed with ACK buffer manufactured by Life Technologies (Carlsbad, CA).

For in vivo experiments, EAE-immunized mice were administered 1.0 mg of siRNA-encapsulated PLG nanoparticles on days 7, 9, and 11 following disease initiation. Behavioral testing of mice was performed daily to determine clinical score, based on a 0-5 scale as follows: 0, healthy; 1, limp tail; 2, limp tail and impaired righting reflex; 3, hind-limp weakness; 4, hind-limb paralysis; and 5, moribund.

6.3.8 Measuring function of siCCR2 *in vitro*

To verify siRNA function, blood cells collected from EAE-immunized C57BL/6 mice were seeded into 24-well flat bottom plates at a density between 2.0×10^5 to 2.5×10^5 cells/mL using non-supplemented RPMI 1640 purchased from Life Technologies (Carlsbad, CA). Complexes of siCCR2 and PEI were added to cells at varying concentrations and analyzed 24 h later using flow cytometry. Cells were blocked in CD16/32, stained with αCCR2-Alexa Fluor 647 (clone SA203G11), and analyzed using a CyAn ADP Analyzer manufactured by Beckman Coulter (Brea, CA). Data was analyzed with FlowJo v10. Cellular events were gated using forward scatter and side scatter. FMO controls were used to identify cells with positive signal.

CCR2 expression was investigated after treating cells with siRNA-encapsulated PLG nanoparticles. Blood cells were seeded as described above in 100 mm dishes. Nanoparticles were added at 100 μg/mL and CCR2 expression was measured 24 h later. Cell types were identified

using αLy6G-Brillian Violet 421 (clone 1A8), αLy6C-APC/Cy7 (clone HK1.4), and αCD45-PerCP (clone 30-F11).

6.3.9 Migration assays

The migratory potential of treated cells was evaluated using Transwell cell culture inserts manufactured by Corning Incorporated (Oneonta, NY). Inserts were submerged in RPMI 1640 containing 100 ng/mL of CCL2, a cytokine that binds CCR2 resulting in extravasation and transmigration, purchased from PeproTech (Rocky Hill, NJ). Blood cells collected from EAE-immunized SJL/J mice or bone marrow-derived macrophages were seeded within inserts at 1.0 x 10^6 cells/mL. After 24 h of treatment with either complexes or nanoparticles, migrated cells were dislodged from inserts using 5 mM EDTA and stained with calcein, AM, cell-permeant dye that was purchased from Thermo Fisher Scientific (Waltham, MA) according to the manufacturer's instructions. Cell fluorescence was measured using a Synergy H1 Multi-Mode Reader manufactured by BioTek Instruments, Inc. (Winooski, VT) and correlated to known quantities of calcein-stained cells.

6.4 Results

6.4.1 Encapsulation of payload enables nanoparticle escape of endocytic pathway

Nanoparticles containing surface-conjugated fluorophore (PLG-FITC) showed strong co-localization with LysoTracker within bone marrow-derived macrophages following 24 h of nanoparticle treatment. (**Fig 6.1a**) The co-localization with LysoTracker, which stains acidic organelles such as lysosomes, suggested the retention of PLG-FITC within the endocytic pathway from cell internalization to lysosomal degradation. Interestingly, nanoparticles encapsulating short double-stranded DNA with an attached fluorophore [PLG(DNA-PEI)] were observed excluded from LysoTracker stains, suggesting escape of these nanoparticles from the

endocytic pathway and into the cytosol. (**Fig 6.1b**) The average diameter and zeta potential of PLG-FITC were 1146 nm and +29.9 mV, respectively, while the same measures for PLG(DNA-PEI) were 480.3 nm and -16.4 mV.

6.4.2 Bioactivity of complexed and encapsulated siCCR2

Complex formation with PEI was verified using a fluorescent dye that emits signal when bound to double-stranded nucleic acids. Fluorescence intensity was linearly correlated with the concentration of double-stranded DNA both before and after complexation with PEI. (**Fig 6.2**) However, the fluorescent sensitivity of complexed DNA decreased dramatically, suggesting hindrance of fluorescent interaction between fluorescent dye and double-stranded nucleic acids due to the presence of PEI.

Surface expression of CCR2 was measured on peripheral blood mononuclear cells (PBMCs) isolated from C57BL/6 mice 8 to 12 days following EAE induction. After 24 h of treatment with complexes of siCCR2 and PEI (siCCR2-PEI), a significant decrease of CCR2 expression was observed among cells receiving 10 nM of siCCR2. (**Fig 6.3a**) This same dose of siCCR2-PEI was administered to PBMCs from SJL/J mice within a Transwell insert before placement inside a reservoir containing CCL2, the chemokine ligand for CCR2. The number of PBMCs migrating was similar to untreated PBMCs placed inside a reservoir without CCL2, both of which were significantly lower than the migration of PBMCs not receiving siCCR2-PEI and placed inside a CCL2-containing reservoir. (**Fig 6.3b**) These results indicate the ability of siCCR2-PEI treatment to inhibit CCL2-mediated cell migration.

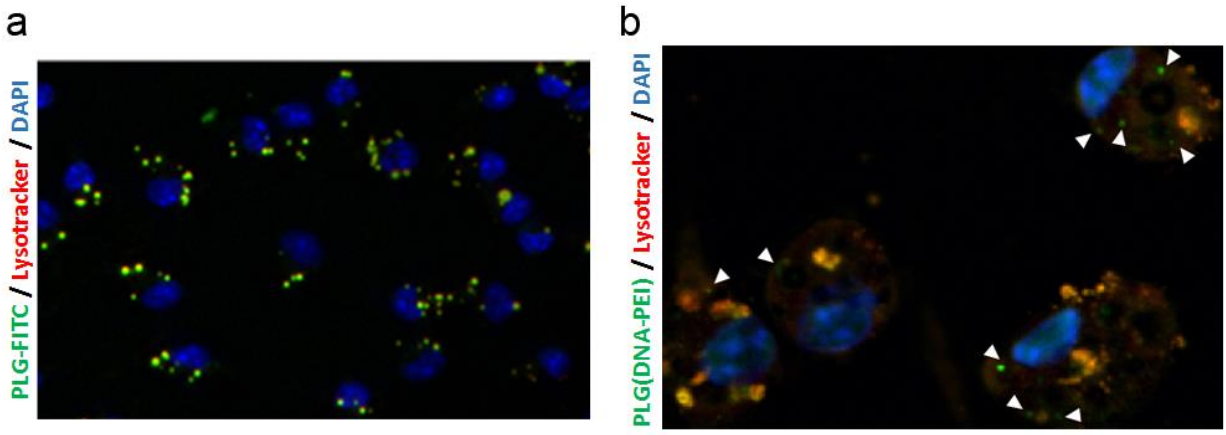

Figure 6.1 Intracellular nanoparticle localization within bone marrow-derived macrophages. MΦs were cultured on chamber slides for 24 h with (**a**) 10 μg/mL of PLG-FITC (green) and imaged using a Leica DM IRB fluorescent microscope or (**b**) 50 μg/mL of PLG(DNA-PEI) (green) and imaged using an Olympus FV 1200 Confocal Microscope. White arrows indicate observations of green fluorescent signal excluded from red fluorescent signal. Cells were stained with lysotracker (red) and slides were mounted with coverslips using Permount Mounting Medium containing DAPI (blue).

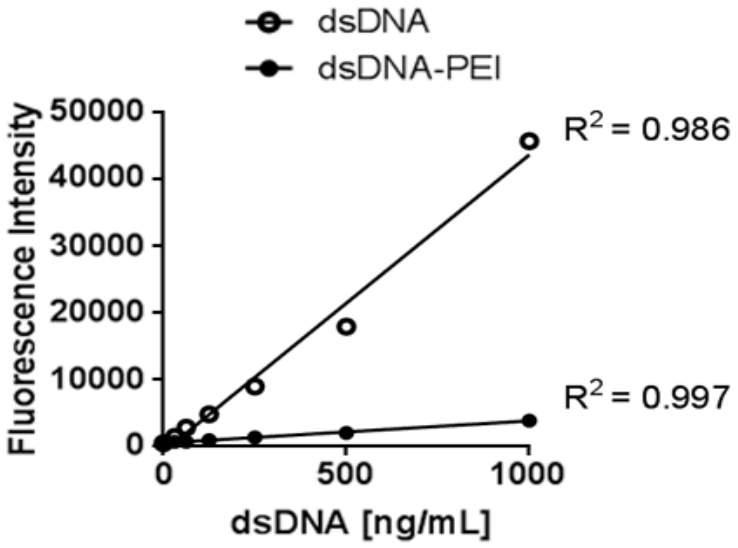

Figure 6.2 Formation of siRNA-PEI polyplexes. The Quant-iT PicoGreen dsDNA Assay Kit was highly sensitive to annealed DNA oligonucleotides (dsDNA) as shown by a steep best-fit line with coefficient of determination equal to 0.986. Mixture of the dsDNA with PEI (dsDNA-PEI) resulted in a dramatic reduction of sensitivity suggesting polyplex formation as shown by a less steep best-fit line with coefficient of determination equal to 0.997.

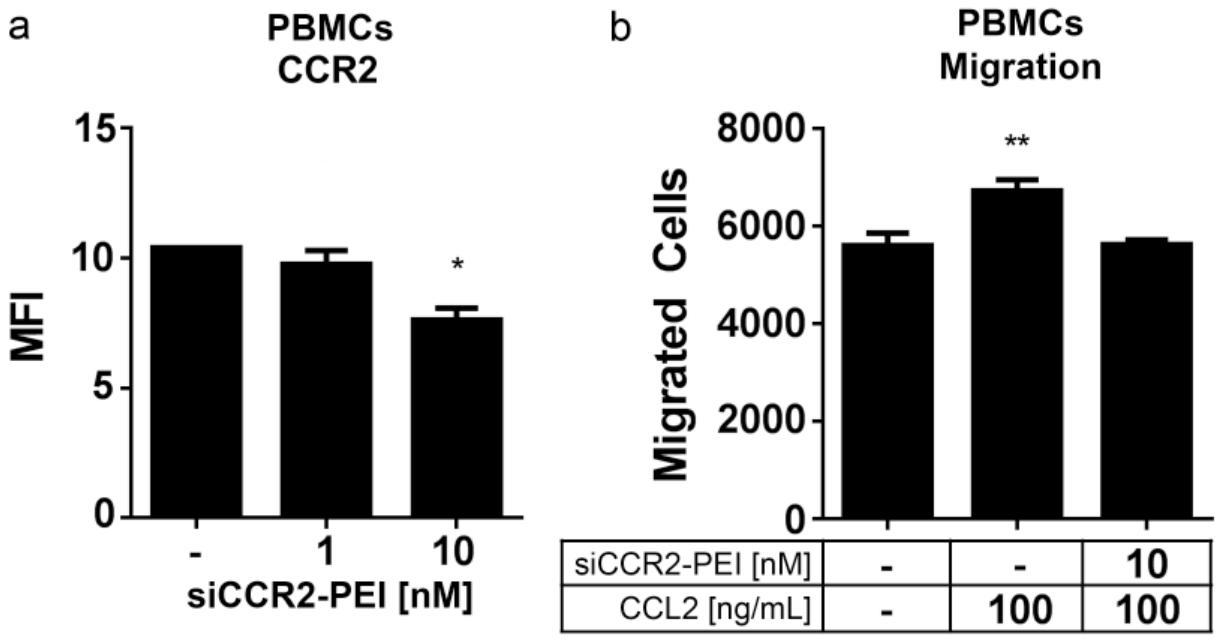

Figure 6.3 Direct measurement and functional detection of siCCR2-PEI activity *in vitro*. (**a**) PBMCs isolated from EAE-immunized mice were cultured with increasing concentrations of siCCR2-PEI for 24 h before CCR2 surface expression analysis using flow cytometry. The mean fluorescence intensity of CCR2 expression significantly decreased on PBMCs treated 10 nM of siCCR2-PEI. (**b**) The number of PBMCs migrating into a Transwell membrane significantly increased in the presence of 100 ng/mL CCL2. The additional migration in response to CCL2 was no longer observed when PBMCs were treated with 10 nM of siCCR2-PEI. Data show averages of three measurements ± standard error of mean (SEM). (*$p < 0.05$, **$p < 0.01$, 1-way ANOVA followed by the Tukey test for multiple comparisons).

6.4.3 Bioactivity of encapsulated siCCR2-PEI

The physicochemical properties of PLG nanoparticles were measured following encapsulation of siCCR2-PEI. The average diameter was 448.6 nm and the average zeta potential was -16.5 mV. Encapsulation efficiency was approximately 7.7%, resulting in total siCCR2 loading of approximately 30.9 pmol per mg of PLG. Blank PLG nanoparticles synthesized in parallel without the encapsulation of siCCR2-PEI had average diameter of 381.9 nm and average zeta potential of -22.6 mV.

Blank nanoparticles (PLG) or nanoparticles containing siRNA complexes [PLG(siCCR2-PEI)] were both administered to PBMCs isolated from SJL/J mice 10 days after EAE induction. After 24 h of nanoparticle treatment, reduced surface expression of CCR2 was measured among PBMCs administered PLG(siCCR2-PEI) compared to PLG. (**Fig 6.4**) This reduction was observed in both Ly6G+ PBMCs and Ly6C+ PBMCs, cell identification markers which are typically associated with neutrophils and monocytes.

To control for differences occurring simply due to siRNA treatment, PLG nanoparticles encapsulating complexes of control siRNA lacking any sequence complementarity within the mouse genome [PLG(siCTRL-PEI)] were administered to bone marrow-derived macrophages alongside PLG(siCCR2-PEI). Both formulations were able to reduce CCR2 expression (**Fig 6.5a**) and migration toward CCL2 (**Fig 6.5b**), although the differences were more significant with PLG(siCCR2-PEI).

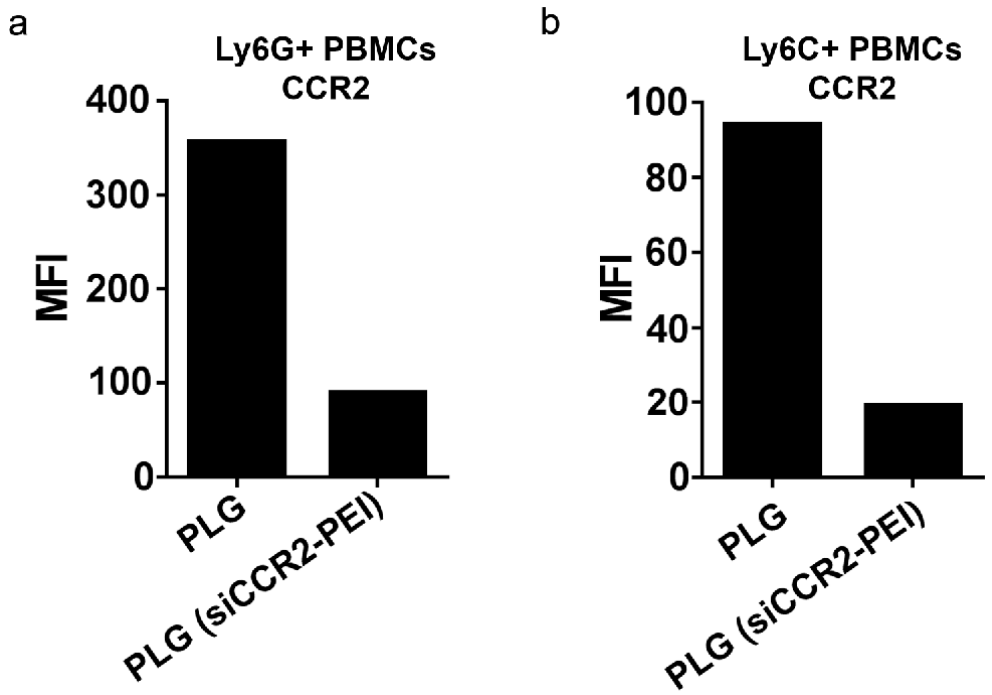

Figure 6.4 Direct measurement of encapsulated siCCR2-PEI activity *in vitro*. PBMCs isolated from EAE-immunized mice were administered either blank nanoparticles (PLG) or nanoparticles containing siCCR2 polyplexes [PLG(siCCR2-PEI)] for 24 h before CCR2 surface expression analysis by flow cytometry. (**a**) The mean fluorescence intensity of CCR2 expression among Ly6G+ PBMCs decreased from 356 to 90 between treating cells with PLG and PLG(siCCR2-PEI). (**b**) The mean fluorescence intensity of CCR2 expressing among Ly6C+ PBMCs decreased from 94 to 19 between treating cells with PLG and PLG(siCCR2-PEI).

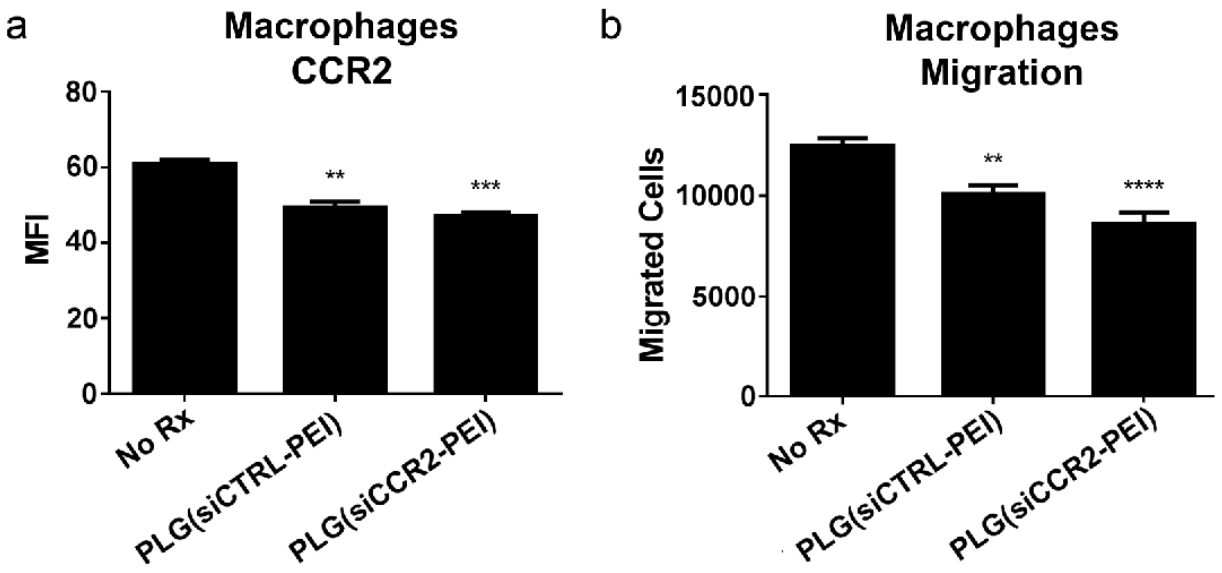

Figure 6.5 Direct measurement and functional detection of encapsulated siCCR2-PEI activity *in vitro*. (**a**) Bone marrow-derived macrophages were administered nanoparticles encapsulating either control siRNA polyplexes [PLG(siCTRL-PEI)] or siCCR2 polyplexes [PLG(siCCR2-PEI)] for 24 h before CCR2 surface expression analysis by flow cytometry. The mean fluorescence intensity of CCR2 expression among macrophages significantly decreased in response to PLG(siCTRL-PEI) and to a greater extent in response to PLG(siCCR2-PEI) compared to macrophages receiving no treatment. (**b**) The number of macrophages migrating into Transwell membranes in the presence of 100 ng/mL of CCL2. Treating macrophages with PLG(siCCR2-PEI) for 24 h prior to Transwell culture resulted in a significant decrease of migration compared to macrophages receiving no treatment. To a lesser extent, treatment with PLG(siCTRL-PEI) also significantly reduced migration compared to macrophages receiving no treatment. Data show averages of three measurements ± standard error of mean (SEM). (**$p < 0.01$, ***$p < 0.001$, 1-way ANOVA followed by the Tukey test for multiple comparisons).

6.4.4 Encapsulated siCCR2 abrogates EAE disease severity

A 1.0 mg dose of nanoparticles encapsulating siRNA was intravenously administered every other day for a total of three injections following EAE induction in C57BL/6 mice. EAE disease course proceeded similarly in all treatment groups for several days following the final injection. (**Fig 6.6)** At around Day 16, mice receiving PLG(siCTRL-PEI) began to show accelerated disease progression compared to mice receiving either PBS or PLG(siCCR2-PEI) which had more similar prognoses. However, beyond Day 30, disease progression in the PLG(siCTRL-PEI) and PBS groups had become indistinguishable, while significantly lower clinical score was observed in the PLG(siCCR2-PEI) group. These observations suggest treatment with PLG(siCCR2-PEI) provided immunosuppressive effects during a critical stage of disease development resulting in a durable abrogation of EAE clinical score.

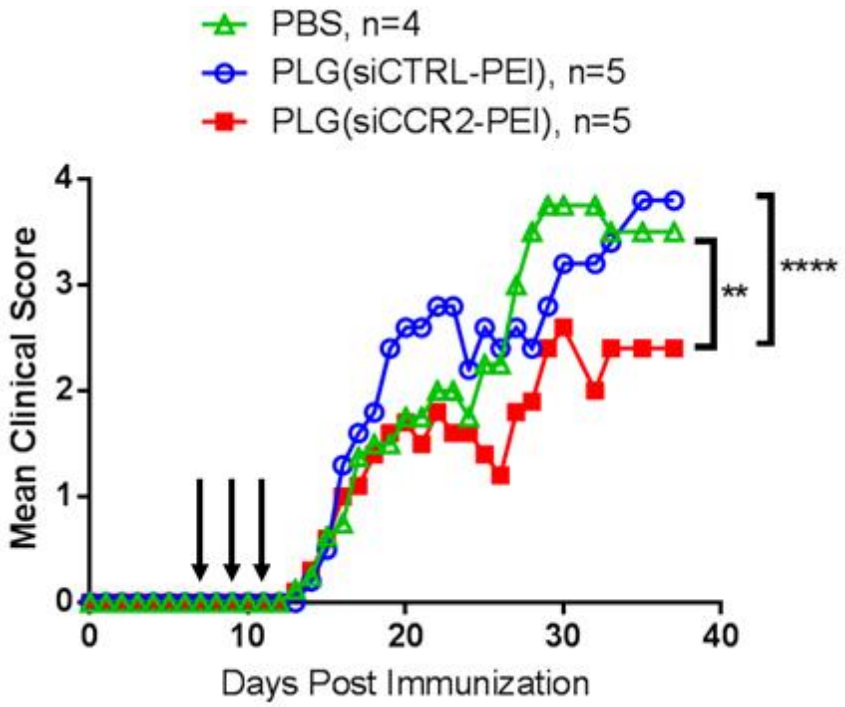

Figure 6.6 EAE disease course following multiple injections of nanoparticles encapsulating siRNA polyplexes. C57BL/6 mice received 1.0 mg injections of the appropriate nanoparticle treatment or phosphate buffer solution (PBS) on days 7, 9, and 11 following induction of EAE disease as indicated by the arrows. In the days following treatment, mice receiving PLG(siCTRL-PEI) had more rapid escalation of disease symptoms compared to the other treatment groups. In later stages of disease, the PBS-treated group also displayed severe EAE symptoms similar to mice receiving PLG(siCTRL-PEI), however, the condition of mice receiving PLG(siCCR2-PEI) stabilized with moderate disease symptoms. Data show averages of four to five mice with error bars omitted for clarity. (**$p < 0.01$, ****$p < 0.0001$, 1-way ANOVA followed by the Tukey test for multiple comparisons).

6.5 Discussion

Delivering siRNA molecules to the cytosol is critical for their proper function, and the location of their intracellular accumulation following administration is strongly influenced by physicochemical properties of the nanoparticles. After PLG nanoparticles are internalized, they are transported along the endocytic pathway, which becomes increasingly acidic in transit to the lysosome, which has an approximate pH of 4.5-5.0. [13] The decrease of pH causes the zeta potential of PLG to increase, such that an initial -15 mV at physiological pH (7.0) can become +2.5 mV at acidic pH (4.0). [140] This transition of zeta potential from negative to positive may disrupt the compartmental membrane entrapping the nanoparticles, allowing the compartmental contents which include the PLG nanoparticles to escape into the cytosol.

Despite the low encapsulation efficiency of siCCR2 molecules, we detected their activity both via direct measurement and indirect functional assays of CCR2 following nanoparticle treatment. Previous reports of delivering siRNA from PLGA nanoparticles found that treating cells with nanoparticles equivalent to 5 pmol of siRNA was sufficient for 80-90% knock-down of luciferase gene expression. [141] Our *in vitro* studies used nanoparticle concentrations of 100 μg/mL, which based on a total siRNA loading of 30.9 pmol per mg of PLG, is on the same order as 5 pmol of siRNA. Thus, the amount of siCCR2 administered *in vitro* was in good agreement with the amount others have reported using to achieve detectable siRNA activity.

The *in vivo* effects of encapsulated siCCR2 suggest a moderate therapeutic potential that may be further improved by adjusting their administration frequencies or dosage. The days on which nanoparticles were administered was determined based on previous dosing regimens. Specifically, it was reported that daily administration of 0.355 mg of blank PLG nanoparticles starting 7 days post EAE induction was effective to reduce disease severity during the acute

phase of relapse-remitting EAE. [142] Moreover, when nanoparticle administration was discontinued, the effect of the nanoparticles slowly faded such that EAE severity eventually became indistinguishable with the group not receiving nanoparticle treatment. Interestingly, we detected a persistent effect of nanoparticle treatment. One explanation for these differences may be due to our use of a chronic-progressive EAE model rather than the relapse-remitting EAE model. Morphological studies of the chronic-progressive model have shown simultaneous inflammation in the brain, spinal cord, and cerebellum while the relapse-remitting model may be characterized by waves of inflammation to the various organs of the central nervous system. [143]

Therefore we hypothesize inflammation in the chronic-progressive model is focused in the initial days of disease which were more effectively curtailed by the short course of nanoparticle treatment which reduced the occurrence of irreversible neuronal damage which occurs over a longer period of time in the relapse-remitting model. This hypothesis could be further supported by studies investigating when in the disease course neuronal damage becomes irreparable. Using siRNA to stimulate the immune system may create additional therapeutic benefits for the specific case of treating multiple sclerosis. The standard treatment of multiple sclerosis currently involves repeated injections of IFN-β which results in skin reactions at the injection site that can be severe enough to cause termination of treatment. [144] Several cell types within the immune system express Toll-like receptors (TLRs), specifically TLR3 and TLR7, which recognize double-stranded and single-stranded RNA, respectively. Activation of these TLRs would initiate signaling cascades that increase production of IFN-β. [145] While the siRNA used in this study contained the 2'-O-methyl modification which reduces immune stimulation, sequence design can be optimized to potentially trigger TLR activation. [146, 147] Using siRNA to induce

endogenous production of IFN-β may provide therapeutic effects for treating multiple sclerosis without causing skin reactions resulting from exogenous IFN-β injection.

Chapter 7: Conclusions and Future Directions

The research investigations described in the preceding chapters examined the mechanism of action used by a nanoparticle-based approach to deliver antigen-specific therapy in the treatment of autoimmune diseases. A direct mechanistic comparison was made between antigen delivery using the nanoparticle-based approach and a cell-based approach also effective for inducing antigen-specific tolerance. Considering instances in which antigen-specific tolerance is not possible or desirable, RNA interference was incorporated within the nanoparticle design to suppress the activity of specific immune signaling pathways correlated with autoimmune pathology. Herein, we discuss the major research findings and their potential implications for the drug delivery research field and development of more targeted autoimmune therapies.

7.1 Peptide-Conjugated Nanoparticles Reduce Positive Co-Stimulatory Expression and T Cell Activity to Induce Tolerance

7.1.1 Conclusions

Identifying cells with MHC-restricted antigen on the surface, and conducting analysis on this subpopulation of cells was a major novel component to this study. Previous mechanistic analyses of nanoparticle-mediated antigen delivery primarily examined co-stimulatory expression on entire populations of antigen-presenting cells (APCs). [148] Depending on the efficiency of antigen delivery and processing, such analysis may include a large number of cells unable to interact with T cells and affect the adaptive immune response. Our studies showed that nanoparticles with the highest amount of antigen coupling, administered at the highest dosage,

resulted in only about 25% of APCs with detectable levels of surface MHC-restricted antigen. The ability for APCs to signal T cells depends on engaging the T cell receptor using MHC-restricted antigen. In the absence of this interaction, levels of co-stimulatory expression on the APC are likely to be inconsequential. Thus, future studies of exogenous antigen delivery may benefit from incorporating strategies to focus analysis on cells expressing detectable levels of MHC-restricted antigen.

APCs had low efficiency of antigen presentation despite a high percentage of nanoparticle internalization. It may be useful to generate APC populations with 0%, 25%, 50% and 100% of cells expressing MHC-restricted antigen, and examine the response of T cells in co-culture. Perhaps not all APCs within the population need to present antigen in order to impact T cell response. It would be interesting to determine if the marginal increase of T cell response reaches a plateau once a certain threshold percentage of APCs expressing MHC-restricted antigen is reached in co-culture with a 2:1 T cell to APC ratio. Previous studies administering a high dose of toxin to APCs reported a positive correlation between the number of APCs and the amount of T cell proliferation which did not reach a plateau even as the T cell to APC ratio decreased from 1000:1 to 1:1, [149] suggesting that availability of MHC-restricted antigen for engaging T cell receptors is typically the limiting factor.

To achieve higher percentages of APCs expressing MHC-restricted antigen, the linker strength connecting antigen and nanoparticle could be further modulated. Reducing the linker strength could liberate additional antigen to bind MHC class II molecules during endocytic transit following nanoparticle internalization. In fact, one hypothesis for the low efficiency of antigen presentation despite the high efficiency of nanoparticle internalization is that antigen remains attached to the nanoparticle which prevents its loading onto MHC molecules. Rather the

antigen is retained in the endocytic pathway until reaching the lysosome for degradation. A reduced linker strength may be similar to the burst release phenomenon, which describes the release of a large percentage of encapsulated payload during the initial timeframe following nanoparticle reconstitution into solution. Studies of antigen-encapsulated nanoparticles with varying propensities for burst release found that nanoparticles with low burst release were more efficient for activating CD8+ T cells compared to nanoparticles with high burst release. [150] Assuming burst release is an adequate approximation for linker strength, these results would then conflict with the aforementioned hypothesis. However, there are considerable differences in the processes of antigen loading onto MHC class I molecules to signal CD8+ T cells compared to antigen loading onto MHC class II molecules to signal CD4+ T cells, and thus a similar study is needed using antigen containing MHC class II epitopes with CD4+ T cells.

The *in vitro* assays involving autoreactive T cells co-cultured with nanoparticle-treated APCs might generate a more clear readout if the T cells receive further purification prior to co-culture. The percentage of T cells in lymphoid organs specific to one particular antigen is initially very low. A moderate increase occurs when an immune response is induced against the antigen, or instead obtaining T cells from mice with transgenic T cell receptors. However, even following successive rounds of antigen stimulation *in vitro*, the percentage of antigen-specific T cells from either source does not exceed 50%. [151] Further enrichment for antigen-specific T cells may improve the readout of the antigen-specific response by removing T cells lacking specificity to the antigen. Various techniques exist to purify antigen-specific cells, although the yield and purity vary dramatically. [152] Raman spectroscopy has demonstrated the ability to distinguish subtle differences among T cells activated by different stimuli. [117] In the years

ahead, Raman spectroscopy may become a critical tool similar to flow cytometry for cell analysis and sorting, but via a label-free approach. [153]

7.1.2 Future Directions

This investigation assembled a useful set of *in vitro* assays to probe the mechanisms that may be involved in the induction of antigen-specific tolerance *in vivo*. These assays could be further assembled into an initial screening approach to explore novel nanoparticle formulations. Nanoparticles can vary in size, shape, and charge due to the fabrication process, not to mention different materials, solvents, and surface coatings. Certain combinations of these physicochemical properties and compositions may offer improved tolerance induction compared to the combinations previously explored and currently used. Testing all of these combinations *in vivo* would be infeasible, however, some of the *in vitro* assays developed here may be useful for early discovery of promising combinations for further investigation.

The number of peptide antigens with an antibody able to detect antigen loading on MHC molecules needs to be dramatically increased. Currently, the available antibodies to detect MHC-restricted antigen presentation are limited to detecting model antigens that have minimal disease relevance. Measuring levels of antigen presentation for disease-relevant antigens would improve data quality, especially as nanoparticles are used *in vivo*. The availability of an antibody library to target various disease-relevant antigens when loaded onto MHC molecules would be a major benefit to mechanistic studies of antigen-specific autoimmune therapies.

The ability to measure levels of MHC-restricted disease-relevant antigens would serve as biomarkers of nanoparticle therapeutic activity. Following nanoparticle administration, a tissue biopsy from the inflammatory site could be purified for APCs and subsequently analyzed for antigen presentation levels. Measuring the amount of antigen presentation and co-stimulatory

expression occurring in sites of inflammation, such as the central nervous system in multiple sclerosis, would be useful for fine-tuning nanoparticle dose and monitoring nanoparticle activity over time. Moreover, these antibodies may have future therapeutic applications as their attachment to disease-relevant antigen loaded onto MHC molecules may specifically disrupt the ability to activate self-reactive T cells.

7.2 The Role of NF-KB Signaling Due to Antigen-Coupled Nanoparticles or Cells Administered for Antigen-Specific T Cell Tolerance

7.2.1 Conclusions

In the presence of αCD3/αCD28, T cells co-cultured with dendritic cells administered antigen-coupled donor cells (SP-OVA) had significant reductions of several activation indicators compared to administering antigen-coupled nanoparticle (PLG-OVA) or soluble antigen (OVA). SP-OVA also reduced levels of pro-inflammatory cytokine (IFNγ) while maintaining levels of anti-inflammatory cytokine (IL-10). Together, these measurements reveal a superior capability for SP-OVA to induce tolerance compared to PLG-OVA or OVA.

A small molecule inhibitor (BAY 11-7085) of the transcription factor NF-KB was also administered in conjunction with antigen. If the improved tolerance effects of SP-OVA had occurred via increased NF-KB signaling, the presence of BAY 11-7085 would have in effect negated SP-OVA treatment resulting in T cell measurements more similar to other treatment groups. Conversely, if SP-OVA induced tolerance via decreased NF-KB signaling, the presence of BAY 11-7085 should have conferred the same advantages to OVA and PLG-OVA. However, there was minimal correlation detected when dendritic cells were administered BAY 11-7085 alongside the different antigen delivery vehicles, suggesting a limited role of NF-KB in the mechanism of tolerance resulting from SP-OVA treatment of dendritic cells. Interestingly, the T

cell response changed dramatically following macrophage treatment with BAY 11-7085 regardless of OVA, PLG-OVA, SP-OVA, suggesting an important role of NF-KB signaling in macrophages, which was confirmed by network analysis of TRanscriptional Activity CEll aRray (TRACER) studies. Network analysis of transcriptional activity in treated macrophages inferred NF-KB as a central hub within the signaling network. Due to its location within the network and based on the observed co-culture responses, we conclude NF-KB plays a critical role in macrophage signaling. This is a similar approach used by others to draw conclusions following network analysis of macrophage transcriptional regulation to focus on the importance of the central hubs. [154]

The TRACER network analysis suggested that other signaling molecules, such as those from the CEBP (CCAAT-enhancer-binding protein) family may be more involved than NF-KB to affect the cell response following SP-OVA treatment of dendritic cells. One important caveat is that the TRACER studies only examined 14 transcription factors, and there are upwards of 1,000 transcription factors in the human genome. [25] The 14 factors evaluated here were selected for their relevance to immune signaling pathways, but it is highly plausible that other signaling molecules not included in this study were triggered by SP-OVA and are important in the subsequent tolerance induction. Additional methods to provide higher analytical throughput may help to further elucidate the mechanism at work. These methods would include microarrays and CyTOF, both of which have been previously used to efficiently investigate transcriptional regulation. [155, 156]

7.2.2 Future Directions

The screening of additional small molecule inhibitors to target alternate signaling pathways may also help to elucidate additional unique tolerance mechanisms triggered by SP-

OVA and not PLG-OVA. Studies of an autoimmune response enhanced by IL-18 treatment detected therapeutic benefits from administering an inhibitor of PI 3-kinase. [122] Other small molecule inhibitors investigated included a MAPK p38 inhibitor, ERK inhibitor, and JNK inhibitor, although they did not reverse the immune response triggered by IL-18. Applying these inhibitors in the same way that BAY 11-7085 was administered to APCs alongside antigen delivery may reveal the involvement of additional signaling molecules in the tolerance mechanism.

TRACER analysis measured the activity and interactions of 14 transcription factors, however improvements to scale up TRACER are necessary to more completely profile the cell signaling response to different treatments. Currently, cells are seeded into wells, and each well receives only one specific reporter. The ability to add additional reporters to the same well would dramatically reduce the size and complexity of a TRACER experiment. This would be possible if reporters emit signal at different wavelengths that a detection instrument could discriminate, similar to the technique of multi-parameter flow cytometry.

However, a more stringent limit for combining TRACER reporters is needed relative to flow cytometry. In flow cytometry, the measured signal is introduced to cells through the various fluorescently-coupled antibodies, and the maximum number of antibodies to apply to a cell is limited by the ability to discriminate the combined signals. In TRACER and other dynamic measurement techniques, measured signal is synthesized by the cell under analysis, and the maximum number of transcription factors to analyze in a cell is limited by toxicity issues from intracellular accumulation of reporter molecules.

Additional experimental tools to dynamically detect transcription factor activity would improve TRACER analysis. These improvements would be to develop transgenic immune cells

with fluorescently-labeled transcription factors. There currently exist only a small number of transgenic mouse lines with fluorescently-labeled gene expression in hematopoietic cells, with a select few of these labeled genes being transcription factors. [157] Increasing the available number of transgenic fluorescently-labeled transcription factors would allow TRACER experiments to be run both *in vitro* and *in vivo* with greater ease. These transgenic mice would also reduce the expense and biosafety concerns of producing viral vectors, as well as the batch-to-batch variability of stable genomic integration following viral transduction. Further improvements of this transgenic approach would modify fluorescent labeling of transcription factors to be conditional with nuclear translocation in order to focus fluorescent measurement on transcription factors actively mediating gene expression.

7.3 Encapsulated CCR2-Targeting SiRNA Reduces Inflammatory Cell Migration and Disease Symptoms in Multiple Sclerosis Model

7.3.1 Conclusions

A major question resulting from this work is whether substantive additional amounts of siRNA can be further encapsulated into PLG nanoparticles. The total loading achieved here was comparable with previous reports using a similar molecular weight (5 kDa) of PLG but in the absence of PEI. [133] This study further showed that increasing to a higher molecular weight of PLG (40 kDa) with PEI resulted in twice the total siRNA loading. Using poly(lactide) nanoparticles, others have shown increasing the N:P ratio from the 8:1 used here to 16:1 results in a marginal increase of siRNA loading. While the amount of siRNA delivered was sufficient to induce a detectable response both *in vitro* and *in vivo*, it would be useful to examine possible improvements in efficacy or duration of siRNA activity due to additional loading. However, increasing polymer molecular weight is anticipated to prolong degradation time and

incorporating additional cationic polymer may create harmful aggregations with serum proteins, both of which would contribute to increased toxicity. [158] It was routinely observed *in vitro* that nanoparticle concentrations above 100 μg/mL as well as siRNA-PEI concentrations above 50 nM resulted in large reductions of cell viability.

Modifying the nanoparticle surface charge may reveal additional formulations to provide greater accumulation of siRNA in the cytosol. The accumulation of free siRNA in the cytosol is critical for its ability to function. Nanoparticle encapsulation assists with delivering siRNA to the intended tissues and cells, but siRNA must then exit the endocytic pathway, shed the nanoparticle, and disentangle from PEI to ensure proper siRNA activity. There is still much debate within the field regarding the intracellular mechanisms governing siRNA accumulation in the cytosol and the potential impacts of polymer-mediated buffering and changes to pH. [159] However, we can expect additional coatings or layers to the nanoparticle will improve their circulation time in the blood to increase targeting of inflammatory cells that contribute to autoimmunity. [160] In lieu of basic principles governing nanoparticle escape of the endocytic pathway and accumulation in the cytosol, empirical testing may be necessary to determine the most optimal formulation to address each therapeutic context.

7.3.2 Future Directions

Extending the work initiated here would involve combining siRNA delivery with antigen delivery to induce more durable, long-lasting antigen-specific immune tolerance. Based on the mechanistic studies examining intracellular and intercellular signaling, more effective tolerance induction may occur when antigen is delivered alongside siRNA molecules targeted against transcription factors, such as NF-KB and AP-1, or cytokines, such as IFN-γ and IL-2. One approach for co-delivery of antigen and siRNA would be to encapsulate siRNA molecules into

antigen-coupled nanoparticles to potentially further enhance their antigen-specific tolerance effects. But multi-functional nanoparticles may be difficult to generate with high loading of all payloads while maintaining good control over physicochemical properties. Therefore designing modular nanoparticles may be more feasible to develop further.

Modular nanoparticles for induction of immune tolerance could be synthesized to contain either antigen or siRNA only. Separating the two payloads may improve the targeting of each to the different intracellular locations necessary for each molecule's bioactivity. Antigen with class II epitopes must encounter MHC-II molecules in the endocytic pathway in order to be presented on the cell surface. In contrast, siRNA must enter the cytosol to associate with RISC in order to degrade mRNA transcripts. These final destinations are largely incompatible, as retention in the endocytic pathway to benefit antigen presentation would reduce siRNA accumulation in the cytosol, and vice versa. Thus separating these two payloads into different nanoparticles would allow physicochemical properties to be separately tuned to facilitate accumulation within the desired intracellular regions.

Modular nanoparticles would also provide greater flexibility in clinical settings that may favor the use of either antigen or siRNA only for treatment. In certain cases of autoimmunity where the risk of anaphylaxis is high or epitope spreading has already occurred, the administration of antigen may not be desirable or effective. In these cases, delivery of nanoparticles carrying siRNA only would be a more effective therapeutic option. But if the autoantigen is well-characterized and serum autoantibody levels have been determined as low, then it may be advantageous to co-deliver nanoparticles carrying antigen and siRNA to induce robust immune tolerance. This approach of developing modular nanoparticles that can be mixed together and administered as a cocktail therapy represent tailored therapeutic approaches for

specific patient needs, in line with precision medicine which will help to advance cutting-edge healthcare in the 21st century.

References

[1] S.M. Hayter, M.C. Cook, Updated assessment of the prevalence, spectrum and case definition of autoimmune disease, Autoimmunity reviews, 11 (2012) 754-765.

[2] G.S. Cooper, B.C. Stroehla, The epidemiology of autoimmune diseases, Autoimmunity reviews, 2 (2003) 119-125.

[3] B.R. Burton, G.J. Britton, H. Fang, J. Verhagen, B. Smithers, C.A. Sabatos-Peyton, L.J. Carney, J. Gough, S. Strobel, D.C. Wraith, Sequential transcriptional changes dictate safe and effective antigen-specific immunotherapy, Nature communications, 5 (2014) 4741.

[4] D.P. McCarthy, Z.N. Hunter, B. Chackerian, L.D. Shea, S.D. Miller, Targeted immunomodulation using antigen-conjugated nanoparticles, Wiley interdisciplinary reviews. Nanomedicine and nanobiotechnology, 6 (2014) 298-315.

[5] S.D. Miller, R.P. Wetzig, H.N. Claman, The induction of cell-mediated immunity and tolerance with protein antigens coupled to syngeneic lymphoid cells, The Journal of experimental medicine, 149 (1979) 758-773.

[6] D.M. Turley, S.D. Miller, Peripheral tolerance induction using ethylenecarbodiimide-fixed APCs uses both direct and indirect mechanisms of antigen presentation for prevention of experimental autoimmune encephalomyelitis, Journal of immunology, 178 (2007) 2212-2220.

[7] J.Q. Chen, P. Szodoray, M. Zeher, Toll-Like Receptor Pathways in Autoimmune Diseases, Clinical reviews in allergy & immunology, 50 (2016) 1-17.

[8] S. McComb, A. Thiriot, L. Krishnan, F. Stark, Introduction to the immune system, Methods in molecular biology, 1061 (2013) 1-20.

[9] T. Lammermann, M. Sixt, The microanatomy of T-cell responses, Immunological reviews, 221 (2008) 26-43.

[10] J.A. Hoffmann, F.C. Kafatos, C.A. Janeway, R.A. Ezekowitz, Phylogenetic perspectives in innate immunity, Science, 284 (1999) 1313-1318.

[11] J.M. Blander, R. Medzhitov, On regulation of phagosome maturation and antigen presentation, Nature immunology, 7 (2006) 1029-1035.

[12] A. Amash, L. Wang, Y. Wang, V. Bhakta, G.D. Fairn, M. Hou, J. Peng, W.P. Sheffield, A.H. Lazarus, CD44 Antibody Inhibition of Macrophage Phagocytosis Targets Fcgamma Receptor- and Complement Receptor 3-Dependent Mechanisms, Journal of immunology, 196 (2016) 3331-3340.

[13] I. Mellman, R. Fuchs, A. Helenius, Acidification of the endocytic and exocytic pathways, Annual review of biochemistry, 55 (1986) 663-700.

[14] E.S. Trombetta, I. Mellman, Cell biology of antigen processing in vitro and in vivo, Annual review of immunology, 23 (2005) 975-1028.

[15] A.M. Norment, R.D. Salter, P. Parham, V.H. Engelhard, D.R. Littman, Cell-cell adhesion mediated by CD8 and MHC class I molecules, Nature, 336 (1988) 79-81.

[16] J. Lustgarten, T. Waks, Z. Eshhar, CD4 and CD8 accessory molecules function through interactions with major histocompatibility complex molecules which are not directly associated with the T cell receptor-antigen complex, European journal of immunology, 21 (1991) 2507-2515.

[17] B. Malissen, C. Gregoire, M. Malissen, R. Roncagalli, Integrative biology of T cell activation, Nature immunology, 15 (2014) 790-797.

[18] R.H. Schwartz, A cell culture model for T lymphocyte clonal anergy, Science, 248 (1990) 1349-1356.

[19] C.A. Chambers, J.P. Allison, Co-stimulation in T cell responses, Current opinion in immunology, 9 (1997) 396-404.

[20] L.M. Francisco, P.T. Sage, A.H. Sharpe, The PD-1 pathway in tolerance and autoimmunity, Immunological reviews, 236 (2010) 219-242.

[21] K. Inaba, S. Turley, F. Yamaide, T. Iyoda, K. Mahnke, M. Inaba, M. Pack, M. Subklewe, B. Sauter, D. Sheff, M. Albert, N. Bhardwaj, I. Mellman, R.M. Steinman, Efficient presentation of phagocytosed cellular fragments on the major histocompatibility complex class II products of dendritic cells, The Journal of experimental medicine, 188 (1998) 2163-2173.

[22] A. Mantovani, A. Sica, M. Locati, Macrophage polarization comes of age, Immunity, 23 (2005) 344-346.

[23] T. Oth, J. Vanderlocht, C.H. Van Elssen, G.M. Bos, W.T. Germeraad, Pathogen-Associated Molecular Patterns Induced Crosstalk between Dendritic Cells, T Helper Cells, and Natural Killer Helper Cells Can Improve Dendritic Cell Vaccination, Mediators of inflammation, 2016 (2016) 5740373.

[24] J.A. Stenken, A.J. Poschenrieder, Bioanalytical chemistry of cytokines--a review, Analytica chimica acta, 853 (2015) 95-115.

[25] J.M. Vaquerizas, S.K. Kummerfeld, S.A. Teichmann, N.M. Luscombe, A census of human transcription factors: function, expression and evolution, Nature reviews. Genetics, 10 (2009) 252-263.

[26] E. Bernstein, A.A. Caudy, S.M. Hammond, G.J. Hannon, Role for a bidentate ribonuclease in the initiation step of RNA interference, Nature, 409 (2001) 363-366.

[27] A. Choo, P. Palladinetti, T. Holmes, S. Basu, S. Shen, R.B. Lock, T.A. O'Brien, G. Symonds, A. Dolnikov, siRNA targeting the IRF2 transcription factor inhibits leukaemic cell growth, International journal of oncology, 33 (2008) 175-183.

[28] T.A.D.C. Committee, Progress in Autoimmune Diseases Research, in: D.o.H.a.H. Services (Ed.), National Institutes of Health, 2005.

[29] S. Gupta, A.G. Louis, Tolerance and autoimmunity in primary immunodeficiency disease: a comprehensive review, Clinical reviews in allergy & immunology, 45 (2013) 162-169.

[30] R. Medzhitov, Toll-like receptors and innate immunity, Nature reviews. Immunology, 1 (2001) 135-145.

[31] L.S. Walker, A.K. Abbas, The enemy within: keeping self-reactive T cells at bay in the periphery, Nature reviews. Immunology, 2 (2002) 11-19.

[32] A. O'Garra, P. Vieira, Regulatory T cells and mechanisms of immune system control, Nature medicine, 10 (2004) 801-805.

[33] S. Hong, L. Van Kaer, Immune privilege: keeping an eye on natural killer T cells, The Journal of experimental medicine, 190 (1999) 1197-1200.

[34] L. Xerri, E. Devilard, J. Hassoun, C. Mawas, F. Birg, Fas ligand is not only expressed in immune privileged human organs but is also coexpressed with Fas in various epithelial tissues, Molecular pathology : MP, 50 (1997) 87-91.

[35] A.G. Sener, I. Afsar, Infection and autoimmune disease, Rheumatology international, 32 (2012) 3331-3338.

[36] R.S. Fujinami, M.G. von Herrath, U. Christen, J.L. Whitton, Molecular mimicry, bystander activation, or viral persistence: infections and autoimmune disease, Clinical microbiology reviews, 19 (2006) 80-94.

[37] J.A. Bluestone, H. Bour-Jordan, Current and future immunomodulation strategies to restore tolerance in autoimmune diseases, Cold Spring Harbor perspectives in biology, 4 (2012).

[38] D. Dix, S. Cellot, V. Price, B. Gillmeister, M.C. Ethier, D.L. Johnston, V. Lewis, B. Michon, D. Mitchell, K. Stobart, R. Yanofsky, C. Portwine, M. Silva, L. Bowes, S. Zelcer, J. Brossard, J. Traubici, U. Allen, J. Beyene, L. Sung, Association between corticosteroids and infection, sepsis, and infectious death in pediatric acute myeloid leukemia (AML): results from the Canadian infections in AML research group, Clinical infectious diseases : an official publication of the Infectious Diseases Society of America, 55 (2012) 1608-1614.

[39] D. Karussis, The diagnosis of multiple sclerosis and the various related demyelinating syndromes: a critical review, Journal of autoimmunity, 48-49 (2014) 134-142.

[40] L. Adorini, Cytokine-based immunointervention in the treatment of autoimmune diseases, Clinical and experimental immunology, 132 (2003) 185-192.

[41] R. Aharoni, R. Eilam, A. Stock, A. Vainshtein, E. Shezen, H. Gal, N. Friedman, R. Arnon, Glatiramer acetate reduces Th-17 inflammation and induces regulatory T-cells in the CNS of mice with relapsing-remitting or chronic EAE, Journal of neuroimmunology, 225 (2010) 100-111.

[42] L. La Mantia, C. Di Pietrantonj, M. Rovaris, G. Rigon, S. Frau, F. Berardo, A. Gandini, A. Longobardi, B. Weinstock-Guttman, A. Vaona, Interferons-beta versus glatiramer acetate for relapsing-remitting multiple sclerosis, The Cochrane database of systematic reviews, 11 (2016) CD009333.

[43] P. Rao, B.M. Segal, Experimental autoimmune encephalomyelitis, Methods in molecular biology, 900 (2012) 363-380.

[44] R.M. Ransohoff, B. Engelhardt, The anatomical and cellular basis of immune surveillance in the central nervous system, Nature reviews. Immunology, 12 (2012) 623-635.

[45] E.L. Sauer, N.C. Cloake, J.M. Greer, Taming the TCR: antigen-specific immunotherapeutic agents for autoimmune diseases, International reviews of immunology, 34 (2015) 460-485.

[46] A.A. Vandenbark, B. Celnik, M. Vainiene, S.D. Miller, H. Offner, Myelin antigen-coupled splenocytes suppress experimental autoimmune encephalomyelitis in Lewis rats through a partially reversible anergy mechanism, Journal of immunology, 155 (1995) 5861-5867.

[47] X.M. Su, S. Sriram, Treatment of chronic relapsing experimental allergic encephalomyelitis with the intravenous administration of splenocytes coupled to encephalitogenic peptide 91-103 of myelin basic protein, Journal of neuroimmunology, 34 (1991) 181-190.

[48] D.R. Getts, D.M. Turley, C.E. Smith, C.T. Harp, D. McCarthy, E.M. Feeney, M.T. Getts, A.J. Martin, X. Luo, R.L. Terry, N.J. King, S.D. Miller, Tolerance induced by apoptotic antigen-coupled leukocytes is induced by PD-L1+ and IL-10-producing splenic macrophages and maintained by T regulatory cells, Journal of immunology, 187 (2011) 2405-2417.

[49] A. Lutterotti, S. Yousef, A. Sputtek, K.H. Sturner, J.P. Stellmann, P. Breiden, S. Reinhardt, C. Schulze, M. Bester, C. Heesen, S. Schippling, S.D. Miller, M. Sospedra, R. Martin, Antigen-specific tolerance by autologous myelin peptide-coupled cells: a phase 1 trial in multiple sclerosis, Science translational medicine, 5 (2013) 188ra175.

[50] D.R. Getts, A.J. Martin, D.P. McCarthy, R.L. Terry, Z.N. Hunter, W.T. Yap, M.T. Getts, M. Pleiss, X. Luo, N.J. King, L.D. Shea, S.D. Miller, Microparticles bearing encephalitogenic peptides induce T-cell tolerance and ameliorate experimental autoimmune encephalomyelitis, Nature biotechnology, 30 (2012) 1217-1224.

[51] N. Huebsch, D.J. Mooney, Inspiration and application in the evolution of biomaterials, Nature, 462 (2009) 426-432.

[52] R. Langer, Biomaterials and biotechnology: from the discovery of the first angiogenesis inhibitors to the development of controlled drug delivery systems and the foundation of tissue engineering, Journal of biomedical materials research. Part A, 101 (2013) 2449-2455.

[53] K. Park, Controlled drug delivery systems: past forward and future back, Journal of controlled release : official journal of the Controlled Release Society, 190 (2014) 3-8.

[54] M. Goldberg, I. Gomez-Orellana, Challenges for the oral delivery of macromolecules, Nature reviews. Drug discovery, 2 (2003) 289-295.

[55] A.C. Anselmo, S. Mitragotri, An overview of clinical and commercial impact of drug delivery systems, Journal of controlled release : official journal of the Controlled Release Society, 190 (2014) 15-28.

[56] J. Panyam, V. Labhasetwar, Biodegradable nanoparticles for drug and gene delivery to cells and tissue, Advanced drug delivery reviews, 55 (2003) 329-347.

[57] M.L. Etheridge, S.A. Campbell, A.G. Erdman, C.L. Haynes, S.M. Wolf, J. McCullough, The big picture on nanomedicine: the state of investigational and approved nanomedicine products, Nanomedicine : nanotechnology, biology, and medicine, 9 (2013) 1-14.

[58] P. Sahdev, L.J. Ochyl, J.J. Moon, Biomaterials for nanoparticle vaccine delivery systems, Pharmaceutical research, 31 (2014) 2563-2582.

[59] F. Danhier, E. Ansorena, J.M. Silva, R. Coco, A. Le Breton, V. Preat, PLGA-based nanoparticles: an overview of biomedical applications, Journal of controlled release : official journal of the Controlled Release Society, 161 (2012) 505-522.

[60] I.D. Rosca, F. Watari, M. Uo, Microparticle formation and its mechanism in single and double emulsion solvent evaporation, Journal of controlled release : official journal of the Controlled Release Society, 99 (2004) 271-280.

[61] E. Cohen-Sela, S. Teitlboim, M. Chorny, N. Koroukhov, H.D. Danenberg, J. Gao, G. Golomb, Single and double emulsion manufacturing techniques of an amphiphilic drug in PLGA nanoparticles: formulations of mithramycin and bioactivity, Journal of pharmaceutical sciences, 98 (2009) 1452-1462.

[62] R. Liang, J. Zhu, Monodisperse PLA/PLGA nanoparticle fabrication through a surfactant-free route, Journal of controlled release : official journal of the Controlled Release Society, 152 Suppl 1 (2011) e129-131.

[63] C.G. Oster, T. Kissel, Comparative study of DNA encapsulation into PLGA microparticles using modified double emulsion methods and spray drying techniques, Journal of microencapsulation, 22 (2005) 235-244.

[64] Y. Xu, C.S. Kim, D.M. Saylor, D. Koo, Polymer degradation and drug delivery in PLGA-based drug-polymer applications: A review of experiments and theories, Journal of biomedical materials research. Part B, Applied biomaterials, (2016).

[65] M.J. Alonso, R.K. Gupta, C. Min, G.R. Siber, R. Langer, Biodegradable microspheres as controlled-release tetanus toxoid delivery systems, Vaccine, 12 (1994) 299-306.

[66] M.S. Shive, J.M. Anderson, Biodegradation and biocompatibility of PLA and PLGA microspheres, Advanced drug delivery reviews, 28 (1997) 5-24.

[67] C.E. Holy, S.M. Dang, J.E. Davies, M.S. Shoichet, In vitro degradation of a novel poly(lactide-co-glycolide) 75/25 foam, Biomaterials, 20 (1999) 1177-1185.

[68] B.S. Zolnik, D.J. Burgess, Effect of acidic pH on PLGA microsphere degradation and release, Journal of controlled release : official journal of the Controlled Release Society, 122 (2007) 338-344.

[69] N. Grabowski, H. Hillaireau, J. Vergnaud, L.A. Santiago, S. Kerdine-Romer, M. Pallardy, N. Tsapis, E. Fattal, Toxicity of surface-modified PLGA nanoparticles toward lung alveolar epithelial cells, International journal of pharmaceutics, 454 (2013) 686-694.

[70] J. Tulinska, A. Kazimirova, M. Kuricova, M. Barancokova, A. Liskova, E. Neubauerova, M. Drlickova, F. Ciampor, I. Vavra, D. Bilanicova, G. Pojana, M. Staruchova, M. Horvathova, E. Jahnova, K. Volkovova, M. Bartusova, M. Cagalinec, M. Dusinska, Immunotoxicity and genotoxicity testing of PLGA-PEO nanoparticles in human blood cell model, Nanotoxicology, 9 Suppl 1 (2015) 33-43.

[71] B.S. Zolnik, A. Gonzalez-Fernandez, N. Sadrieh, M.A. Dobrovolskaia, Nanoparticles and the immune system, Endocrinology, 151 (2010) 458-465.

[72] S.K. Sahoo, J. Panyam, S. Prabha, V. Labhasetwar, Residual polyvinyl alcohol associated with poly (D,L-lactide-co-glycolide) nanoparticles affects their physical properties and cellular uptake, Journal of controlled release : official journal of the Controlled Release Society, 82 (2002) 105-114.

[73] M.J. Heslinga, G.M. Willis, D.J. Sobczynski, A.J. Thompson, O. Eniola-Adefeso, One-step fabrication of agent-loaded biodegradable microspheroids for drug delivery and imaging applications, Colloids and surfaces. B, Biointerfaces, 116 (2014) 55-62.

[74] W.Y. Liao, H.J. Li, M.Y. Chang, A.C. Tang, A.S. Hoffman, P.C. Hsieh, Comprehensive characterizations of nanoparticle biodistribution following systemic injection in mice, Nanoscale, 5 (2013) 11079-11086.

[75] A.K. Mohammad, J.J. Reineke, Quantitative detection of PLGA nanoparticle degradation in tissues following intravenous administration, Molecular pharmaceutics, 10 (2013) 2183-2189.

[76] G. Cappellano, A.D. Woldetsadik, E. Orilieri, Y. Shivakumar, M. Rizzi, F. Carniato, C.L. Gigliotti, E. Boggio, N. Clemente, C. Comi, C. Dianzani, R. Boldorini, A. Chiocchetti, F. Reno, U. Dianzani, Subcutaneous inverse vaccination with PLGA particles loaded with a MOG peptide and IL-10 decreases the severity of experimental autoimmune encephalomyelitis, Vaccine, 32 (2014) 5681-5689.

[77] N. Aghdami, F. Gharibdoost, S.M. Moazzeni, Experimental autoimmune encephalomyelitis (EAE) induced by antigen pulsed dendritic cells in the C57BL/6 mouse: influence of injection

route, Experimental animals / Japanese Association for Laboratory Animal Science, 57 (2008) 45-55.

[78] R. Nicolete, D.F. dos Santos, L.H. Faccioli, The uptake of PLGA micro or nanoparticles by macrophages provokes distinct in vitro inflammatory response, International immunopharmacology, 11 (2011) 1557-1563.

[79] A. Haddadi, P. Elamanchili, A. Lavasanifar, S. Das, J. Shapiro, J. Samuel, Delivery of rapamycin by PLGA nanoparticles enhances its suppressive activity on dendritic cells, Journal of biomedical materials research. Part A, 84 (2008) 885-898.

[80] J.A. Hubbell, S.N. Thomas, M.A. Swartz, Materials engineering for immunomodulation, Nature, 462 (2009) 449-460.

[81] R.A. Maldonado, R.A. LaMothe, J.D. Ferrari, A.H. Zhang, R.J. Rossi, P.N. Kolte, A.P. Griset, C. O'Neil, D.H. Altreuter, E. Browning, L. Johnston, O.C. Farokhzad, R. Langer, D.W. Scott, U.H. von Andrian, T.K. Kishimoto, Polymeric synthetic nanoparticles for the induction of antigen-specific immunological tolerance, Proceedings of the National Academy of Sciences of the United States of America, 112 (2015) E156-165.

[82] M. Gharagozloo, S. Majewski, M. Foldvari, Therapeutic applications of nanomedicine in autoimmune diseases: From immunosuppression to tolerance induction, Nanomedicine : nanotechnology, biology, and medicine, (2015).

[83] A. Boster, G. Edan, E. Frohman, A. Javed, O. Stuve, A. Tselis, H. Weiner, B. Weinstock-Guttman, O. Khan, D.o.N.W.S.U.S.o.M. Multiple Sclerosis Clinical Research Center, Intense immunosuppression in patients with rapidly worsening multiple sclerosis: treatment guidelines for the clinician, The Lancet. Neurology, 7 (2008) 173-183.

[84] A. Winkelmann, M. Loebermann, E.C. Reisinger, U.K. Zettl, Multiple sclerosis treatment and infectious issues: update 2013, Clinical and experimental immunology, 175 (2014) 425-438.

[85] S.D. Miller, W.J. Karpus, T.S. Davidson, Experimental autoimmune encephalomyelitis in the mouse, Current protocols in immunology / edited by John E. Coligan ... [et al.], Chapter 15 (2010) Unit 15 11.

[86] E.R. Mari, J.N. Moore, G.X. Zhang, A. Rostami, Mechanisms of immunological tolerance in central nervous system inflammatory demyelination, Clinical & experimental neuroimmunology, 6 (2015) 264-274.

[87] N.D. Pennock, J.T. White, E.W. Cross, E.E. Cheney, B.A. Tamburini, R.M. Kedl, T cell responses: naive to memory and everything in between, Advances in physiology education, 37 (2013) 273-283.

[88] R. Elgueta, M.J. Benson, V.C. de Vries, A. Wasiuk, Y. Guo, R.J. Noelle, Molecular mechanism and function of CD40/CD40L engagement in the immune system, Immunological reviews, 229 (2009) 152-172.

[89] J. Bryant, K.A. Hlavaty, X. Zhang, W.T. Yap, L. Zhang, L.D. Shea, X. Luo, Nanoparticle delivery of donor antigens for transplant tolerance in allogeneic islet transplantation, Biomaterials, 35 (2014) 8887-8894.

[90] R.M. Boehler, R. Kuo, S. Shin, A.G. Goodman, M.A. Pilecki, R.M. Gower, J.N. Leonard, L.D. Shea, Lentivirus delivery of IL-10 to promote and sustain macrophage polarization towards an anti-inflammatory phenotype, Biotechnology and bioengineering, 111 (2014) 1210-1221.

[91] E. Gianchecchi, D.V. Delfino, A. Fierabracci, Recent insights into the role of the PD-1/PD-L1 pathway in immunological tolerance and autoimmunity, Autoimmunity reviews, 12 (2013) 1091-1100.

[92] Z. Hunter, D.P. McCarthy, W.T. Yap, C.T. Harp, D.R. Getts, L.D. Shea, S.D. Miller, A biodegradable nanoparticle platform for the induction of antigen-specific immune tolerance for treatment of autoimmune disease, ACS nano, 8 (2014) 2148-2160.

[93] B. Penalver Bernabe, S. Shin, P.D. Rios, L.J. Broadbelt, L.D. Shea, S.K. Seidlits, Dynamic transcription factor activity networks in response to independently altered mechanical and adhesive microenvironmental cues, Integrative biology : quantitative biosciences from nano to macro, 8 (2016) 844-860.

[94] G.K. Smyth, J. Michaud, H.S. Scott, Use of within-array replicate spots for assessing differential expression in microarray experiments, Bioinformatics, 21 (2005) 2067-2075.

[95] D.B. Murphy, D. Lo, S. Rath, R.L. Brinster, R.A. Flavell, A. Slanetz, C.A. Janeway, Jr., A novel MHC class II epitope expressed in thymic medulla but not cortex, Nature, 338 (1989) 765-768.

[96] C.L. Vanderlugt, S.D. Miller, Epitope spreading in immune-mediated diseases: implications for immunotherapy, Nature reviews. Immunology, 2 (2002) 85-95.

[97] L. Cavone, B. Peruzzi, R. Caporale, A. Chiarugi, Long-term suppression of EAE relapses by pharmacological impairment of epitope spreading, British journal of pharmacology, 171 (2014) 1501-1509.

[98] J.J. O'Shea, R. Plenge, JAK and STAT signaling molecules in immunoregulation and immune-mediated disease, Immunity, 36 (2012) 542-550.

[99] W.B. Wang, D.E. Levy, C.K. Lee, STAT3 negatively regulates type I IFN-mediated antiviral response, Journal of immunology, 187 (2011) 2578-2585.

[100] Y. Sun, J. Sun, T. Tomomi, E. Nieves, N. Mathewson, H. Tamaki, R. Evers, P. Reddy, PU.1-dependent transcriptional regulation of miR-142 contributes to its hematopoietic cell-specific expression and modulation of IL-6, Journal of immunology, 190 (2013) 4005-4013.

[101] M. Nakayama, Antigen Presentation by MHC-Dressed Cells, Frontiers in immunology, 5 (2014) 672.

[102] H. Shen, A.L. Ackerman, V. Cody, A. Giodini, E.R. Hinson, P. Cresswell, R.L. Edelson, W.M. Saltzman, D.J. Hanlon, Enhanced and prolonged cross-presentation following endosomal escape of exogenous antigens encapsulated in biodegradable nanoparticles, Immunology, 117 (2006) 78-88.

[103] S. Hirosue, I.C. Kourtis, A.J. van der Vlies, J.A. Hubbell, M.A. Swartz, Antigen delivery to dendritic cells by poly(propylene sulfide) nanoparticles with disulfide conjugated peptides: Cross-presentation and T cell activation, Vaccine, 28 (2010) 7897-7906.

[104] F. Ronchi, C. Basso, S. Preite, A. Reboldi, D. Baumjohann, L. Perlini, A. Lanzavecchia, F. Sallusto, Experimental priming of encephalitogenic Th1/Th17 cells requires pertussis toxin-driven IL-1beta production by myeloid cells, Nature communications, 7 (2016) 11541.

[105] H. Zhou, Y. Wang, Q. Lian, B. Yang, Y. Ma, X. Wu, S. Sun, Y. Liu, B. Sun, Differential IL-10 production by DCs determines the distinct adjuvant effects of LPS and PTX in EAE induction, European journal of immunology, 44 (2014) 1352-1362.

[106] R.M. Steinman, D. Hawiger, M.C. Nussenzweig, Tolerogenic dendritic cells, Annual review of immunology, 21 (2003) 685-711.

[107] J.A. Quaresma, G.T. Yoshikawa, R.V. Koyama, G.A. Dias, S. Fujihara, H.T. Fuzii, HTLV-1, Immune Response and Autoimmunity, Viruses, 8 (2015).

[108] R.W. Nelson, D. Beisang, N.J. Tubo, T. Dileepan, D.L. Wiesner, K. Nielsen, M. Wuthrich, B.S. Klein, D.I. Kotov, J.A. Spanier, B.T. Fife, J.J. Moon, M.K. Jenkins, T cell receptor cross-reactivity between similar foreign and self peptides influences naive cell population size and autoimmunity, Immunity, 42 (2015) 95-107.

[109] S.I. Mannering, J. Zhong, C. Cheers, T-cell activation, proliferation and apoptosis in primary Listeria monocytogenes infection, Immunology, 106 (2002) 87-95.

[110] S. Spath, J. Komuczki, M. Hermann, P. Pelczar, F. Mair, B. Schreiner, B. Becher, Dysregulation of the Cytokine GM-CSF Induces Spontaneous Phagocyte Invasion and Immunopathology in the Central Nervous System, Immunity, 46 (2017) 245-260.

[111] L. Northrup, M.A. Christopher, B.P. Sullivan, C. Berkland, Combining antigen and immunomodulators: Emerging trends in antigen-specific immunotherapy for autoimmunity, Advanced drug delivery reviews, 98 (2016) 86-98.

[112] M.T. Krishna, A.P. Huissoon, Clinical immunology review series: an approach to desensitization, Clinical and experimental immunology, 163 (2011) 131-146.

[113] D.P. McCarthy, J. Bryant, J.P. Galvin, S.D. Miller, X. Luo, Tempering Allorecognition to Induce Transplant Tolerance With Chemically Modified Apoptotic Donor Cells, American journal of transplantation : official journal of the American Society of Transplantation and the American Society of Transplant Surgeons, (2015).

[114] P. Saas, E. Daguindau, S. Perruche, Concise Review: Apoptotic Cell-Based Therapies-Rationale, Preclinical Results and Future Clinical Developments, Stem cells, 34 (2016) 1464-1473.

[115] K. Inaba, M. Inaba, N. Romani, H. Aya, M. Deguchi, S. Ikehara, S. Muramatsu, R.M. Steinman, Generation of large numbers of dendritic cells from mouse bone marrow cultures supplemented with granulocyte/macrophage colony-stimulating factor, The Journal of experimental medicine, 176 (1992) 1693-1702.

[116] A.M. Rasmussen, G. Borelli, H.J. Hoel, K. Lislerud, G. Gaudernack, G. Kvalheim, T. Aarvak, Ex vivo expansion protocol for human tumor specific T cells for adoptive T cell therapy, Journal of immunological methods, 355 (2010) 52-60.

[117] K.L. Brown, O.Y. Palyvoda, J.S. Thakur, S.L. Nehlsen-Cannarella, O.R. Fagoaga, S.A. Gruber, G.W. Auner, Differentiation of alloreactive versus CD3/CD28 stimulated T-lymphocytes using Raman spectroscopy: a greater specificity for noninvasive acute renal allograft rejection detection, Cytometry. Part A : the journal of the International Society for Analytical Cytology, 75 (2009) 917-923.

[118] D.M. Lindell, T.A. Moore, R.A. McDonald, G.B. Toews, G.B. Huffnagle, Distinct compartmentalization of CD4+ T-cell effector function versus proliferative capacity during pulmonary cryptococcosis, The American journal of pathology, 168 (2006) 847-855.

[119] B. Haastert, R.J. Mellanby, S.M. Anderton, R.A. O'Connor, T cells at the site of autoimmune inflammation show increased potential for trogocytosis, PloS one, 8 (2013) e81404.

[120] J. Zhang, K.V. Salojin, T.L. Delovitch, CD28 co-stimulation restores T cell responsiveness in NOD mice by overcoming deficiencies in Rac-1/p38 mitogen-activated protein kinase signaling and IL-2 and IL-4 gene transcription, International immunology, 13 (2001) 377-384.

[121] E. Toubi, Y. Shoenfeld, Toll-like receptors and their role in the development of autoimmune diseases, Autoimmunity, 37 (2004) 183-188.

[122] S.M. Dai, H. Matsuno, H. Nakamura, K. Nishioka, K. Yudoh, Interleukin-18 enhances monocyte tumor necrosis factor alpha and interleukin-1beta production induced by direct contact with T lymphocytes: implications in rheumatoid arthritis, Arthritis and rheumatism, 50 (2004) 432-443.

[123] N. Ade, D. Antonios, S. Kerdine-Romer, F. Boisleve, F. Rousset, M. Pallardy, NF-kappaB plays a major role in the maturation of human dendritic cells induced by NiSO(4) but not by DNCB, Toxicological sciences : an official journal of the Society of Toxicology, 99 (2007) 488-501.

[124] A.E. Morelli, A.T. Larregina, W.J. Shufesky, A.F. Zahorchak, A.J. Logar, G.D. Papworth, Z. Wang, S.C. Watkins, L.D. Falo, Jr., A.W. Thomson, Internalization of circulating apoptotic cells by splenic marginal zone dendritic cells: dependence on complement receptors and effect on cytokine production, Blood, 101 (2003) 611-620.

[125] M. Elsabahy, K.L. Wooley, Cytokines as biomarkers of nanoparticle immunotoxicity, Chemical Society reviews, 42 (2013) 5552-5576.

[126] K. Schinnerling, P. Garcia-Gonzalez, J.C. Aguillon, Gene Expression Profiling of Human Monocyte-derived Dendritic Cells - Searching for Molecular Regulators of Tolerogenicity, Frontiers in immunology, 6 (2015) 528.

[127] G.J. Hannon, J.J. Rossi, Unlocking the potential of the human genome with RNA interference, Nature, 431 (2004) 371-378.

[128] A.A. Seyhan, RNAi: a potential new class of therapeutic for human genetic disease, Human genetics, 130 (2011) 583-605.

[129] K. Garber, Worth the RISC?, Nature biotechnology, (2017).

[130] J. Lieberman, E. Song, S.K. Lee, P. Shankar, Interfering with disease: opportunities and roadblocks to harnessing RNA interference, Trends in molecular medicine, 9 (2003) 397-403.

[131] K.A. Whitehead, R. Langer, D.G. Anderson, Knocking down barriers: advances in siRNA delivery, Nature reviews. Drug discovery, 8 (2009) 129-138.

[132] D.J. Gary, N. Puri, Y.Y. Won, Polymer-based siRNA delivery: perspectives on the fundamental and phenomenological distinctions from polymer-based DNA delivery, Journal of controlled release : official journal of the Controlled Release Society, 121 (2007) 64-73.

[133] Y. Patil, J. Panyam, Polymeric nanoparticles for siRNA delivery and gene silencing, International journal of pharmaceutics, 367 (2009) 195-203.

[134] T. Brunner, S. Cohen, A. Monsonego, Silencing of proinflammatory genes targeted to peritoneal-residing macrophages using siRNA encapsulated in biodegradable microspheres, Biomaterials, 31 (2010) 2627-2636.

[135] B.C. te Boekhorst, L.B. Jensen, S. Colombo, A.K. Varkouhi, R.M. Schiffelers, T. Lammers, G. Storm, H.M. Nielsen, G.J. Strijkers, C. Foged, K. Nicolay, MRI-assessed therapeutic effects of locally administered PLGA nanoparticles loaded with anti-inflammatory siRNA in a murine arthritis model, Journal of controlled release : official journal of the Controlled Release Society, 161 (2012) 772-780.

[136] R.M. Ruggieri, N. Settipani, L. Viviano, M. Attanasio, L. Giglia, P. Almasio, V. La Bella, F. Piccoli, Long-term interferon-beta treatment for multiple sclerosis, Neurological sciences : official journal of the Italian Neurological Society and of the Italian Society of Clinical Neurophysiology, 24 (2003) 361-364.

[137] B. Ajami, J.L. Bennett, C. Krieger, K.M. McNagny, F.M. Rossi, Infiltrating monocytes trigger EAE progression, but do not contribute to the resident microglia pool, Nature neuroscience, 14 (2011) 1142-1149.

[138] B.T. Fife, G.B. Huffnagle, W.A. Kuziel, W.J. Karpus, CC chemokine receptor 2 is critical for induction of experimental autoimmune encephalomyelitis, The Journal of experimental medicine, 192 (2000) 899-905.

[139] F. Leuschner, P. Dutta, R. Gorbatov, T.I. Novobrantseva, J.S. Donahoe, G. Courties, K.M. Lee, J.I. Kim, J.F. Markmann, B. Marinelli, P. Panizzi, W.W. Lee, Y. Iwamoto, S. Milstein, H. Epstein-Barash, W. Cantley, J. Wong, V. Cortez-Retamozo, A. Newton, K. Love, P. Libby, M.J. Pittet, F.K. Swirski, V. Koteliansky, R. Langer, R. Weissleder, D.G. Anderson, M. Nahrendorf, Therapeutic siRNA silencing in inflammatory monocytes in mice, Nature biotechnology, 29 (2011) 1005-1010.

[140] J. Panyam, W.Z. Zhou, S. Prabha, S.K. Sahoo, V. Labhasetwar, Rapid endo-lysosomal escape of poly(DL-lactide-co-glycolide) nanoparticles: implications for drug and gene delivery, FASEB journal : official publication of the Federation of American Societies for Experimental Biology, 16 (2002) 1217-1226.

[141] J. Nguyen, T.W. Steele, O. Merkel, R. Reul, T. Kissel, Fast degrading polyesters as siRNA nano-carriers for pulmonary gene therapy, Journal of controlled release : official journal of the Controlled Release Society, 132 (2008) 243-251.

[142] D.R. Getts, R.L. Terry, M.T. Getts, C. Deffrasnes, M. Muller, C. van Vreden, T.M. Ashhurst, B. Chami, D. McCarthy, H. Wu, J. Ma, A. Martin, L.D. Shae, P. Witting, G.S. Kansas, J. Kuhn, W. Hafezi, I.L. Campbell, D. Reilly, J. Say, L. Brown, M.Y. White, S.J. Cordwell, S.J. Chadban, E.B. Thorp, S. Bao, S.D. Miller, N.J. King, Therapeutic inflammatory monocyte modulation using immune-modifying microparticles, Science translational medicine, 6 (2014) 219ra217.

[143] S. Kuerten, D.N. Angelov, Comparing the CNS morphology and immunobiology of different EAE models in C57BL/6 mice - a step towards understanding the complexity of multiple sclerosis, Annals of anatomy = Anatomischer Anzeiger : official organ of the Anatomische Gesellschaft, 190 (2008) 1-15.

[144] M. Conroy, L. Sewell, O.F. Miller, T. Ferringer, Interferon-beta injection site reaction: review of the histology and report of a lupus-like pattern, Journal of the American Academy of Dermatology, 59 (2008) S48-49.

[145] K.A. Whitehead, J.E. Dahlman, R.S. Langer, D.G. Anderson, Silencing or stimulation? siRNA delivery and the immune system, Annual review of chemical and biomolecular engineering, 2 (2011) 77-96.

[146] A.D. Judge, G. Bola, A.C. Lee, I. MacLachlan, Design of noninflammatory synthetic siRNA mediating potent gene silencing in vivo, Molecular therapy : the journal of the American Society of Gene Therapy, 13 (2006) 494-505.

[147] M.P. Gantier, Strategies for designing and validating immunostimulatory siRNAs, Methods in molecular biology, 942 (2013) 179-191.

[148] L.J. Cruz, R.A. Rosalia, J.W. Kleinovink, F. Rueda, C.W. Lowik, F. Ossendorp, Targeting nanoparticles to CD40, DEC-205 or CD11c molecules on dendritic cells for efficient CD8(+) T cell response: a comparative study, Journal of controlled release : official journal of the Controlled Release Society, 192 (2014) 209-218.

[149] T. Rothoeft, A. Gonschorek, H. Bartz, O. Anhenn, U. Schauer, Antigen dose, type of antigen-presenting cell and time of differentiation contribute to the T helper 1/T helper 2 polarization of naive T cells, Immunology, 110 (2003) 430-439.

[150] A.L. Silva, R.A. Rosalia, A. Sazak, M.G. Carstens, F. Ossendorp, J. Oostendorp, W. Jiskoot, Optimization of encapsulation of a synthetic long peptide in PLGA nanoparticles: low-burst release is crucial for efficient CD8(+) T cell activation, European journal of pharmaceutics and biopharmaceutics : official journal of Arbeitsgemeinschaft fur Pharmazeutische Verfahrenstechnik e.V, 83 (2013) 338-345.

[151] J. Reddy, E. Bettelli, L. Nicholson, H. Waldner, M.H. Jang, K.W. Wucherpfennig, V.K. Kuchroo, Detection of autoreactive myelin proteolipid protein 139-151-specific T cells by using MHC II (IAs) tetramers, Journal of immunology, 170 (2003) 870-877.

[152] A.P. Kodituwakku, C. Jessup, H. Zola, D.M. Roberton, Isolation of antigen-specific B cells, Immunology and cell biology, 81 (2003) 163-170.

[153] R. Smith, K.L. Wright, L. Ashton, Raman spectroscopy: an evolving technique for live cell studies, The Analyst, 141 (2016) 3590-3600.

[154] J. Xue, S.V. Schmidt, J. Sander, A. Draffehn, W. Krebs, I. Quester, D. De Nardo, T.D. Gohel, M. Emde, L. Schmidleithner, H. Ganesan, A. Nino-Castro, M.R. Mallmann, L. Labzin, H. Theis, M. Kraut, M. Beyer, E. Latz, T.C. Freeman, T. Ulas, J.L. Schultze, Transcriptome-based network analysis reveals a spectrum model of human macrophage activation, Immunity, 40 (2014) 274-288.

[155] M. Gorte, A. Horstman, R.B. Page, R. Heidstra, A. Stromberg, K. Boutilier, Microarray-based identification of transcription factor target genes, Methods in molecular biology, 754 (2011) 119-141.

[156] S.C. Bendall, E.F. Simonds, P. Qiu, A.D. Amir el, P.O. Krutzik, R. Finck, R.V. Bruggner, R. Melamed, A. Trejo, O.I. Ornatsky, R.S. Balderas, S.K. Plevritis, K. Sachs, D. Pe'er, S.D. Tanner, G.P. Nolan, Single-cell mass cytometry of differential immune and drug responses across a human hematopoietic continuum, Science, 332 (2011) 687-696.

[157] A.M. Vacaru, J. Vitale, J. Nieves, M.H. Baron, Generation of transgenic mouse fluorescent reporter lines for studying hematopoietic development, Methods in molecular biology, 1194 (2014) 289-312.

[158] H.Y. Xue, S. Liu, H.L. Wong, Nanotoxicity: a key obstacle to clinical translation of siRNA-based nanomedicine, Nanomedicine (Lond), 9 (2014) 295-312.

[159] R.V. Benjaminsen, M.A. Mattebjerg, J.R. Henriksen, S.M. Moghimi, T.L. Andresen, The possible "proton sponge " effect of polyethylenimine (PEI) does not include change in lysosomal pH, Molecular therapy : the journal of the American Society of Gene Therapy, 21 (2013) 149-157.

[160] Z.J. Deng, S.W. Morton, E. Ben-Akiva, E.C. Dreaden, K.E. Shopsowitz, P.T. Hammond, Layer-by-layer nanoparticles for systemic codelivery of an anticancer drug and siRNA for potential triple-negative breast cancer treatment, ACS nano, 7 (2013) 9571-9584.